



Universiteit  
Leiden  
The Netherlands

## Comprehensive metabolomics of the experimental opisthorchiasis

Kokova, D.

### Citation

Kokova, D. (2021, September 15). *Comprehensive metabolomics of the experimental opisthorchiasis*. Retrieved from <https://hdl.handle.net/1887/3210397>

Version: Publisher's Version

License: [Licence agreement concerning inclusion of doctoral thesis in the Institutional Repository of the University of Leiden](#)

Downloaded from: <https://hdl.handle.net/1887/3210397>

**Note:** To cite this publication please use the final published version (if applicable).

Cover Page



## Universiteit Leiden



The handle <https://hdl.handle.net/1887/3210397> holds various files of this Leiden University dissertation.

**Author:** Kokova, D.

**Title:** Comprehensive metabolomics of the experimental opisthorchiasis

**Issue Date:** 2021-09-15

# **Comprehensive metabolomics of the experimental opisthorchiasis**

Daria Kokova

Copyright © 2021 by D. Kokova. All rights reserved. No part of this book may be reproduced, stored in a retrieval system, or transmitted in any form or by any means, without prior permission of the author.  
Printing:

# Comprehensive metabolomics of the experimental opisthorchiasis

## PROEFSCHRIFT

ter verkrijging van  
de graad van doctor aan de Universiteit Leiden,  
op gezag van de rector magnificus prof.dr.ir. H. Bijl,  
volgens besluit van het college voor promoties  
te verdedigen op woensdag 15 september 2021  
klokke 11:15 uur

*door*

**Daria Kokova**

geboren te Abakan, de USSR

in 1986

Promotor: prof. dr. M. Yazdanbakhsh

Co-promotor: dr. O.A. Mayboroda

Promotiecommissie: prof. dr. C.H. Hokke  
dr. E. Want (Imperial College London, UK)  
prof. dr. A.G.M. Tielens (Utrecht University)

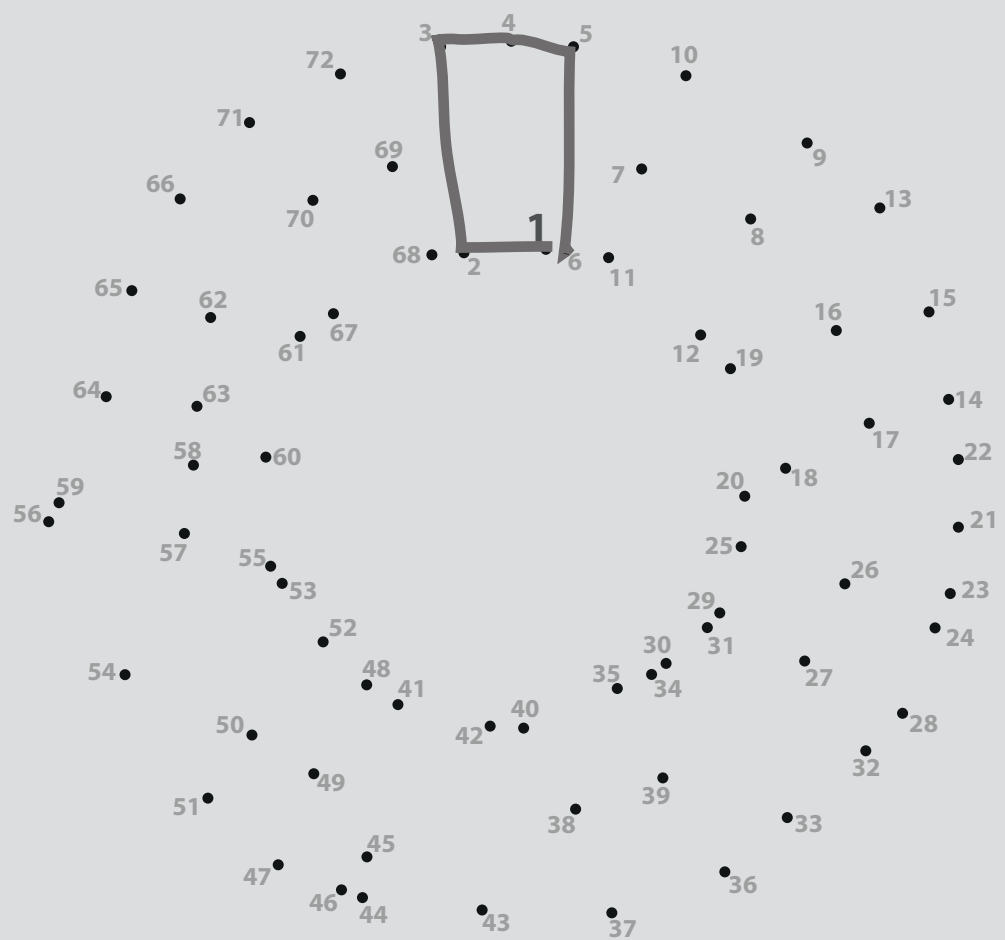
“Глядя на мир, нельзя не удивляться”  
Kozma Prutkov, 1884

for Matthias

# Table of contents

<b>Chapter 1</b>	11
General introduction	
<b>Chapter 2</b>	23
Twenty years on: metabolomics in helminth research	
<i>D. Kokova, O.A. Mayboroda. Trends in Parasitology, V. 35, I. 4, pp 282-288 (2019). <a href="https://doi.org/10.1016/j.pt.2019.01.012">https://doi.org/10.1016/j.pt.2019.01.012</a></i>	
<b>Chapter 3</b>	41
Exploratory metabolomics study of the experimental opisthorchiasis in a laboratory animal model (golden hamster, <i>Mesocricetus auratus</i> )	
<i>D. Kokova, S. Kostidis, J. Morello, N. Dementeva, E.A. Perina, V.V. Ivanov, L.M. Ogorodova, A.E. Sazonov, I.V. Saltykova, O.A. Mayboroda. PLoS Negl Trop Dis 11(10): e0006044 (2017). <a href="https://doi.org/10.1371/journal.pntd.0006044">https://doi.org/10.1371/journal.pntd.0006044</a></i>	
<b>Chapter 4</b>	69
Plasma metabolomics of the time resolved response to <i>Opisthorchis felineus</i> infection in an animal model (golden hamster, <i>Mesocricetus auratus</i> )	
<i>D. Kokova, A. Verhoeven, E.A. Perina, V.V. Ivanov, E.M. Knyazeva, I.V. Saltykova, O.A. Mayboroda. PLoS Negl Trop Dis 14(1): e0008015 (2020). <a href="https://doi.org/10.1371/journal.pntd.0008015">https://doi.org/10.1371/journal.pntd.0008015</a></i>	
<b>Chapter 5</b>	95
<sup>1</sup> H-NMR analysis of feces: new possibilities in the helminthes infections research	
<i>S. Kostidis, D. Kokova, N. Dementeva, I.V. Saltykova, H.K. Kim, Y.H. Choi, O.A. Mayboroda. BMC Infectious Diseases. 17:275 (2017). DOI 10.1186/s12879-017-2351-7</i>	
<b>Chapter 6</b>	115
Metabolic homeostasis in chronic helminth infection is sustained by organ specific metabolic rewiring	
<i>D. Kokova, A. Verhoeven, E.A. Perina, V.V. Ivanov, M. Heijink, M. Yazdankhosh, O.A. Mayboroda. ACS Infect. Dis. 7: 4 (2021). <a href="https://doi.org/10.1021/acsinfecdis.1c00026">https://doi.org/10.1021/acsinfecdis.1c00026</a></i>	

<b>Chapter 7</b>	153
General discussion	
<b>Appendices</b>	163
Nederlandse samenvatting	
Acknowledgements	
Curriculum Vitae	
List of publications	
PhD portfolio	



# 1

## General introduction

## Opisthorchiasis: a brief overview

Food-borne trematodes are one of the big groups of human helminthiases, includes liver, lung, and intestinal flukes. They affect more than 56 million people around the world and 900 million at the risk [1, 2]. These parasites are mostly prevalent in developing countries with tropical climate: Asia, Africa, and South America [1]. The flukes of *Opisthorchiidae* family are responsible for the largest "share" of infected population with approximately 46 million people infected and 600 people – at risk. *Opisthorchis viverrini* (*O. viverrini*), and *Clonorchis sinensis* (*C. sinensis*) have tropical and subtropical endemic areas such us Thailand and China, respectively [3, 4]. However, food-borne trematode *Opisthorchis felineus* (*O. felineus*), which belongs to the same family, has another unique prevalence area around the middle and lower Ob and Irtysh rivers (Western Siberia) where average annual temperature is +1 °C. *O. felineus* was described for the first time at the end of the XIX century in the Northern Italy as a parasite of the cats. In 1891, the Russian scientist K. N. Vinogradov described this parasite in the human liver during post-mortem examination and named it the "Siberian liver fluke" [5]. In the last decade of the 20<sup>th</sup> century (1990-2000) up to 80% of population were infected with *O. felineus* in the Siberian region [6]. Today, despite availability of the affordable treatments and relatively straightforward diagnostics, the infection still impacts the Russian health care system (Figure 1). Furthermore, the cases of *O. felineus* infection are being reported in the Far East, Southeast Asia, and Eastern Europe and well as in North America, which may be attributed largely to global mobility or migration [7].

All three species of *Opisthorchiidae* have endemic areas around rivers or lakes, which is due to a complex life cycle of the flukes. There are two intermediate hosts; the first intermediate host is a susceptible snail, and the second – a fish of *Cyprinidae* family. In the first intermediate host, parasite eggs develop from miracidia to cercariae through sporocysts and rediae. Then metacercariae enter the second intermediate host – freshwater fish, where the cercaria develop to metacercaria. After eating contaminated undercooked fish, the parasite enters the final host (human or other fish-eating mammals). When the metacercaria



Figure 1. Numbers of reported new cases of *O. felineus* infection per 100 000 population per year in Russia in 2011-2013 (the figure was generated using the data summarised by Fedorova O.S. et al., [6])

reach the duodenum of the final host, they ascend through the ampulla of Vater into biliary ducts (their final destination), where they become adults and start to pass eggs from 3<sup>rd</sup> to 4<sup>th</sup> week post-infection [8].

A clinical presentation of opisthorchiasis is not very specific; neither for acute, nor for chronic forms of the disease. For example, the main symptoms of the acute phase such as fever and abdominal pain, are strongly dependent on the intensity of infection and, previous exposure to the parasite, commonly, opisthorchiasis with worm burden less than 100 flukes is asymptomatic, and nonspecific mild symptoms are associated with 100 to 1000 worms [9]. Yet, with a typical, for a *Trematoda*, life span of 25-30 years, the flukes obstructing the bile ducts of the host may trigger multiple local and systemic complications due to the bile duct obstruction and usually presented in a form of fibrosis, cholangitis, obstructive jaundice, hepatomegaly, abdominal pain, and nausea [3]. Importantly, epidemiological and animal studies show that *O. viverrini* and *C. sinensis* infections can lead to cholangiocarcinoma (bile duct cancer), which has resulted in the classification of these parasites to the Group I carcinogens by the International Agency for Research on Cancer [10]. Discovery of an association between opisthorchiasis and an increased risk of cholangiocarcinoma has triggered

interest in the disease as evident from the number of publications overtime (Figure 2). Most of the publications cover the common areas of parasitology and epidemiology. Yet, in the last twenty years the pattern of opisthorchiasis research has changed; studies on diagnosis,

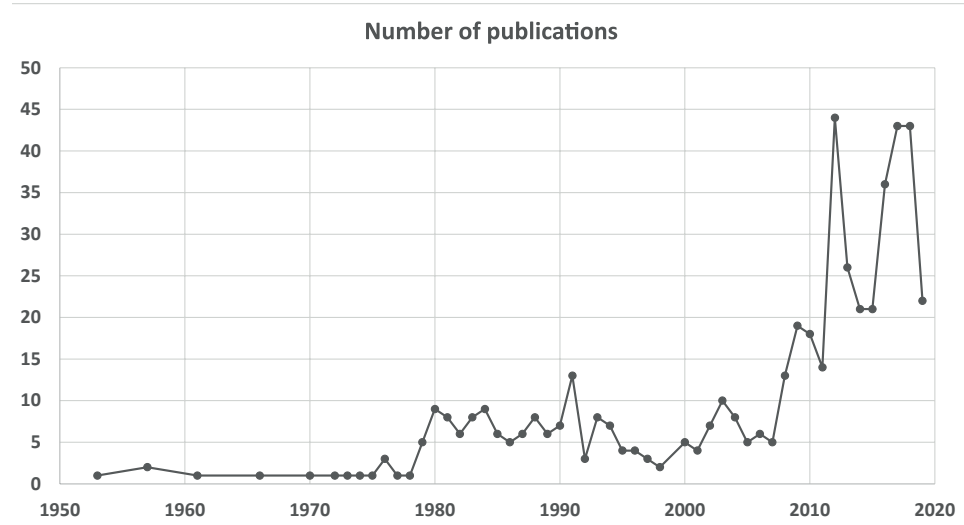


Figure 2. Dynamics of the publications on opisthorchiasis based on an online bibliographic database "Web of Science"

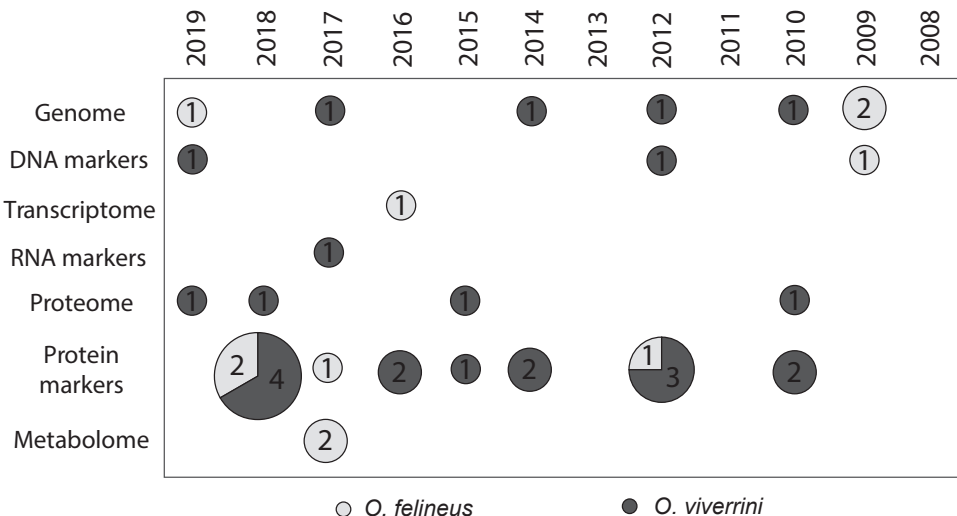


Figure 3. The frequency of the publications on opisthorchiasis related to "omics" sciences; light-grey – *O. felineus*, dark-grey – *O. viverrini*

treatment, and additionally, opisthorchis-induced cholangiocarcinoma started to be performed taking new molecular-based approaches.

New, enabling molecular and analytical techniques are used more and more frequently to generate data, which describe the parasite and its interaction with its host at a molecular level (Figure 3). Therefore, genomes of *O. viverrini* and *O. felineus* have been well studied [11-14]; genomes of the three species (*O. viverrini*, *O. felineus*, *C. sinensis*) have been compared [14] and, the mitochondrial genome of *O. felineus* was sequenced [15]. At the same time, DNA markers of oxidative stress, such as 8-oxo-7,8-dihydro-2'-deoxyguanosine, were discovered as significant markers that predict the initiation, promotion and progression of opisthorchiasis-induced cholangiocarcinoma [16, 17]. The transcriptomic study of *O. felineus* has obtained four highly encoded proteins myoglobin, vitelline proteins, cathepsin F, and 28 kDa glutathione S-transferase which participate in adaptation of the fluke in the bile duct [18, 19]. One of important study was exploring and comparing transcriptome of *O. viverrini* and *C. sinensis* [20], which also generated data on differences between transcriptome of juvenile and adult stages of *O. viverrini* [21]. Most notable are differences among the C13-peptide and cathepsin L-like cysteine peptidases, which play key roles in tissue migration, immune evasion and feeding, and, thus, represent potential drug and/or vaccine targets [21].

Proteomics is probably the best studied area when it comes to biology of *Opisthorchiidae*. For instance, the excretory/secretory products of adult stage of *O. viverrini* were shown to include proteins that have been associated with cancers, including proteases with different characteristics, orthologues of mammalian growth factors and anti-apoptotic proteins [22]. Moreover, it has been shown in animal models that a liver antioxidant enzyme, peroxiredoxin 6, plays a key role in host response to the infection and be both a biomarker and a therapeutic target for opisthorchiasis [23]. In addition, the studies at different “omics” levels, have allowed integration of results transcriptomics and proteomics. The identification of cathepsin B-1 protease as a possible serodiagnostic antigen was guided by transcriptomic data and confirmed by excretory/secretory proteome analysis of *O. viverrini*. Also, a recombinant form of cathepsin B-1 protein was produced and tested as a serodiagnostic antigen in enzyme linked immunosorbent assays that showed a sensitivity and specificity 67% and 81%, respectively [24]. There are also a few protein markers of

cholangiocarcinoma detectable during chronic opisthorchiasis: plasma exostosin 1, liver 14-3-3-eta, cadherin-related family member 2 and lysosome associated membrane glycoprotein 1 and 2 in urine, provide the basis for development of novel diagnostic biomarkers [25-27].

However, the metabolome is not investigated at all, apart from 2 publications that are part of this thesis [28, 29]. It is important to have a full overview of an infection at multiomics level and therefore data on the metabolome of the parasite and changes in host metabolism are still needed. To address this need, the aim of our studies is to fill the existing data gap; we concentrate on the contemplation of risks associated with the *O. felineus* infection using metabolomics. The hypothesis is that the parasite remodels host metabolism, which leads to the development of the associated pathologies.

## Thesis outline

Metabolomics is a post-genomic discipline that offers the researcher a combination of advanced analytical techniques capable of simultaneously detecting multiple compounds and the multivariate data modeling. In this way, the physiological status or “metabolic phenotype” of an organism can be represented as a combination of metabolite concentrations/abundances in biofluids. This thesis is focused on application of the metabolomics to study experimental opisthorchiasis.

**Chapter 2** presents a critical overview of the current status, merits, and limitations of metabolomics in helminthology. The comparison of the published results was systematically assessed for the first time. Animal studies on trematode infections where NMR spectroscopy was used were included, to allow cross-comparison of the results published in different laboratories.

**Chapter 3** and **Chapter 4** are focused on exploratory NMR-based metabolomics study of biofluids in *O. felineus*-associated opisthorchiasis. **Chapter 3** is dedicated to the metabolic changes detected in urine samples; **Chapter 4** covers the changes upon infection in blood plasma samples. Both sets of samples (urine and plasma) were collected within the same study, which was designed as a longitudinal study with two levels of infection intensity. The studies had allowed us to analyze metabolites associated with development of the infection in time, gender-specific reaction to the infection and response to the different infection burden.

**Chapter 5** is focused on the development of a method for the NMR-based metabolic profiling/phenotyping of stool samples, the method is then used in **Chapter 6**.

**Chapter 6** is a quantitative NMR metabolomics study of experimental opisthorchiasis which describes metabolic changes at the chronic stage of infection. The unique feature of this study is that we describe a metabolic landscape of the infection using a combined analysis of the host’s body fluids and the most relevant tissue samples. We show which data blocks/samples are most affected by the infection and provide an optimal combination of the metabolites which could be considered as a signature of infection.

Finally, **Chapter 7** consists of a general discussion of the principal findings.

## References

1. Keiser J, Utzinger J. Food-borne trematodiases. *Clin Microbiol Rev*. 2009;22(3):466-83.
2. Furst T, Keiser J, Utzinger J. Global burden of human food-borne trematodiasis: a systematic review and meta-analysis. *Lancet Infect Dis*. 2012;12(3):210-21.
3. Keiser J, Utzinger J. Food-Borne Trematodiases. *Clinical Microbiology Reviews*. 2009;22(3):466-83.
4. Keiser J, Utzinger J. Emerging foodborne trematodiasis. *Emerging Infectious Diseases*. 2005;11(10):1507-14.
5. Marquardt, William C. et al. *Parasitology and Vector Biology*. 2nd Edition. Academic Press, 2000
6. Fedorova OS, Kovshirina YV, Kovshirina AE, Fedotova MM, Deev IA, Petrovskiy FI, et al. *Opisthorchis felineus* infection and cholangiocarcinoma in the Russian Federation: A review of medical statistics. *Parasitology International*. 2017;66(4):365-71.
7. Hotez PJ, Gurwith M. Europe's neglected infections of poverty. *International Journal of Infectious Diseases*. 2011;15(9):E611-E9.
8. <https://www.cdc.gov/parasites/opisth-orchis/biology.html>
9. Liu LX, Harinasuta KT. Liver and intestinal flukes. *Gastroenterology Clinics of North America*. 1996;25(3):627.
10. Bouvard V, Baan R, Straif K, Grosse Y, Secretan B, El Ghissassi F, et al. A review of human carcinogens-Part B: biological agents. *Lancet Oncology*. 2009;10(4):321-2.
11. Young ND, Nagarajan N, Lin SLJ, Korhonen PK, Jex AR, Hall RS, et al. The *Opisthorchis viverrini* genome provides insights into life in the bile duct. *Nature Communications*. 2014;5.
12. Gasser RB, Tan P, Teh B, Wongkham S, Young ND. Genomics of worms, with an emphasis on *Opisthorchis viverrini* - opportunities for fundamental discovery and biomedical outcomes. *Parasitol Int*. 2017;66(4):341-5.
13. Young ND, Gasser RB. *Opisthorchis viverrini* Draft Genome - Biomedical Implications and Future Avenues. *Asiatic Liver Fluke - from Ba-*

sic Science to Public Health, Pt A. 2018;101:125-+.

14. Ershov NI, Mordvinov VA, Prokhortchouk EB, Pakharukova MY, Gunbin KV, Ustyantsev K, et al. New insights from *Opisthorchis felineus* genome: update on genomics of the epidemiologically important liver flukes. *Bmc Genomics*. 2019;20.

15. Mordvinov VA, Mardanov AV, Ravin NV, Shekhovtsov SV, Demakov SA, Katokhin AV, et al. Complete Sequencing of the Mitochondrial Genome of *Opisthorchis felineus*, Causative Agent of Opisthorchiasis. *Acta Naturae*. 2009;1(1):99-104.

16. Yongvanit P, Pinlaor S, Loilome W. Risk biomarkers for assessment and chemo-prevention of liver fluke-associated cholangiocarcinoma. *Journal of Hepato-Biliary-Pancreatic Sciences*. 2014;21(5):309-15.

17. Jamnongkan W, Techasen A, Thanan R, Duenngai K, Sithithaworn P, Mairiang E, et al. Oxidized alpha-1 antitrypsin as a predictive risk marker of opisthorchiasis-associated cholangiocarcinoma. *Tumor Biol*. 2013;34(2):695-704.

18. Pomaznay M, Tatkov S, Katokhin A, Afonnikov D, Babenko V, Furman D, et al. Adult *Opisthorchis felineus* major protein fractions deduced from transcripts: Comparison with liver flukes *Opisthorchis viverrini* and *Clonorchis sinensis*. *Exp Parasitol*. 2013;135(2):297-306.

19. Pomaznay MY, Logacheva MD, Young ND, Penin AA, Ershov NI, Katokhin AV, et al. Whole transcriptome profiling of adult and infective stages of the trematode *Opisthorchis felineus*. *Parasitology International*. 2016;65(1):12-9.

20. Young ND, Campbell BE, Hall RS, Jex AR, Cantacessi C, Laha T, et al. Unlocking the Transcriptomes of Two Carcinogenic Parasites, *Clonorchis sinensis* and *Opisthorchis viverrini*. *Plos Neglected Tropical Diseases*. 2010;4(6).

21. Jex AR, Young ND, Sripa J, Hall RS, Scheerlinck JP, Laha T, et al. Molecular Changes in *Opisthorchis viverrini* (South-east Asian Liver Fluke) during the Transition from the Juvenile to the Adult Stage. *Plos Neglect Trop D*. 2012;6(11).

22. Mulvenna J, Sripa B, Brindley PJ, Gorman J, Jones MK, Colgrave ML, et al. The secreted and surface proteomes of the adult stage of the carcinogenic human liver fluke *Opisthorchis viverrini*. *Proteomics*. 2010;10(5):1063-78.

23. Khoontawad J, Wongkham C, Hiraku Y, Yongvanit P,

Prakobwong S, Boonmars T, et al. Proteomic identification of peroxiredoxin 6 for host defence against *Opisthorchis viverrini* infection. *Parasite Immunol.* 2010;32(5):314-23.

24. Sripa J, Brindley PJ, Sripa B, Loukas A, Kaewkes S, Laha T. Evaluation of liver fluke recombinant cathepsin B-1 protease as a serodiagnostic antigen for human opisthorchiasis. *Parasitol Int.* 2012;61(1):191-5.

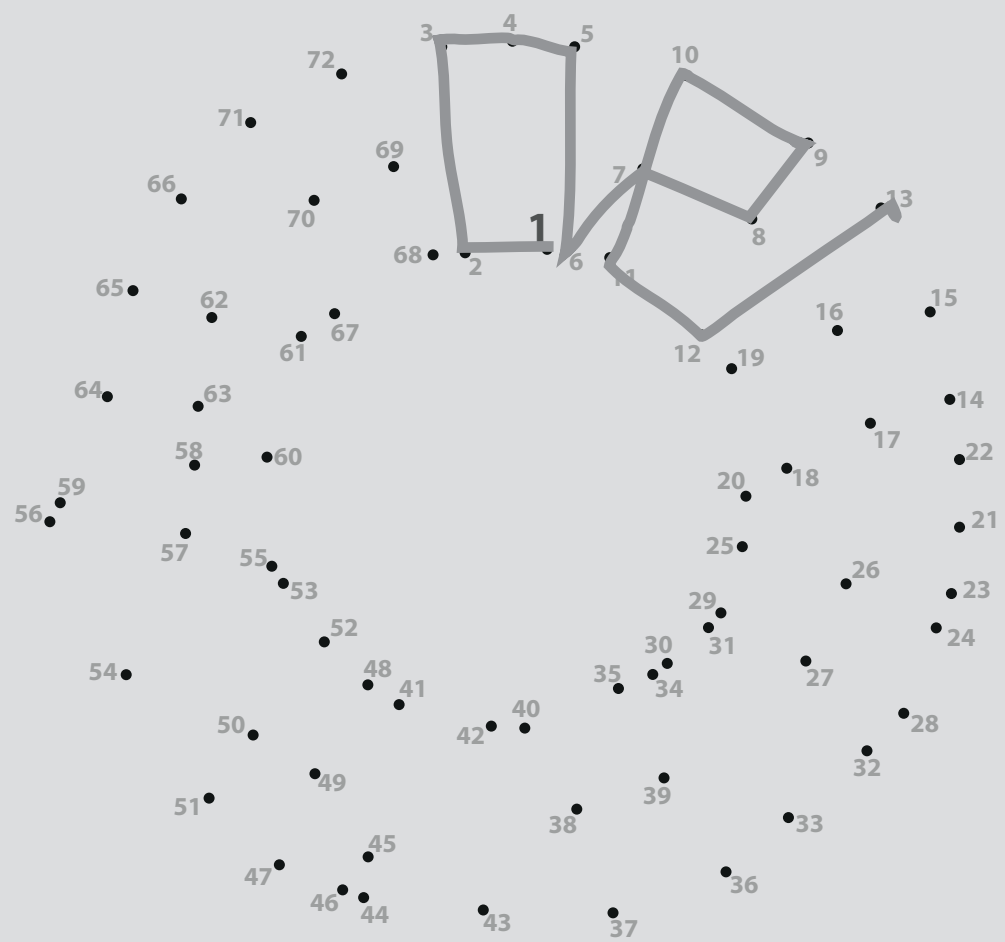
25. Khoontawad J, Hongsrichan N, Chamgramol Y, Pinlaor P, Wongkham C, Yongvanit P, et al. Increase of exostosin 1 in plasma as a potential biomarker for opisthorchiasis-associated cholangiocarcino-ma. *Tumor Biol.* 2014;35(2):1029-39.

26. Haonon O, Rucksaken R, Pinlaor P, Pairojkul C, Chamgramol Y, Intuyod K, et al. Upregulation of 14-3-3 eta in chronic liver fluke infection is a potential diagnostic marker of cholangiocarcinoma. *Proteom Clin Appl.* 2016;10(3):248-56.

27. Duangkumpha K, Stoll T, Phetcharaburanin J, Yongvanit P, Thanan R, Techasen A, et al. Urine proteomics study reveals potential biomarkers for the differential diagnosis of cholangiocarcinoma and periductal fibrosis. *Plos One.* 2019;14(8).

28. Kokova DA, Kostidis S, Morel-  
lo J, Dementeva N, Perina EA, Ivanov VV, et al. Exploratory metabolomics study of the experimental opisthorchiasis in a laboratory animal model (golden hamster *Mesocricetus auratus*). *Plos Neglect Trop D.* 2017;11(10).

29. Kostidis S, Kokova D, Dementeva N, Saltykova IV, Kim HK, Choi YH, et al. H-1-NMR analysis of feces: new possibilities in the helminthes infections research. *Bmc Infectious Diseases.* 2017;17.



# 2

## Twenty years on: metabolomics in helminth research

D. Kokova  
O.A. Mayboroda

Trends in Parasitology, V. 35, I. 4, pp 282-288 (2019)  
<https://doi.org/10.1016/j.pt.2019.01.012>

## Abstract

This contribution makes a critical assessment of the metabolomics application to helminthic infection research. To ensure a cross-comparison of the results published by different laboratories over a period of almost two decades, we restrict the discussion to only the publications where nuclear magnetic resonance (NMR) spectroscopy is used as the analytical platform. We review the metabolites consistently reported for the body fluids of animals infected with the parasitic helminths and the characteristic metabolic patterns, arguing that the field needs a complete integration of metabolomics into research lines that examine host-helminth interactions.

## Highlights

- » Helminth infections were among the very first experimental models used in metabolomics; the first results were positive, and they inspired great expectations.
- » Robustness of the NMR metabolomics analysis enables comparison of the data obtained for a period of two decades.
- » There are three major metabolic traits which NMR metabolomics studies of the helminth infections revealed: remodeling of the amino acid metabolism, strong change in the metabolism of lipids, and dysregulation of the microbiota.
- » Metabolomics research generated a number of functional hypotheses, but the follow-up studies are often missing.

# In the beginning: metabolomics meets parasitology

For a parasitic worm, coexistence with its host is a “long-term project”. The time of this coexistence is measured in years or decades, during which the host and the parasite are competing for the available energy resources, as well as metabolic building blocks; that profoundly affects the metabolic homeostasis of each other. Hence, it is not surprising that, with the emerging of a novel discipline, metabolomics (see Glossary), parasitic helminth infections were among the first experimental models to which it was applied. Of course, the metabolic effects of helminths on the host were studied before the “omics” era. For instance, the changes in serum lipids were described for rabbits infected with *Schistosoma japonicum* [1]. Moreover, an attenuation of the key metabolic enzymes in liver and the consequent shift in the metabolic homeostasis of the host were shown for humans infected with *Schistosoma mansoni* [2]. Yet, metabolomics boded something completely new: a combination of the advanced analytical techniques capable of simultaneously detecting multiple compounds and the multivariate modeling or machine-learning algorithms, which offered a strong alternative to the conventional biochemical experimentation [3]. New and more accurate diagnostic methods based on the multiparametric metabolic readouts, as well as novel approaches for estimating morbidity or monitoring host-parasite interaction, appeared to be within a hand’s reach. The first reports on metabolomics of *S. mansoni* infection appeared promising [4]. A clear biological response to this parasitic infection was discovered that involved changes in the pattern of amino acids as well as the composition of the microbiota-related metabolites. Since then, despite the enormous progress in analytical instrumentation and, most importantly, the data analysis routines, metabolomics of the body fluids in helminth infections has not provided the field with much in-depth insight. Here, we would like to give our point of view on the disagreement between a highly promising methodology and the rather disappointing results. We have restricted our discussion to studies that: (i) involve only members of the *Trematoda*, (ii) are conducted in animal models, and (iii) use the method of nuclear magnetic resonance (NMR) spectroscopy

as the analytical platform (Box 1) to ensure a cross-comparison of the results published in different laboratories. Of course, any restriction introduces a bias, but we believe that consistency of the discussed data is more important than extensive coverage of the literature.

**Box 1.** NMR-Based Metabolomics NMR spectroscopy, in essence, is a physical tool for investigating matter. NMR exploits the properties of the atomic nuclei (Nuclear) in a strong magnetic field (Magnetic) using radiofrequency waves (Resonance) to gain information about the composition and quantity of the molecular entities in the complex mixtures. The first published biological application of NMR goes back to the 1950s when the method was applied to study the hydration properties of DNA in solution [32]. A proton NMR or  $^1\text{H}$ -NMR used in the above-mentioned work became, after several instrumental improvements, an analytical core of NMR metabolomics.  $^1\text{H}$  is the most commonly used nucleus for NMR analysis of biofluids, thanks to its natural abundance of 99.98% and its invariable presence in organic molecules.  $^1\text{H}$ -NMR cannot match the sensitivity of

mass spectrometric techniques, but it offers superior reproducibility and facile quantitation based on a linear relation between the peak area and the concentration of the corresponding analyte [33, 34]. A truly unique feature of NMR metabolomics is the possibility to analyze the data with an exploratory untargeted or targeted approach to the same set of raw data. Finally, the automated workflows that integrate data acquisition, preprocessing, and modeling algorithms are making the platform accessible to a broad scientific community [35].

## The numbers: how many metabolites are there, and how many do we see?

We start with the numbers. The last version of the human metabolome database (HMDB 4.0) includes over 100 000 structures [5]. Yet, by searching the database for body-fluid-specific metabolites, we get only 2025 features for urine and 3189 for blood (the search was performed using the filters “detected and quantified” and “detected but not quantified”, thus limiting it only to the metabolites that were in fact measured and excluding the predicted ones). Furthermore, the diversity of the physicochemical properties of the metabolites makes it impossible for a single analytical method to provide a full coverage of the metabolome within a given biological sample. Consequently, a choice of the analytical method will always skew the analysis towards one or another group of metabolites, for example, polar (e.g., amino acids, sugars, nucleosides, nucleobases) or nonpolar (e.g., fatty acids, lipids). NMR is not an exception, though the limitations are due to the sensitivity rather than chemical selectivity (as it is in the case of mass spectrometry analysis). For instance, the introductory paper of the human urine metabolome database, published in 2013, included only 200 structures detectable by NMR [6], while the serum database published 2 years earlier included just 59 [7]. An open-access resource comparable to HMDB is not available for the rodents, but the numbers reported for human body fluids can be safely taken as a first approximation of the metabolome coverage offered by NMR for the animal rodent models. An analysis of the preselected literature revealed a set of 67 metabolites reported in the context of the trematode infections [4, 8–19]. The metabolites are summarized in Figure 1 (Key Figure). At a first glance, the number might appear low. But considering the restrictions discussed above, we can conclude that the number is just within a possible range. An additional explanation for a limited number of the reported metabolites could be due to the data analysis strategies routinely used in the exploratory metabolomics studies (Figure 2) – only the metabolites relevant to the study design that passed the selection criteria (e.g., variable ranking or variable importance for the multivariate methods or P value cut-off for the univariate ones) are reported and discussed. Thus, a typical output would have something

like 10–20 structures per report.

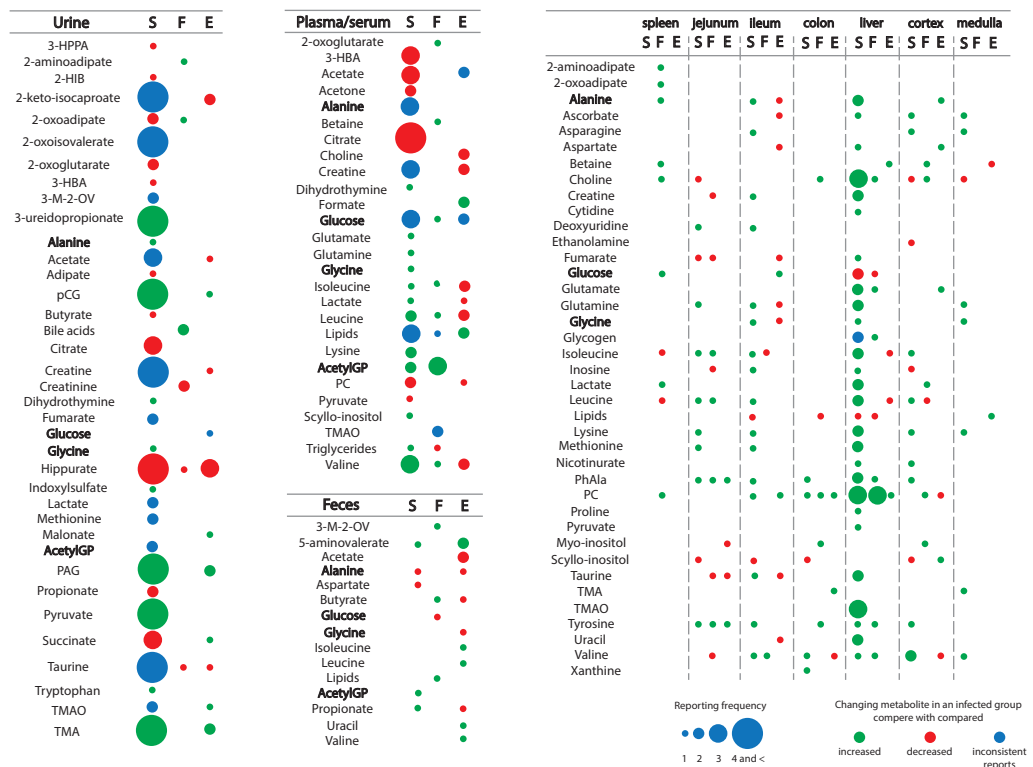


Figure 1. The included metabolites were reported as the ones with the highest contribution to multivariate models using case-control (infected versus noninfected) as the class ID [3–15]. The entries are organized according to the biological material used in the experiments and the frequency of reporting. There are 67 metabolites in total, but only 3 (highlighted in bold) are reported for all types of biomaterial; urine has the largest number (17) of the 'unique' metabolites. S, *Schistosoma mansoni* and *Schistosoma japonicum*; F, *Fasciola hepatica*; E, *Echinostoma caproni*. The size of the dots indicates reporting frequency. The colour indicates the concentration change: green, consistently increased; red, consistently decreased; blue, inconsistent data. Metabolites abbreviations: 3-HPPA, 3-hydroxyphenylpropionic acid; 2-HIB, 2-hydroxyisobutyrate; 3-HBA, 3-hydroxybutyrate; 3-M-2-OV, 3-methyl-2-oxovalerate; pCG, 4-cresol glucuronide; acetylGP, acetyl glycoproteins; PAG, phenylacetylglycine; TMAO, trimethylamine-N-oxide; TMA, trimethylamine; PC, phosphocholine; PhAla, phenylalanine.

## The numbers: how many metabolites are there, and how many do we see?

Thus, what can we extract from the metabolomics studies of helminth infections? In fact, there are several consistent trends reported from different studies. The first one is the change in the metabolism of amino acids observed in helminth-infected animals (mouse, *Mus musculus*, and Syrian hamster, *Mesocricetus auratus*, are the most used models). For some amino acids, the reported changes are helminth-specific; an example is taurine, a key metabolite for bile formation and one of the frequently mentioned amino acids affected by these infections [4, 10, 11, 15, 17]. In the *Schistosoma mansoni* infection model, the change in direction (whether the concentration of a metabolite increases or decreases in the infected animals in comparison to the noninfected ones) of urinary taurine varies, but it is consistently elevated in the liver [4, 10, 18]. In *Fasciola hepatica* infection, a decreased concentration of urinary taurine in combination with an increase in urinary bile acids [11, 16] fits nicely into a physiological paradigm which explains urinary excretion of the bile acids as a consequence of a duodenal obstruction [20]. This, in turn, may lead to the increased production of the bile acids and depletion of the taurine pool. As is the case with many other hypotheses derived from metabolomics data, this one is waiting for experimental confirmation. Another interesting example was reported for the first time in the seminal manuscript of Wang et al. [4]. The authors, as pioneers in the field, made a few interesting observations. One of them is a distinct pattern characterized by increased concentration of urinary pyruvate alongside a simultaneous decrease in citrate, succinate, and 2-oxoglutarate, which was associated with *S. mansoni* infection. The pattern proved to be consistent with further reports [4, 10]. Moreover, an original interpretation of the observation as a consequence of a systemic impairment of the pyruvate dehydrogenase was supported by an independent proteomics study [21]. Some changes in the urinary amino acid patterns, such as the decreased levels of 2-oxoisovalerate and 2-oxoisocaproate [4], are interpreted as a sign of impaired liver function, suggesting that one could estimate morbidity from a single urine sample. Yet, despite the fact that the amino acids always appear on the list of the metabolites affected by an infection, the variability

in the reported patterns remains high. With a single but notable exception: the concentration of essential amino acids, such as valine, is lower in the experimental models of *Echinostoma caproni* and is increased in the *Schistosoma* and *Fasciola* models [9–11, 15, 17, 19]. The first could be explained by the intestinal location of the parasite and as a consequence of impaired absorption of the dietary material. The second could suggest that the parasite is capable of impairing the insulin-stimulated absorption of the essential amino acids by the tissues (and muscle in the first place) to benefit from an increased pool of this important carbon and energy source in blood.

The second general observation is the infection-driven shift in lipid metabolism. The critical changes in the entire system of lipid homeostasis during the acute phase of infection were known for a long time, and the differences between rodents and primates are well documented. For example, it has been shown that, during the acute phase of an infection, the cholesterol increases in the serum of animals with low baseline values of low-density lipoprotein cholesterol (rodents) but remains stable in primates where the baseline values are higher [22]. Moreover, next to their role as the lipid transporters and regulators of cholesterol bioavailability, the lipoproteins are playing a part in the innate immune response. Thus, in the context of helminth infections, the observation that resistance to *Schis-*

## Glossary

**Biocomplexity:** complexity as exhibited by living organisms in their structure, composition, function, and interactions, or the study of complex structures and behaviors that arise from nonlinear interactions of the biological systems.

**Biofluid:** any bio-organic fluid produced by an organism, such as blood, urine, saliva, cerebrospinal fluid, sperm etc.

**Mass spectrometry:** an analytic technique by which chemical substances are identified by the sorting of ions in electric and magnetic fields according to their mass-to-charge ratios.

**Metabolite:** a chemical substance that is a product of metabolic action or that is involved in a metabolic process.

**Metabolome:** the complete set of the metabolites (such as metabolic intermediates, hormones and other signaling molecules, and secondary metabolites) to be found within a biological sample.

**Metabolomics:** a postgenomic discipline studying multiparametric metabolic responses of living systems to the internal and environmental stimuli.

**Multivariate modeling:** an application of multivariate statistics that encompasses the simultaneous observation and analysis of more than one outcome variable.

**Nuclear magnetic resonance (NMR):** spectroscopy is an analytic technique which measures local magnetic fields around atomic nuclei to obtain information about the molecular entities in the complex mixtures.

*tosoma* in rodents (rats) could be mediated by lipoproteins [23] makes the infection-related changes in lipid metabolism an important trend. Although  $^1\text{H}$  NMR provides only an overview of the major lipids (fatty acids, glycerolipids, phospholipids, sterols) and lipoprotein classes, detailed analysis of the structurally diverse lipometabolites is beyond the reach of the method. Recently, quantitative analysis of more than 100 lipoprotein subclasses directly from  $^1\text{H}$  NMR of serum/plasma samples has been made possible [24, 25]. Application of the standardized and quantitative method to the helminth infection models could help to resolve the existing inconsistencies in the reported changes in the lipid-related resonance regions. Finally, practically all metabolomics studies on helminth infections published so far show changes in metabolites associated with the gut microbiota. Today, it is widely accepted that the microbiota plays an essential role in the control of host physiological processes, forming a symbiotic “super-organism” [26]. One of the most pronounced metabolic traits is indirect urinary depletion of gut microbiota metabolites, namely hippurate (a conjugate of the benzoic acid and glycine), propionate, and butyrate [4]. The effect appears so consistent that it is reported not only for the rodent models of helminth infections but also in human studies in endemic regions [8, 27]. The exact physiological consequences of this depletion remain unexplored. However, considering the common symptoms of intestinal schistosomiasis (abdominal pain, diarrhea, and blood in the stool), a suppressed metabolic activity of the microbiota could be expected as a result, leading to a depletion of the main intermediates of the microbiota. However, this purely causal reasoning gives no insight into the mechanism of interaction between the intestinal metabolic pool and the excretion of the microbiotic metabolites in urine. Another interesting microbiota-related metabolic trait is the inverse relationship between the concentrations of two glycine conjugates: hippurate and phenylacetylglucine (PAG, a conjugate of phenylacetic acid and glycine) [8, 10–19]. The effect appears to be common to all helminth infections studied to date and is confirmed by independent analytical approaches [13, 14, 17, 28]. Both compounds depend on a pool of free glycine and could be synthesized by the microorganisms as well as by the host. To explain whether the observed dependency is a spurious correlation or an effect pointing to the mechanisms of response/adaptation to helminth infection, a properly designed follow-up study is required.

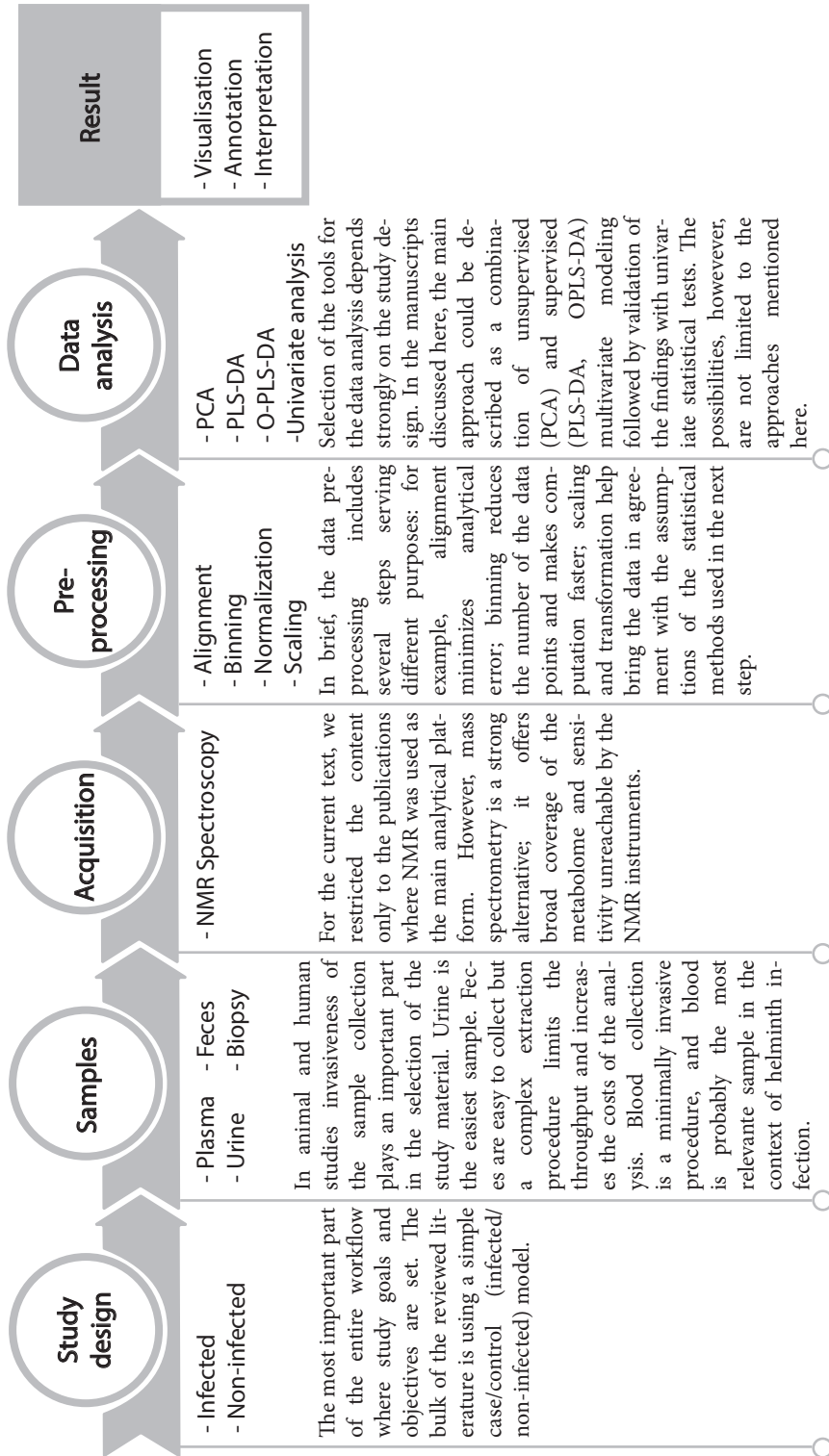


Figure 2. A generic workflow for a metabolomics study. A generic experimental workflow outlines the main steps of a metabolomic study and summarizes the special points for every step: types of sample, possible analytical solution, essential steps in the data preprocessing and analysis.

## The numbers: how many metabolites are there, and how many do we see?

One rationale for using animal models of human pathologies is the possibility to work in a highly controlled manner, minimizing the sources of the variance common for the human studies, reducing unwanted complexity, and revealing otherwise blurred patterns. Our approach to writing this text was similar: define the area of the analysis and try to grasp a general pattern. Hence, what do we have at the end? A limited set of the discriminative metabolites (Figure 1), many of which belong to a notorious list of the 'usual suspects' (a set of metabolites which appears on the top of the classification lists in any metabolomics study), and a few consistent metabolic trends. Does this imply that the discussed methodological approach leads to a dead end? We do not believe that there are grounds for such a conclusion. Not yet, at least. Firstly, the bulk of the metabolomics projects was designed and executed as exploratory studies and, as such, should generate a number of hypotheses for further testing, thus it is mainly a hypothesis-generating tool. Indeed, some interesting hypotheses (for example, a hypothesis on a systemic impairment of the pyruvate dehydrogenase during infection) have been generated. What is missing is a strategy for the follow-up studies. Secondly, the exploratory metabolomics studies used a rather limited set of data-modeling tools (see the data analysis section of Figure 2), which often address only case-control (infected versus noninfected) differences. Integration of the metabolomic data with clinical chemistry laboratory tests, demographic data, and genomic traits can broaden the data analysis repertoire. The positive examples from other fields of research (cardiology, metabolic syndrome) encourage such an approach [29, 30]. The manuscripts of Kettunen et al. [29] and Sliz et al. [30] are good examples showing that a combination of NMR metabolomics with genomic traits and an advanced data modeling made possible an accurate estimation of the heritability and risk of cardiovascular disorders. Thirdly, the host-parasite interaction is a complex phenomenon affecting all physio-logical systems of the host. Using a single biofluid to study it leads to an incomplete view of the problem. This issue was recognized from the very early days of metabolomics when parasitic

infections were considered as special cases of the increased biocomplexity [26]. Attempts at integrative analysis, using multiple biofluids, were made [9], but the available data are still too fragmentary to reveal the full advantage of such an approach. One could propose here a need for a more systematic, “multi-omics” approach; we recommend a recent review on this topic for a detailed overview [31]. Finally, in the early days of metabolomics, the discipline was presented as a solution to the open questions in biomedical sciences that conventional hypothesis-testing experimental models failed to solve. It is true that a holistic nature of the methodology is indeed its main ‘added value’. What is missing here is a real ‘embedding’ of the methodology into a problem-solving process in the field. Or, in other words, the method has to earn its place in the ‘toolbox’ of contemporary parasitology research. Thus, in our opinion, the future of metabolomics in helminth research is to be integrated with the standard physiological readouts routinely used in parasitological studies. The detailed process of such integration is difficult to predict. From the perspective of those who practice metabolomics research, we could mention a current trend towards automation and standardization of the complex metabolomics workflows as a practical way to make the technology and the data more accessible [32]. Furthermore, the current field of metabolomics is not limited to  $^1\text{H}$  NMR spectroscopy. Mass spectrometry is a strong alternative; it offers broad coverage of the metabolome and the sensitivity unreachable by NMR instruments. A balanced combination of the methodologies, as well as a knowledge of their advantages and limitations, would help us to make a right choice of the method, best fitted to a biological question or to the metabolites of interest (see Outstanding Questions).

## Outstanding Questions

- » Given that metabolomics offers a number of methodologies, including both the well-known ones (such as NMR or mass spectrometry) and the exotic ones (e.g., Raman spectroscopy), how does one find a realistically simple set of rules that facilitate a choice of the analytical platforms that, meanwhile, optimally fit a given study design?
- » How many metabolites need to be measured to make a meaningful physiological/pathophysiological description of the studied organism?
- » Is the host's metabolic response to helminth parasites specific, or does it represent the systemic response to infection? What does medical helminthology need from metabolomics to address the current challenges?

## Acknowledgments

We thank Professor Maria Yazdanbakhsh for helpful discussions and a critical reading of the text.

## References

1. Nishina, M. et al. (1994) Nuclear magnetic resonance (NMR) analysis on the serum-lipids of rabbits infected with *Schistosoma japonicum* – oxidative modifications of Diene system in fatty chains. *Int. J. Parasitol.* 24, 417–419
2. Sheweita, S.A. et al. (1998) Different levels of *Schistosoma mansoni* infection induce changes in drug-metabolizing enzymes. *J. Helminthol.* 72, 71–77
3. Holmes, E. and Nicholson, J.K. (2007) Human metabolic phenotyping and metabolome wide association studies. *Ernst-Schering Found. Symp. Proc.* 4, 227–249
4. Wang, Y. et al. (2004) Metabonomic investigations in mice infected with *Schistosoma mansoni*: an approach for biomarker identification. *Proc. Natl. Acad. Sci. U. S. A.* 101, 12676–12681
5. Wishart, D.S. et al. (2018) HMDB 4.0: the human metabolome database for 2018. *Nucleic Acids Res.* 46, D608–D617
6. Bouatra, S. et al. (2013) The human urine metabolome. *PLoS One* 8, e73076
7. Psychogios, N. et al. (2011) The human serum metabolome. *PLoS One* 6, e16957
8. Psychogios, N. et al. (2011) The human serum metabolome. *PLoS One* 6, e16957
9. Balog, C.I.A. et al. (2011) Metabonomic investigation of human *Schistosoma mansoni* infection. *Mol. Biosyst.* 7, 1473–1480
10. Saric, J. et al. (2009) Panorganismal metabolic response modeling of an experimental *Echinostoma caproni* infection in the mouse. *J. Proteome Res.* 8, 3899–38911
11. Li, J.V. et al. (2011) Chemometric analysis of biofluids from mice experimentally infected with *Schistosoma mansoni*. *Parasites Vectors* 4, 179
12. Saric, J. et al. (2010) Integrated cytokine and metabolic analysis of pathological responses to parasite exposure in rodents. *J. Proteome Res.* 9, 2255–2264
13. Wang, Y. et al. (2006) System level metabolic effects of a *Schistosoma japonicum* infection in the Syrian hamster. *Mol. Biochem. Parasitol.* 146, 1–9
14. Wang, Y. et al. (2009) Systems

metabolic effects of a *Necator americanus* infection in Syrian hamster. *J. Proteome Res.* 8, 5442–5450

14. Wu, J.F. et al. (2010) Metabolic alterations in the hamster co-infected with *Schistosoma japonicum* and *Necator americanus*. *Int. J. Parasitol.* 40, 695–703

15. Wu, J. et al. (2010) Metabolic changes reveal the development of schistosomiasis in mice. *PLoS Negl. Trop. Dis.* 4, 8

16. Saric, J. et al. (2010) Systems parasitology: effects of *Fasciola hepatica* on the neurochemical profile in the rat brain. *Mol. Syst. Biol.* 6, 396

17. Saric, J. et al. (2008) Metabolic profiling of an *Echinostoma caproni* infection in the mouse for biomarker discovery. *PLoS Negl. Trop. Dis.* 2, e254

18. Li, J.V. et al. (2009) Metabolic profiling of a *Schistosoma mansoni* infection in mouse tissues using magic angle spinning-nuclear magnetic resonance spectroscopy. *Int. J. Parasitol.* 39, 547–558

19. Zhu, X. et al. (2017) *Salmonella typhimurium* infection reduces *Schistosoma japonicum* worm burden in mice. *Sci. Rep.* 7, 1349

20. Corbett, C.L. et al. (1981) Urinary excretion of bile acids in cholestasis – evidence for renal tubular secretion in man. *Clin. Sci.* 61, 773–780

21. Harvie, M. et al. (2007) Differential liver protein expression during schistosomiasis. *Infect. Immun.* 75, 736–744

22. Hardardottir, I. et al. (1994) Effects of endotoxin and cytokines on lipid metabolism. *Curr. Opin. Lipidol.* 5, 207–215

23. Bout, D. et al. (1986) Rat resistance to schistosomiasis: platelet-mediated cytotoxicity induced by C-reactive protein. *Science* 231, 153–156

24. Jimenez, B. et al. (2018) Quantitative lipoprotein subclass and low molecular weight metabolite analysis in human serum and plasma by  $^1\text{H}$  NMR spectroscopy in a multilaboratory trial. *Anal. Chem.* 90, 11962–11971

25. Barrilero, R. et al. (2018) Lip-Spin: a new bioinformatics tool for quantitative  $^1\text{H}$  NMR lipid profiling. *Anal. Chem.* 90, 2031–2040

26. Nicholson, J.K. et al. (2004) The challenges of modeling mammalian biocomplexity. *Nat. Biotechnol.* 22, 1268–1274

27. Singer, B.H. et al. (2007) Exploiting the potential of metabonomics in large population studies: three venues. In *The Handbook of Metabonomics and Metabolomics* (Lindon,

J.C. et al., eds), pp. 289–325, Elsevier

28. Garcia-Perez, I. et al. (2008) Metabolic fingerprinting of *Schistosoma mansoni* infection in mice urine with capillary electrophoresis. *Electrophoresis* 29, 3201–3206

29. Kettunen, J. et al. (2012) Genome-wide association study identifies multiple loci influencing human serum metabolite levels. *Nat. Genet.* 44, 269–276

30. Sliz, E. et al. (2018) NAFLD risk alleles in PNPLA3, TM6SF2, GCKR and LYPLAL1 show divergent metabolic effects. *Hum. Mol. Genet.* 27, 2214–2223

31. Sotillo, J. et al. (2017) Exploiting helminth–host interactomes through big data. *Trends Parasitol.* 33, 875–888

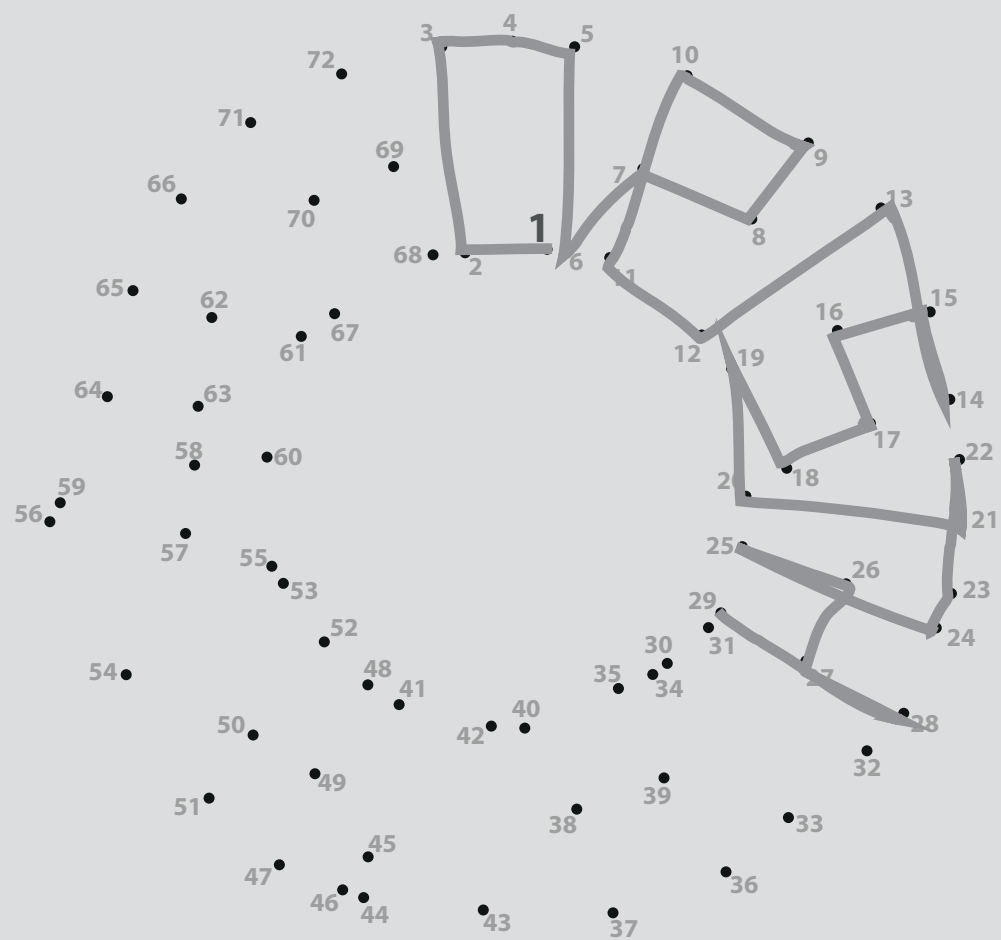
32. Jacobson, B. et al. (1954) A proton magnetic resonance study of the hydration of deoxyribonucleic acid. *Nature* 173, 772–773

33. Verhoeven, A. et al. (2017) Automated quantification of metabolites in blood-derived samples by NMR. *Anal. Chim. Acta* 976, 52–62

34. Lenz, E.M. and Wilson, I.D. (2007) Analytical strategies in metabolomics. *J. Proteome Res.* 6, 443–458

35. Nicholson, J.K. et al. (1999) ‘Metabonomics’: understanding the metabolic responses of living systems to pathophysiological stimuli via multivariate statistical analysis of biological NMR spectroscopic data. *Xenobiotica* 29, 1181–1189





# 3

## Exploratory metabolomics study of the experimental opisthorchiasis in a laboratory animal model

**D. Kokova**

S. Kostidis

J. Morello

N. Dementeva

E.A. Perina

V.V. Ivanov

L.M. Ogorodova

A.E. Sazonov

I.V. Saltykova

O.A. Mayboroda

PLoS Negl Trop Dis 11(10): e0006044 (2017)  
<https://doi.org/10.1371/journal.pntd.0006044>

## Abstract

### Background

Opisthorchiasis is a parasitic infection caused by the liver flukes of the *Opisthorchiidae* family. Both experimental and epidemiological data strongly support a role of these parasites in the etiology of the hepatobiliary pathologies and an increased risk of intrahepatic cholangiocarcinoma. Understanding a functional link between the infection and hepatobiliary pathologies requires a detailed description a host-parasite interaction on different levels of biological regulation including the metabolic response on the infection. The last one, however, remains practically undocumented. Here we are describing a host response on *Opisthorchiidae* infection using a metabolomics approach and present the first exploratory metabolomics study of an experimental model of *O. felineus* infection.

### Methodology and Principal findings

We conducted a NMR-based longitudinal metabolomics study involving a cohort of 30 animals with two degrees of infection and a control group. An exploratory analysis shows that the most noticeable trend (30% of total variance) in the data was related to the gender differences. Therefore, further analysis was done of each gender group separately applying a multivariate extension of the ANOVA-ASCA (ANOVA simultaneous component analysis). We show that in the males the infection specific time trends are present in the main component (43.5% variance), while in the females it is presented only in the second component and covers 24% of the variance. We have selected and annotated 24 metabolites associated with the observed effects and provided a physiological interpretation of the findings.

### Conclusions

The first exploratory metabolomics study an experimental model of *O. felineus* infection is presented. Our data show that at early stage of infection a response of an organism unfolds in a gender specific manner. Also, main physiological mechanisms affected appear rather nonspecific (a status of the metabolic stress) the data provides a set of the hypothesis for a search of the more specific metabolic markers of the *Opisthorchiidae* infection.

## Author summary

Opisthorchiasis is a parasitic infection caused by the liver flukes of the *Opisthorchiidae* family (*Trematoda; Platyhelminthes*). The liver fluke infections trigger development of the hepatobiliary pathologies such as chronic forms of cholecystitis, cholangitis, pancreatitis, and cholelithiasis. However, the most threatening effect of the *Opisthorchiidae* infection is an increased risk of intrahepatic cholangiocarcinoma. With this work we are getting an insight into a host response on *Opisthorchiidae* infection using a metabolomics approach. Metabolomics is a post-genomic discipline studying the metabolome. The dynamic character of the metabolome, its ability to change in response to the external stimuli makes it an optimal “readout” for exploratory studies aiming for the description of the systemic responses of an organism. Using this approach, we demonstrate that that early response to the *O. felineus* infection unfolds in a gender-dependent manner. Moreover, with this first exploratory analysis of the metabolic response to *O. felineus* infection in an animal model we present a subset of the metabolites changing during the early phase of the infection and offer a possible physiological interpretation.

## Introduction

Opisthorchiasis is a parasitic infection caused by the liver flukes of the *Opisthorchiidae* family (*Trematoda; Platyhelminthes*). The family includes the three most important species for human health: *C. sinensis*, *O. viverrini*, *O. felineus*; together they are responsible for more than 45 million infections worldwide; 600-750 million people are currently at risk [1, 2]. *O. viverrini* and *C. sinensis* are endemic to the Far East regions and South East Asia remaining an important public health problem [3]. *O. felineus* infection is highly prevalent in Eastern Europe (Ukraine and the European part of Russia), Central Asia (northern Kazakhstan) and North Asia (Siberia) [2]. Both experimental and epidemiological data strongly support a role of liver fluke infections in the etiology of the hepatobiliary pathologies such as chronic forms of cholecystitis, cholangitis, pancreatitis, and cholelithiasis [2-5]. However, the most threatening effect of the *Opisthorchiidae* infection is an increased risk of intrahepatic cholangiocarcinoma [6].

Unlike other pathogens, e.g. viruses and microbes, parasitic helminths do not proliferate within their mammalian host. Accordingly, the intensity of infection is one of the leading causes of the morbidity. For instance, *O. viverrini*-associated symptoms occurred more frequently in those with high intensities of infection [7] and positive association between hepatobiliary pathology and *O. viverrini* infection intensity is well documented [4]. Moreover, the biliary tract abnormalities more often detected by ultrasonography in the patients with heavy *O. viverrini* infections than light or moderate ones [8]. However, despite clear phenomenological and epidemiological evidence linking *Opisthorchiidae* infection and hepatobiliary pathology, our understanding of the mechanistic and descriptive biochemistry of the association is still rather poor. Only the humoral response to *O. viverrini* is reasonably well documented; for instance, a study on the infected hamsters showed that a titer of the parasite specific IgG in the acute stage is directly correlated to the intensity of infection, as determined by both worm burden and eggs per gram (EPG) counts. A more discriminative approach where the pathogen specific antibodies were divided according to their specificity to egg, excretory-secretory and somatic

antigens, shows an interesting kinetic of humoral response: while in the acute phase of infection the antibody response was higher in the animals infected with higher dose of metacercariae, in chronic phase higher responses, particularly to somatic and egg antigens, were found in the lightly infected hamsters [9]. A recent report of Khoontawad et al [10] represents the most detailed proteomics work on *O. viverrini* infection published so far. The authors explore the differential protein expression in the host tissue with a chronic inflammation versus the tissue samples from the subjects with *O. viverrini* induced cancer. With regard to the metabolomics, a post-genomic discipline aiming at studying the metabolites – the end points and the intermediate products of the metabolism, the data is simply not available. The metabolome of body fluids is the closest approximation of the physiological phenotype of an organism and, as such, it represents an important, but still undervalued, source of clinical/physiological information [11]. The dynamic character of the metabolome, its ability to change in response to the external stimuli makes it an optimal “readout” for exploratory studies describing the systemic responses of an organism. Whereas in schistosomiasis a number of exploratory metabolomics studies have been performed in animal models and patient material [12-16], there are so far no such studies in opisthorchiasis.

Here we present the first exploratory metabolomics study of an experimental model of *O. felineus* infection. Using an established hamster infection model, we conducted a nuclear magnetic resonance (NMR) based metabolomics study involving a cohort of 30 animals with two degrees of infection (severe and mild) and a control group. Urine samples were collected every two weeks for a period over several months. Using a combination of unsupervised and supervised multivariate statistical analysis we were able to discriminate the time-resolved urinary metabolic patterns of the infection.

# Material and methods

## Ethics statement

All hamsters used in the study were handled according the recommendations of the national guidelines for animal caring: 12.08.1977 N 755 "On measures to further improve the organizational forms of work using experimental animals". The study was approved by the local ethical committee of Siberian State Medical University with a license number 3296 issued on 29.04.2013.

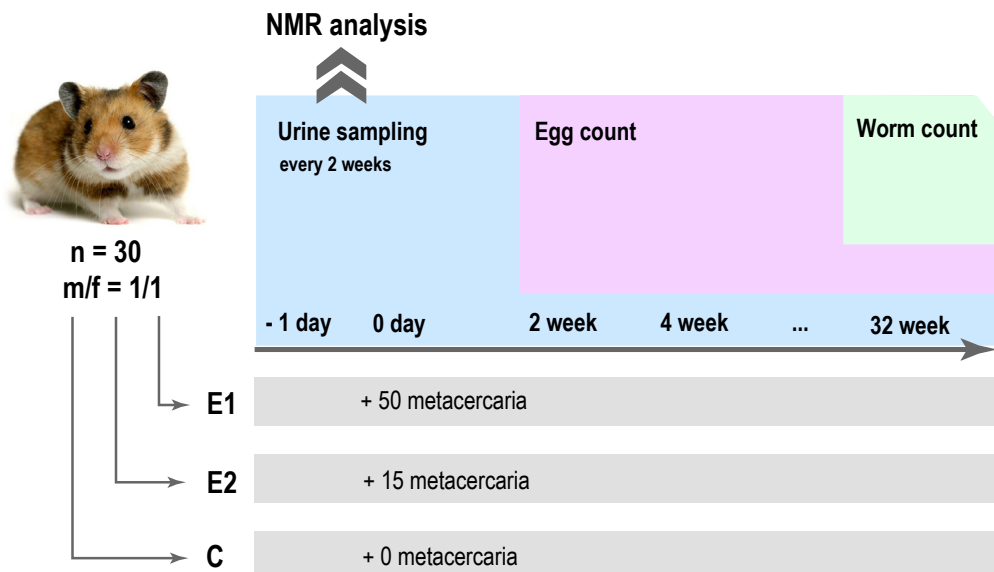


Figure 1. A graphical outline of the experimental design

## Experimental opisthorchiasis model

Hamsters *Mesocricetus auratus* were purchased from the animal facility of the Institute of Bioorganic Chemistry Academicians M.M. Shemyakin and U. A. Ovchinnikov. Metacercariae of *O. felineus* were obtained from naturally infected fishes sold in the local supermarkets as a consumption product. The muscular tissue and the subcutaneous tissue were digested by pepsin-HCl and viable metacercariae were collected and identified by microscopy. Hamsters were divided in 3 groups: high intensity of infection (50 metacercariae/hamster), low in-

tensity of infection (15 metacercariae/hamster) and uninfected (vehicle-PBS) groups. Each group consisted of 10 animals – five males and five females. Hamsters were housed in separate cages, maintained on a 12:12 light-dark cycle (06.00-18.00:18.00-06.00 hs), and provided food and water *ad libitum* for the duration of the experiment. Hamsters were approximately five weeks old at the time of infection. Animals were sacrificed after 46 weeks of infection. Livers were collected at the time of the sacrifice to count the adult worms. Urine and feces were collected every two weeks, specifically at the weeks 0, 2, 4, 6, 8, 10, 12, 14, 16, 18, 20, 22, 24, 26, 28, 30 and 32 after infection. For urine and feces collection hamster were placed individually into sterile empty glass crater and observed until urine and feces pellets were generated. Urine and fecal samples were collected into individually labelled Eppendorf tubes, and transferred to a freezer (-80°C) for long term storage.

### Eggs counts

The mean number of eggs per gram of feces was calculated following the modified Kato method (Katz et al. 1972). The fecal sample from each animal in the examined time point were mixed by Mini-Beadbeater-16 (Bio-Spec) for 5 minutes. A sample 25 mg of the feces was weighed with an electronic scale (Sartorius type 1702, sensitivity 0.1 mg) immediately after homogenization. Two slides were prepared for each 25 mg of feces. The extrapolation of the egg counts per 25 mg sample to the eggs per gram values was done by a simple multiplication (x 40).

### Urine sample preparation

All chemicals used for the buffer solution were purchased from Sigma-Aldrich except for the  $^{2}\text{H}_2\text{O}$  which was purchased from Cortecnet and the 3-(trimethylsilyl)propionic-2,2,3,3-d4 acid sodium salt (TSP) from Cambridge Isotope Laboratories Inc. 96-well plates and NMR tubes were purchased from Bruker Biospin Ltd (Germany).

Aliquots of 0.5 ml urine per sample were thawed overnight at 4°C. Cellular components and other insoluble material were then spun down by centrifugation for 10 min at 3184 g and 4°C and the supernatants were transferred into 96-well plates. 270  $\mu\text{L}$  of urine from each sample were mixed with 30  $\mu\text{L}$  buffer solution in  $^{2}\text{H}_2\text{O}$  (pH = 7.4) containing 1.5M  $\text{K}_2\text{HPO}_4$ , 2 mM  $\text{NaN}_3$  and 4mM of TSP-2,2,3,3-d4 as an in-

ternal standard and chemical shift reference (0.4 mM final concentration in each sample). Finally, 165  $\mu$ L of each urine-buffer mixture were transferred to 3 mm SampleJet NMR tubes and placed in refrigerated racks (6°C) of a SampleJet system until the NMR measurements. Both mixing of urine with buffer and transfer of the mixture to NMR tubes were performed by two 215 Gilson liquid handler robots and controlled by the SampleTrack software (Bruker Biospin Ltd).

### NMR data acquisition

NMR data were recorded using a Bruker 14.1T AVANCE II spectrometer for  $^1\text{H}$  600 MHz, equipped with a triple resonance inverse cryoprobe (TCI). Each sample was allowed to sit in the probe for 5 min to adopt a stable temperature at 27°C before starting the calibration routines and data acquisition. The probe was then automatically tuned and matched, followed by shimming and proton pulse calibration. One-dimensional (1D)  $^1\text{H}$  NMR spectra were recorded using the first increment of a NOESY pulse sequence [17] (noesygppr1d in Topspin 3.0 library). Water signal suppression was achieved with pre-saturation, a continuous wave irradiation of 50 Hz soft pulse during the relaxation delay of 4 s and the mixing time of 10 ms. The spectral width was set to 20 ppm (12335 Hz) and 16 scans of 65536 points were collected. The recorded free induction decays (FIDs) were Fourier transformed and a line broadening of 1.0 Hz was applied. The spectra were automatically phased, and baseline corrected and referenced to the internal standard chemical shift (TSP;  $\delta$  0.0 ppm). An evaluation of spectra quality was performed after processing. Peaks linewidth was evaluated with the TSP singlet and Alanine's methyl protons doublet. In addition, the efficiency of water suppression and the quality of the baseline were also checked. Spectra which failed to fulfil the quality criteria were discarded from further analysis.

Two-dimensional J-resolved spectra (2D Jres) were also collected for each sample using the same water suppression scheme as described above during the relaxation delay of 2 s. The spectral width was set to 16.66 ppm (12288 Hz) for the direct dimension and 78 Hz for the indirect one and 2 scans were acquired over 40 increments. The FIDs were automatically processed with Fourier transformation and spectra were referenced to the TSP signal at 0.0 ppm in the F2 dimension and at 0.0 Hz in the F1 dimension.

For assignment purpose, 2D NMR spectra were also acquired for

a sample is made as mix all urine samples. The set of 2D experiments included  $^1\text{H}$ - $^1\text{H}$  correlation spectroscopy (COSY),  $^1\text{H}$ - $^1\text{H}$  total correlation spectroscopy (TOCSY),  $^1\text{H}$ - $^{13}\text{C}$  heteronuclear single quantum correlation (HSQC) and  $^1\text{H}$ - $^{13}\text{C}$  heteronuclear multiple bond correlation spectroscopy (HMBC) using the standard parameters implemented in Topspin 3.0 library (Bruker Biospin Ltd.).

### Spectral data processing and data analysis

Pre-processing of NMR data to be suitable for statistical analysis was performed with in house routines written in Matlab 2014a (The Mathworks, Inc., USA) and Python 2.7 (Python Software Foundation, [www.python.org](http://www.python.org)). All 1D NMR  $^1\text{H}$  spectra were re-evaluated for incorrect baselines and corrected using a polynomial fit of degree 5. The spectral region from 0.5 to 9.5 ppm was binned using an in-house algorithm for adaptive intelligent binning [18]. Initial bin width was set to 0.02 ppm and final variable bins sizes were calculated based on the peaks edges in the spectra by using a lowest standard deviation criterion. The spectral region including the residual water and the urea peaks ( $\delta$  4.5-6.2 ppm) was excluded from the data.

The final data consisted of 392 bins of variable size  $\times$  490 observations (samples), which were normalized by the Probabilistic Quotients Normalization method (PQN) [19] to correct for dilution differences from sample to sample. Finally, the normalized data was scaled to unit variance for the statistical analysis.

The data analysis was performed with R statistical environment (<http://www.r-project.org/>, R versions 3.3.2). For exploratory analysis “Rcpm”, “pcaMethods” and “caret” packages were used. ASCA modeling was performed using “lmdme” package [20]. The visualizations were made using “ggplot2”, “cowplot” and “gridExtra” packages.

### Identification of the metabolites

Identification of metabolites was performed by exhausting search of the total 1D and 2D Jres data using the proprietary Bbioréfcode (Bruker Biospin Ltd.) and ChenomX NMR suite 8.1 (Chenonx Inc.) databases. The IDs of the annotated resonances were further verified by the collected 2D NMR data.

## Results

### Adult worm and eggs counts

The study design involves 30 animals divided in three groups: a control uninfected group and the two experimental groups infected with fifteen and fifty metacercaria Figure 1. Each experimental group consisted of an equal number of male and female animals. The data-set described in the current manuscript includes the samples from the baseline up to the thirty-two weeks collected every two weeks. The median of adult worm count at the end of the study was 35 for severe and 6 for mild infection intensity group respectively (p-value = 0.003) (S1A Figure). Eggs of *O. felineus* were detected in all fecal samples starting from 4 weeks post infection. S1B Figure shows the time course of the egg production over the entire period of the experiment. It shows a coherent increase in the egg production for both experimental groups over a period from 4 till 10 weeks. We consider changes in the egg production related to the different stage of the infection, namely an acute (till 10 weeks) and chronic one (from 10 weeks on). From week 12 till week 30 of the experiment, egg output is stable and the group with high infection has constantly higher egg output. The output is significantly higher at the weeks 12 (p-value = 0.002), 14 (p-value = 0.004), 16 (p-value = 0.030), 20 (p-value = 0.001), 26 (p-value = 0.001) and 28 (p-value = 0.009).

### An exploratory analysis of urinary metabolic profiles

The first step of an exploratory study is to identify the main sources of the variance in the data and influence of the confounding factors. The principal component analysis (PCA) is a commonly accepted approach. Figure 2 shows the score plots of the first two principle components of a PCA model built on the entire data set. The model required 5 components to explain 50% of the variance with 34% explained by the first two components. Every block of the figure represents the same model colored according to different factors. Surprisingly, the intensity of the infection (Figure 2A) is not contributing to the main sources of the variance in the data. Gender influences the profile profoundly; the influence is clearly represented in the first two

principal components (Figure 2C). Another recognizable source of the variance is the time of sample collection (Figure 2B and 2D). The S2 Figure shows the PCA models built separately for male (A, B) and female (C, D) animals. The models have similar characteristics to the “global” one, both require 5 components to explain 50% of the variance; the first two components explain 37% and 32% of the variance in the male and female models, respectively. Again, the intensity of infection is not explaining the main variance within the data (S2A and S2C Figure), but the time trend is clearly visible (S2B and S2D Figure). Moreover, the directions of the time trends in the models built on gender specific subsets appear to be different.

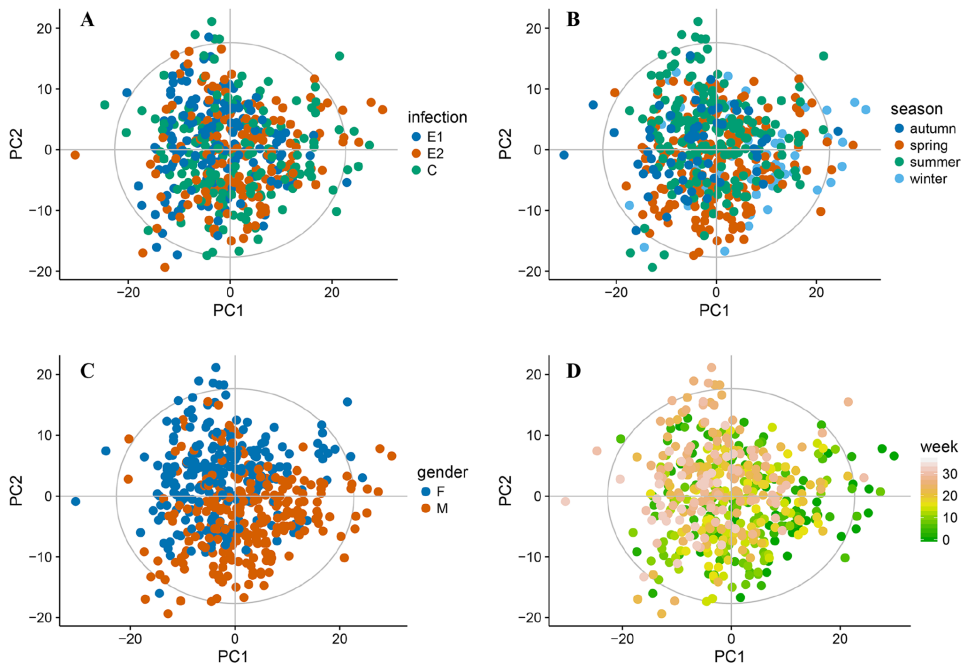


Figure 2. The score plots of the first two principal components of a PCA model built on the entire dataset; Every block of the figure represents the same model colored according to different factors; A – infection group, B – season, C – gender, D – time in weeks

### Analysis of the gender specific metabolic changes in the acute phase of the infection

The data shown in Figure 2 indicates clearly that a straightforward analysis of the infection dependent changes will be hampered by the influence of the gender and time trend. Thus, to reduce the

complexity of the analysis we decided to concentrate on the period from 0 to 10 weeks of the experiment: a time frame when egg output was steadily increasing (S1B Figure). The analysis was performed separately on the male and female subsets. Figure 3 shows the PCA models built on the data from week 0 up to the week 10 of the experiment. The “male model” (Figure 3A, 3B and 3C) required four components to explain 50% of the variance with 42% explained by the first two. The model was built of the data including only females (Figure 3D, 3E and 3F) required 6 components to explain 50% of the variance with the first two explain 34%. Both models appear quite similar, however applying the geometric trajectory analysis [21] (Figure 3C and 3F) some underlying differences can be revealed. The geometric time trajectories for the infected animals (groups E1 and E2) are clearly pronounced in the male model (Figure 3C). The same time in the female subset (Figure 3F) only a trajectory for highly infected animals (E1) has a distinct form, a trajectory for the lower infection group appears as random as the control one.

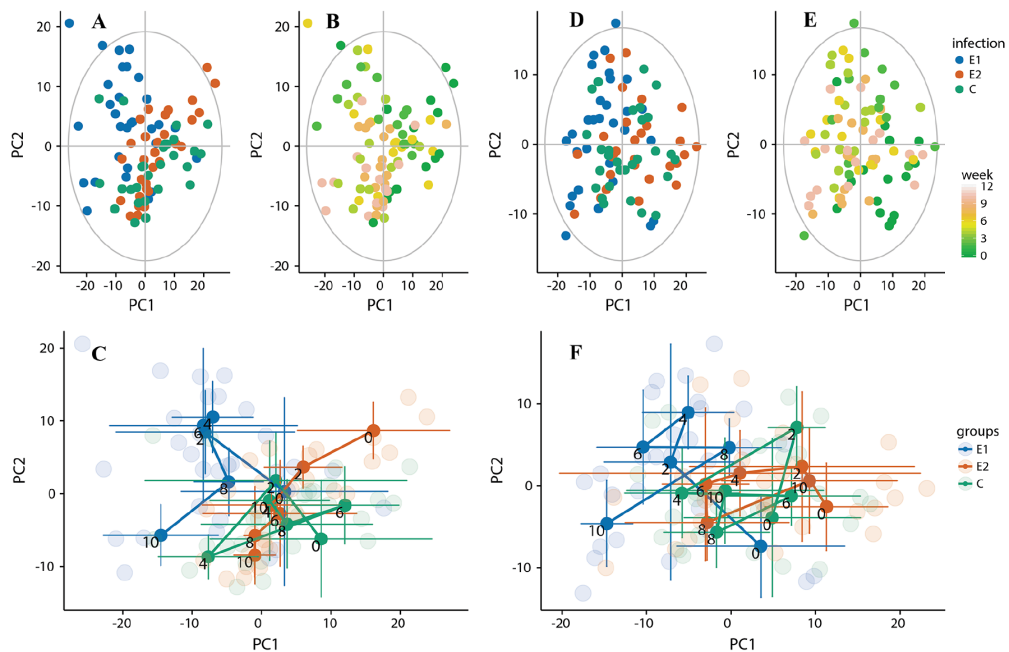


Figure 3. PCA models build for each gender group separately on a subset of the samples collected between 0 and 10 weeks; A, B – males, D, E – females. Geometric time trajectories: C – males, F – females

## ANOVA simultaneous component analysis (ASCA) modeling

To dissect the metabolic features related to the infection one needs a data analysis approach which enables simultaneous analysis of the experimental design and time. The choice is rather limited. One of the “stress tested” methods is ANOVA simultaneous component analysis or ASCA [22, 23]. In a nutshell, ASCA is a multivariate extension of the ANOVA and the strongest asset of the method is a possibility of modelling of the experimental designs with several factors. With regards to our study those factors are the time, intensity of the infection and gender. To avoid a complex interpretation of the multiple cross-factor interactions we applied ASCA separately to each gender subset. Figure 4 shows the results of the analysis for the first two components. The trends are looking similar, but not identical. In the male subset the infection specific time trends are present in the main component (43.5% variance). The time trends for non-infected and infected with 50 metacercaria animals have almost opposite behavior in the first component showing somewhat random pattern in the second one. In the female subset, the infection related trends are not presented in the first component, but well presented in the second one. The last one, however, covers only 24% of the variance, almost the half of what was seen in males.

## Selection and annotation of the variables

Figure 4 shows the time/infection specific trends and the systemic differences between the males and females in the reaction on the infection challenge. Yet, it gives no information on the nature of the biochemical entities involved in the observed phenomena. Thus, using a leverage as a measure of the variable importance we extracted a subset of the variables influencing the models shown at Figure 4. Table 1 summarizes the selected variables. Most of the variables can be annotated, but few complex regions (1.63-1.69, 1.71-1.74 and 2.46 ppm) simply cannot be assigned to a single metabolite. S1 Figure 3 shows the 24 week time trends of the every individual feature included in the table. The traces are plotted as the median values per experimental group, the original values are included in the plots in a form of transparency graphics. A visual inspection of the graphs shows that only few compounds demonstrate a consistent trend over the entire period. For most of them, the changes are evident only in the early weeks; some compounds (e.g. 2-amino adipic acid and nicotinuric

acid) shows a distinct trend for the group of the animals infected with 50 metacercaria.

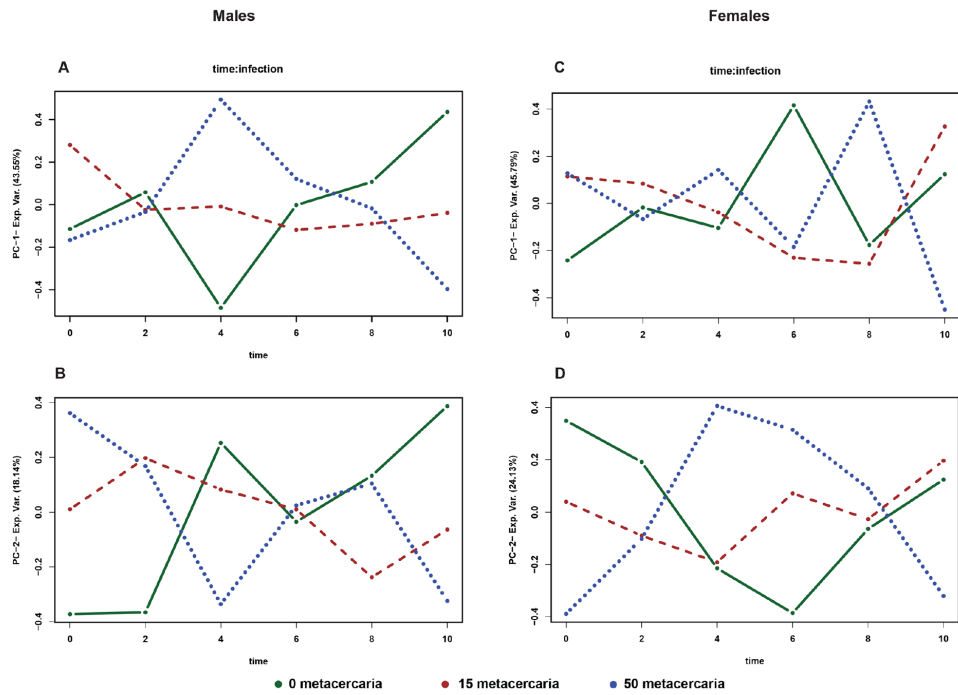


Figure 4. ANOVA simultaneous component analysis loading plot on metabolites satisfying the F test with  $p$ -value  $< 0.005$  on the interaction coefficients: Time  $\times$  infection. A, B – males, C,D – females

Table 1. The annotation of variables selected on basis of the ASCA modeling

	Bin	Compound ID*	Gender group **
1	0.7198	Bile acids	f, m
2	0.8924, 0.929	Pantothenic acid	m
3	1.0258	L-Isoleucine	m
4	1.6366, 1.6562, 1.6798, 1.6942	5-aminopentanoic acid & 2-amino adipic acid	f
5	1.7138, 1.7386, 1.7472	Leucine, Lysine	f
6	1.833	Crotonic acid	m
7	2.4634	3-(3-hydroxyphenyl) propionic acid, hydroxyferulic acid, glutamine & pyridoxine	f
8	3.4394	Taurine, glucose	m
9	3.6704, 7.4332	Phenylacetyl glycine*	m
10	3.7128	Threitol	m
11	3.7872	Guanidinoacetate	m
12	6.4	Urocanic acid	m
13	6.78	Homovanillic acid	f
14	6.8798	Tyrosine	f
15	6.8948	Trigonelline*	f
16	6.9596	Hydroferulic acid	f
17	7.029	5-Hydroxyindoleacetic acid	f
18	7.34, 7.3728, 7.4	Phenylacetate	m
19	8.6798	Nnicotinic acid	f
20	8.7	Nicotinuric acid	f, m
21	8.7282	Nicotinamide-N-oxide	f, m

\* compound(s) ID protons of which resonate within the selected bins

\*\* column shows whether bins were selected from model built on the male or female subgroup (m - males, f - females)

## Discussion

Here we present for the first time an exploratory analysis of the metabolic response to *O. felineus* infection in an animal model. Following an established routine of a descriptive study we started the analysis by exploring the main sources of the variance in the data. Using unsupervised projections methods namely PCA we have shown that neither infection status nor the time are representing the major sources of the variance in the data. In fact, the most noticeable trend in the data was related to the gender differences. At first glance, this observation may appear contradictory to the earlier publications on the animal models infected with other trematodes *S. japonicum* [13] and *S. mansoni* [12] as well as to our own report on a human study [15] where clear differences between infected and non-infected subjects were reported. Yet, to reveal the infection related differences authors of the above mentioned studies had to use the supervised modeling techniques and an unbiased assessment of the main sources of the variance in the data as a rule showed the influence of the physiological confounding factors such as for example age [15, 24]. A gender related bias in human studies was concealed by age factor due to the broad age range of the participants. In the animal studies the single gender models were used: the female animals for mice [12, 14, 25] and the males for hamsters [13, 26]. Since the animals included in our study were age matched, gender is now the strongest physiological cofounder [27]; consequently, the gender bias observed in the data should be expected. Of course, one should keep in mind the all the above-mentioned examples are taken from the publications on the metabolic effects of Schistosomiasis, no information on opisthorchiasis has been published yet.

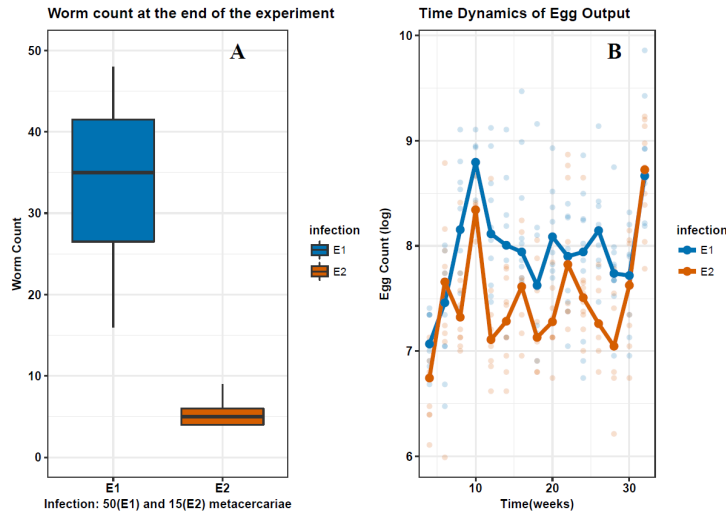
A gender related trend explains approximately 30% of variance in the data; therefore, further analysis was done of each sub-group separately. Both unsupervised multivariate modelling and ASCA-based analysis showed that a time related response to the infection unfolds differently in the males and females. Moreover, the Figure 4 which provides an overview of the main patterns associated with time-infection interaction clearly shows that in the male model the distinct trend

is present in the first principle component covering twice as much variance as the female model where the similar trend is visible only in the second component. Naturally, a discussion of the biological relevance of the observed effects is only possible if we know the identity of the metabolites influencing the models. A subset of the most influential entities is presented in the Table 1. In overall it appears as a more or less standard set of the metabolites which are regularly reported in the NMR-based metabolomics studies of urine. It also has a strong overlap with the metabolites reported in the publications on schistosomiasis mentioned above.

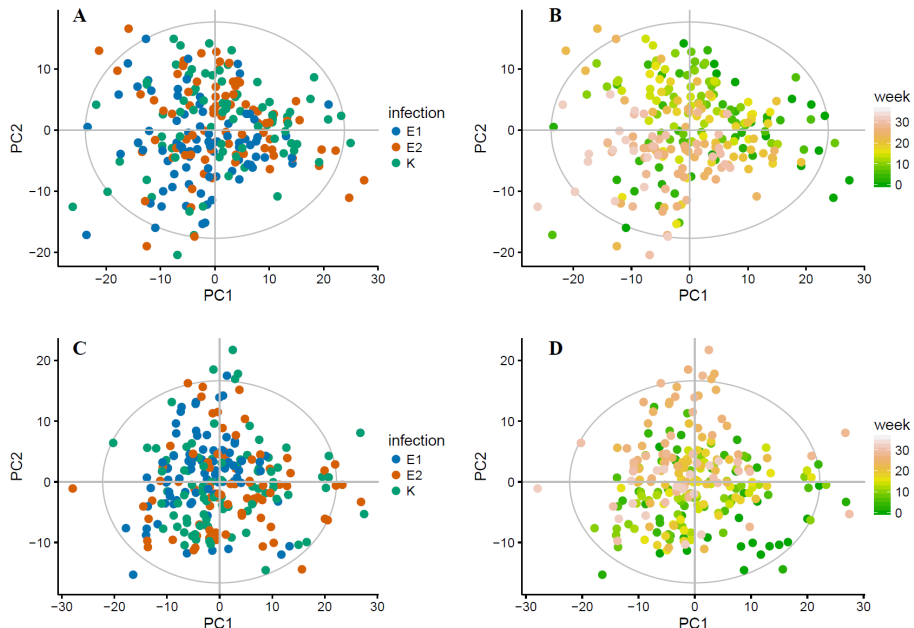
In the context of an acute opisthorchiasis, a state of the energetic stress, one particular trend, namely the bile acids becomes interesting. S1 Figure 3 shows that in the group of heavy infected animals urinary excretion of the bile acids is increasing starting from the beginning of the experiment reaching the peak at four weeks and going down after that point. A current physiological paradigm links an increased urinary excretion of the bile acids with the possible obstructions of the main duodenal path [28]. We can only speculate about the exact physiological mechanisms which leads to the increase of the bile acids secretion but the timing of the observed effect overlaps perfectly with a period when the parasite “settles down” in the host’s bile ducts. Of course, our method catches only a gross effect and cannot provide the exact annotation of the bile acids. From the literature we know that the bulk of the urinary bile acids are excreted as the sulphonated species [29] but to our best knowledge there is no published report on urinary bile acids profiles in opisthorchiasis. A similar transient pattern to the bile acids was also observed for the spectral areas where resonate lysine and a product of its catabolism 5-aminopentanoic acid are located. Despite an intriguing similarity, a “simple” interpretation where lysine would be considered as a breakdown product of the conjugated bile acids is difficult to accept; the lysine conjugates are rather unusual and were reported only as the minor products of lithocholic acid in the liver [30]. Another group of the metabolites which are related to the physiological control of the lipid metabolism consist of nicotinic acid and its metabolites nicotinuric acid and nicotinamide-N-oxide. The last two compounds show a transient decrease with a peak at four weeks. The effect is more pronounced in the male group. It is logical to assume that the host energy metabolism works in a stress mode during invasion of the parasite the bulk of nicotinic acid pool will be utilized

for NAD<sup>+</sup> production, in turn this can lead to a reduced production and urinary clearance of nicotinuric acid and nicotinamide-N-oxide. Another metabolite which nicely fits into a pattern of the stress mode of the energy metabolism is guanidinoacetate – a precursor of creatine [31]. Of course, an interpretation of the data from a point of view of the metabolic stress has a weakness. None of the described changes can be considered as specific for opisthorchiasis; all the changes reflect a general reaction of an organism to acute infection. Yet, an exploratory study, especially the one that enters a relatively uncharted territory should provide the leads and hypothesis for further investigation. To this end, we have fulfilled a purpose of the study. A logical follow up of our study appears to be an in-depth analysis of the urinary and fecal profiles of the bile acids using more sensitive techniques namely mass spectrometry. Already the last decades of twentieth century the analytical methods enabled detection and quantitation of several of the bile acids [32], the state-of-the-art technology offers a reliable analysis of more than hundred species [33]. Besides, the existing reports on alteration in the urinary bile acids profiles during the pathological conditions of liver [34] supports our hypothesis. Considering the other mentioned compounds and trends they fit a context of the energetic stress and metabolic redistribution of the bulk metabolites in the circulation, it remains to be seen however whether our findings can be translated to the human infection.

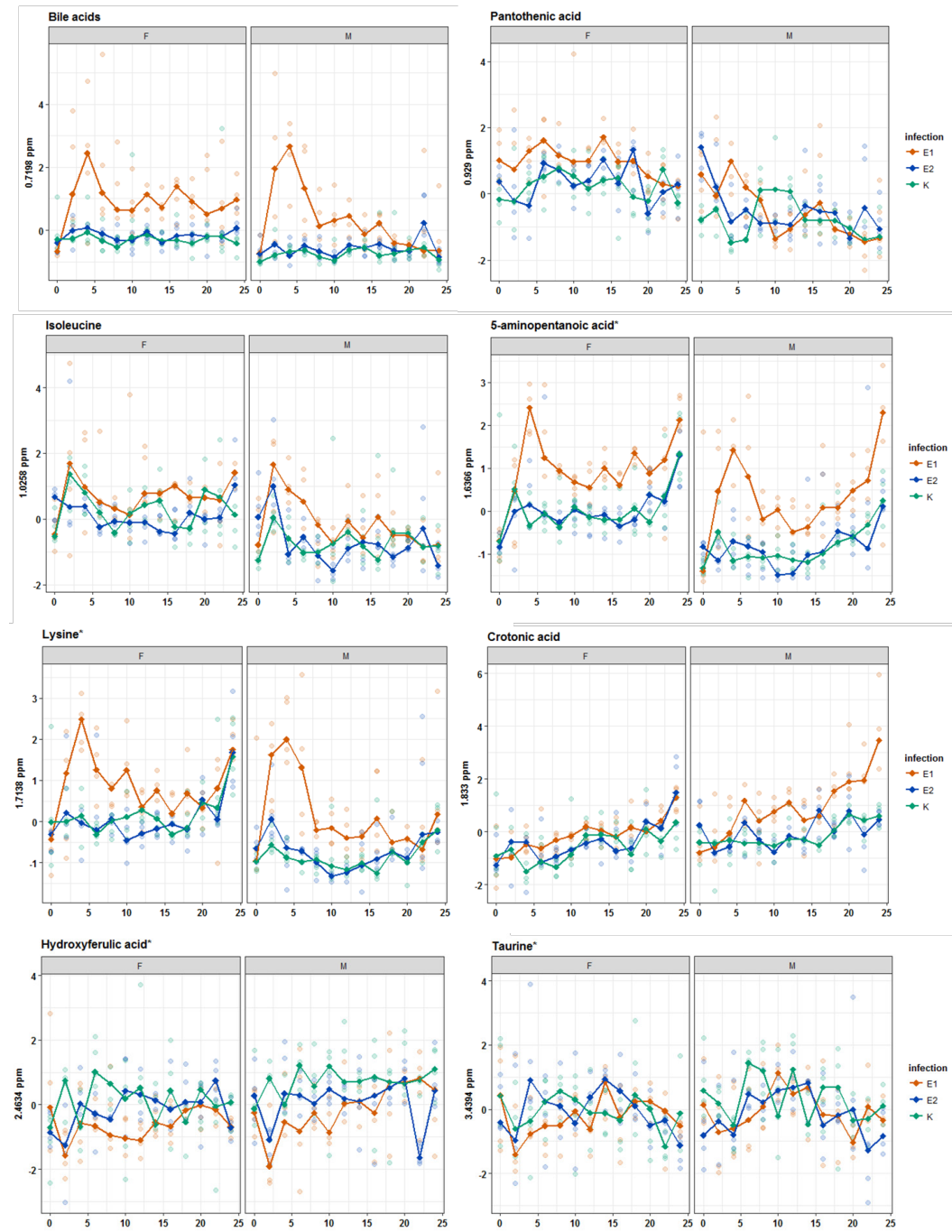
# Supplementary information



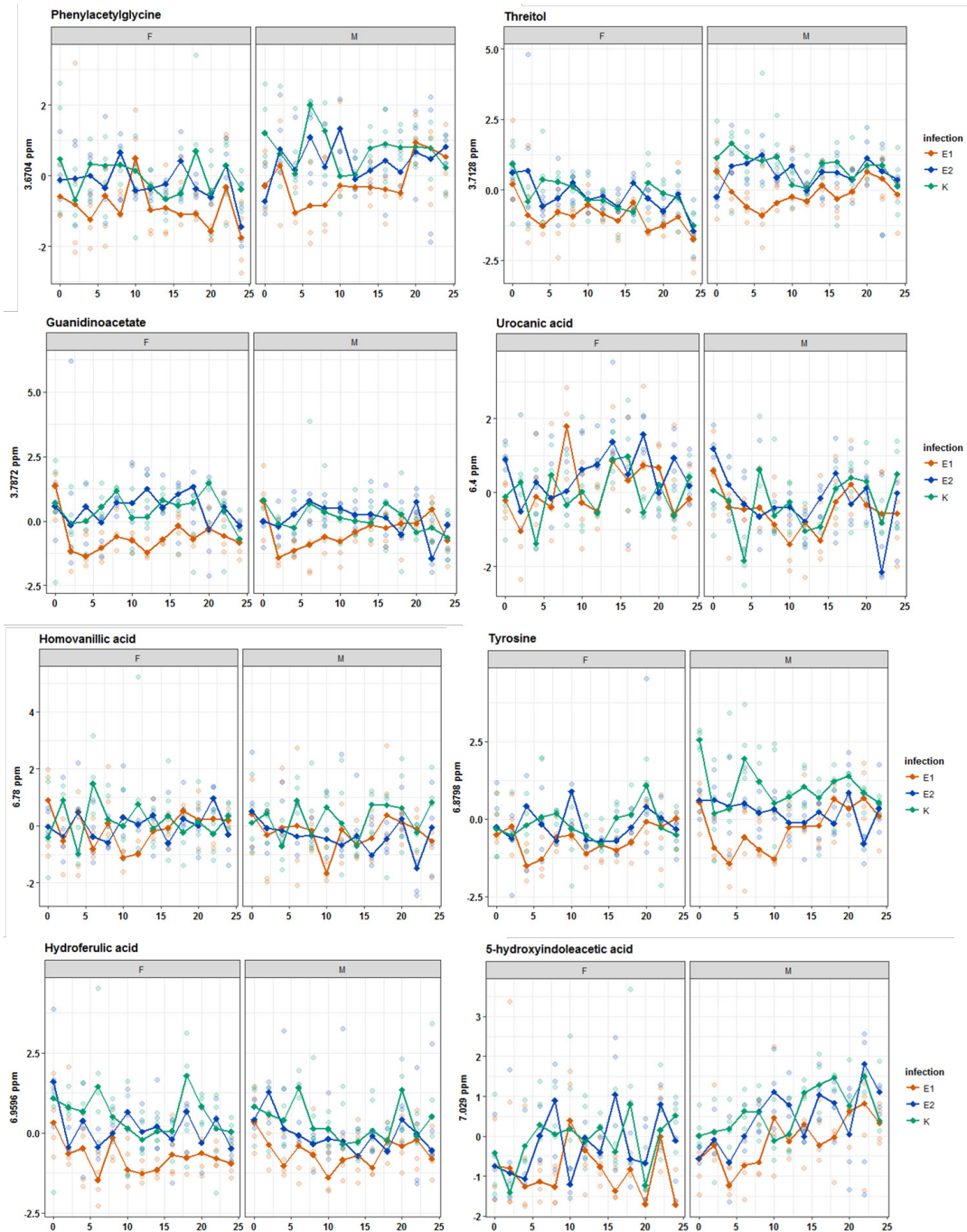
*S1 Figure. An overview of infection intensity. A. Worm count at the end of the experiment; B. Time dynamics of egg output.*



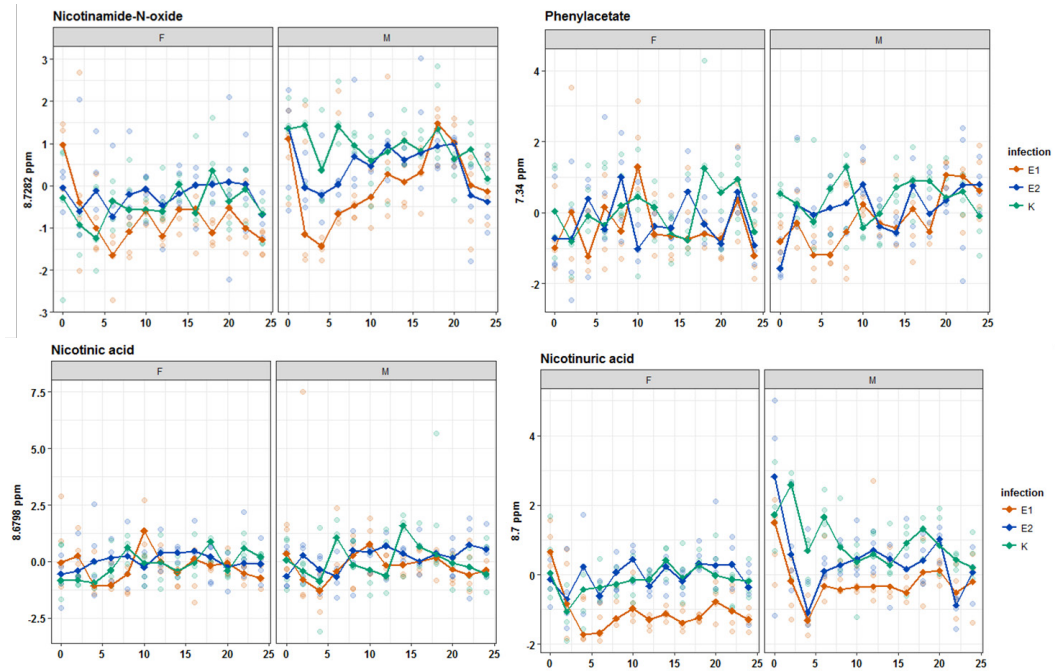
*S2 Figure. PCA models built separately for male (A, B) and female (C, D) animals*



S1 Figure. 3 Time trajectories for the metabolites included in the Table 1



*S1 Figure. 3 Time trajectories for the metabolites included in the Table 1 (continue)*



*S1 Figure. 3 Time trajectories for the metabolites included in the Table 1 (continue)*

## References

1. Petney TN, Andrews RH, Sajjuntha W, Wenz-Mucke A, Sithithaworn P: The zoonotic, fish-borne liver flukes *Clonorchis sinensis*, *Opisthorchis felineus* and *Opisthorchis viverrini*. International journal for parasitology 2013, 43(12-13):1031-1046.
2. Fedorova OS, Kovshirina YV, Kovshirina AE, Fedotova MM, Deev IA, Petrovskiy FI, Filimonov AV, Dmitrieva AI, Kudyakov LA, Saltykova IV et al: *Opisthorchis felineus* infection and cholangiocarcinoma in the Russian Federation: A review of medical statistics. Parasitol Int 2016.
3. Sripa B, Bethony JM, Sithithaworn P, Kaewkes S, Mairiang E, Loukas A, Mullen J, Laha T, Hotez PJ, Brindley PJ: Opisthorchiasis and *Opisthorchis*-associated cholangiocarcinoma in Thailand and Laos. Acta tropica 2011, 120:S158-S168.
4. Elkins DB, Mairiang E, Sithithaworn P, Mairiang P, Chaiyakum J, Chamadol N, Loapabiboon V, Haswell-Elkins MR: Cross-sectional patterns of hepatobiliary abnormalities and possible precursor conditions of cholangiocarcinoma associated with *Opisthorchis viverrini* infection in humans. Am J Trop Med Hyg 1996, 55(3):295-301.
5. Sriamporn S, Pisani P, Pipitgool V, Suwanrungruang K, Kamsa-ard S, Parkin DM: Prevalence of *Opisthorchis viverrini* infection and incidence of cholangiocarcinoma in Khon Kaen, Northeast Thailand. Tropical medicine & international health : TM & IH 2004, 9(5):588-594.
6. Sripa B, Kaewkes S, Sithithaworn P, Mairiang E, Laha T, Smout M, Pairojkul C, Bhudhisawasdi V, Tesana S, Thinkamrop B et al: Liver fluke induces cholangiocarcinoma. Plos Med 2007, 4(7):1148-1155.
7. Upatham ES, Viyanant V, Kurathong S, Rojborwonwitaya J, Brockelman WY, Ardsungnoen S, Lee P, Vajrathira S: Relationship between prevalence and intensity of *Opisthorchis viverrini* infection, and clinical symptoms and signs in a rural community in north-east Thailand. Bull World Health Organ 1984,

62(3):451-461.

8. Mairiang E, Elkins DB, Mairiang P, Chaiyakum J, Chamadol N, Loapaiboon V, Posri S, Sithithaworn P, Haswell-Elkins M: Relationship between intensity of *Opisthorchis viverrini* infection and hepatobiliary disease detected by ultrasonography. *J Gastroenterol Hepatol* 1992, 7(1):17-21.

9. Sripa B, Kaewkes S: Relationship between parasite-specific antibody responses and intensity of *Opisthorchis viverrini* infection in hamsters. *Parasite Immunology* 2000, 22(3):139-145.

10. Khoontawad J, Pairojku C, Rucksaken R, Pinlaor P, Wongkham C, Yongvanit P, Pugkhem A, Jones A, Plieskatt J, Potriquet J et al: Differential protein expression marks the transition from infection with *Opisthorchis viverrini* to cholangiocarcinoma. *Molecular & cellular proteomics* : MCP 2017.

11. Wang YL, Holmes E, Nicholson JK, Cloarec O, Chollet J, Tanner M, Singer BH, Utzinger J: Metabonomic investigations in mice infected with *Schistosoma mansoni*: An approach for biomarker identification. *Proceedings of the National Academy of Sciences of the United States of America* 2004, 101(34):12676-12681.

12. Wang YL, Utzinger J, Xiao SH, Xue J, Nicholson JK, Tanner M, Singer BH, Holmes E: System level metabolic effects of a *Schistosoma japonicum* infection in the Syrian hamster. *Molecular and biochemical parasitology* 2006, 146(1):1-9.

13. Wu JF, Xu WX, Ming ZP, Dong HF, Tang HR, Wang YL: Metabolic Changes Reveal the Development of Schistosomiasis in Mice. *Plos Neglected Tropical Diseases* 2010, 4(8).

14. Balog CIA, Meissner A, Goraler S, Bladergroen MR, Vennervald BJ, Mayboroda OA, Deelder AM: Metabonomic investigation of human *Schistosoma mansoni* infection. *Molecular Biosystems* 2011, 7(5):1473-1480.

15. Balog C, Alexandrov T, Derkx R, Hensbergen P, van Dam G, Tukahebwa E, Kabatereine N, Thiele H, Vennervald B, Mayboroda O et al: The feasibility of MS and advanced data processing for monitoring *Schistosoma mansoni* infection. *Proteomics Clinical Applications* 2010, 4(5):499-510.

16. Nicholson G, Rantalainen M, Maher AD, Li JV, Malmordin D, Ahmadi KR, Faber JH, Hallgrimsdottir IB, Barrett A, Toft H et al: Human metabol-

ic profiles are stably controlled by genetic and environmental variation. *Mol Syst Biol* 2011, 7.

17. Kumar A, Ernst RR, Wuthrich K: A Two-Dimensional Nuclear Overhauser Enhancement (2d Noe) Experiment for the Elucidation of Complete Proton-Proton Cross-Relaxation Networks in Biological Macromolecules. *Biochem Biophys Res Co* 1980, 95(1):1-6.

18. De Meyer T, Sinnaeve D, Van Gasse B, Tsimporkova E, Rietzschel ER, De Buyzere ML, Gillebert TC, Bekaert S, Martins JC, Van Criekinge W: NMR-based characterization of metabolic alterations in hypertension using an adaptive, intelligent binning algorithm. *Analytical chemistry* 2008, 80(10):3783-3790.

19. Dieterle F, Ross A, Schlotterbeck G, Senn H: Probabilistic quotient normalization as robust method to account for dilution of complex biological mixtures. Application in H-1 NMR metabonomics. *Analytical chemistry* 2006, 78(13):4281-4290.

20. Keun HC, Ebbels TMD, Bolland ME, Beckonert O, Antti H, Holmes E, Lindon JC, Nicholson JK: Geometric trajectory analysis of metabolic responses to toxicity can define treatment specific profiles. *Chem Res Toxicol* 2004, 17(5):579-587.

21. Smilde AK, Jansen JJ, Hoefsloot HCJ, Lamers RJAN, van der Greef J, Timmerman ME: ANOVA-simultaneous component analysis (ASCA): a new tool for analyzing designed metabolomics data. *Bioinformatics* 2005, 21(13):3043-3048.

22. Jansen JJ, Hoefsloot HCJ, van der Greef J, Timmerman ME, Westerhuis JA, Smilde AK: ASCA: analysis of multivariate data obtained from an experimental design. *J Chemometr* 2005, 19(9):469-481.

23. Singer BH, Utzinger J, Ryff CD, Wang Y, Holmes E: Exploiting the Potential of Metabonomics in Large Population Studies: Three Venues. In: *The Handbook of Metabonomics and Metabolomics*. edn. Edited by Holmes E, Nicholson JK. Oxford: Elsevier B.V.; 2007: 289-325.

24. Li JV, Holmes E, Saric J, Keiser J, Dirnhofer S, Utzinger J, Wang YL: Metabolic profiling of a *Schistosoma mansoni* infection in mouse tissues using magic angle spinning-nuclear magnetic resonance spectroscopy. *International journal for parasitology* 2009, 39(5):547-558.

25. Wu JF, Holmes E, Xue J, Xiao SH, Singer BH, Tang HR, Utzinger J, Wang YL: Metabol-

ic alterations in the hamster co-infected with *Schistosoma japonicum* and *Necator americanus*. International journal for parasitology 2010, 40(6):695-703.

26. Bolland ME, Stanley EG, Lindon JC, Nicholson JK, Holmes E: NMR-based metabonomic approaches for evaluating physiological influences on biofluid composition. *Nmr Biomed* 2005, 18(3):143-162.

27. Corbett CL, Bartholomew TC, Billing BH, Summerfield JA: Urinary-Excretion of Bile-Acids in Cholestasis - Evidence for Renal Tubular Secretion in Man. *Clin Sci* 1981, 61(6):773-780.

28. Alnouti Y: Bile Acid Sulfation: A Pathway of Bile Acid Elimination and Detoxification. *Toxicol Sci* 2009, 108(2):225-246.

29. Nair PP, Mendeloff AI, Vocci M, Bankoski J, Gorelik M, Herman G, Plapinger R: Lithocholic Acid in Human Liver - Identification of Epsilon-Lithocholyl Lysine in Tissue Protein. *Lipids* 1977, 12(11):922-929.

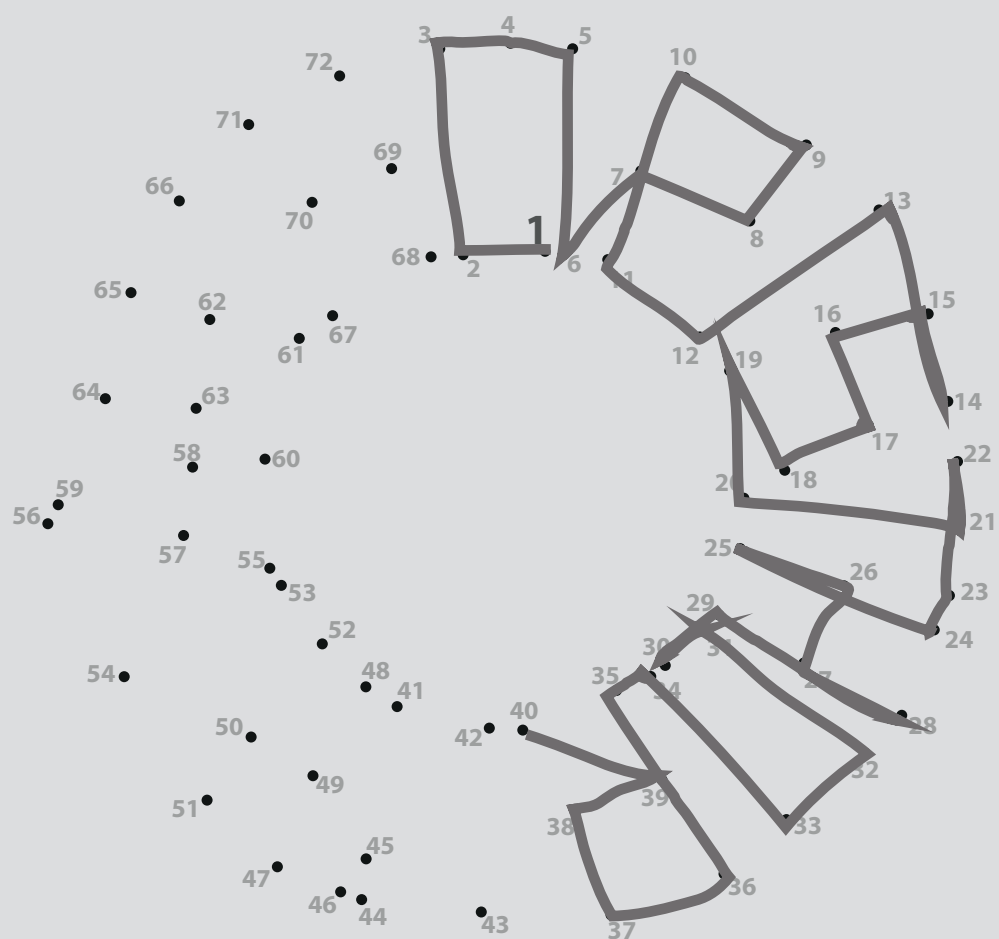
30. Wyss M, Kaddurah-Daouk R: Creatine and creatinine metabolism. *Physiological reviews* 2000, 80(3):1107-1213.

31. Alme B, Bremmelgaard A, Sjovall J, Thomassen P: Analysis of Metabolic Profiles of Bile-Acids in Urine Using a Lipophilic Anion-Exchanger and Computerized Gas-Liquid Chromatography Mass Spectrometry. *Journal of lipid research* 1977, 18(3):339-362.

32. Sarafian MH, Lewis MR, Pechlivanis A, Ralphs S, McPhail MJW, Patel VC, Dumas ME, Holmes E, Nicholson JK: Bile Acid Profiling and Quantification in Biofluids Using Ultra-Performance Liquid Chromatography Tandem Mass Spectrometry. *Analytical chemistry* 2015, 87(19):9662-9670.

33. Bremmelgaard A, Sjovall J: Bile-Acid Profiles in Urine of Patients with Liver-Diseases. *Eur J Clin Invest* 1979, 9(5):341-348.





# 4

## Plasma metabolomics of the time resolved response to *Opisthorchis felineus* infection in an animal model

D. Kokova  
A. Verhoeven  
E.A. Perina  
V.V. Ivanov

E.M. Knyazeva  
I.V. Saltykova  
O.A. Mayboroda

PLoS Negl Trop Dis 14(1): e0008015 (2020)  
<https://doi.org/10.1371/journal.pntd.0008015>

## Abstract

### Background

Opisthorchiasis is a hepatobiliary disease caused by flukes of the trematode family *Opisthorchiidae*. Opisthorchiasis can lead to severe hepatobiliary morbidity and is classified as a carcinogenic agent. Here we investigate the time-resolved metabolic response to *Opisthorchis felineus* infection in an animal model.

### Methodology

Thirty golden hamsters were divided in three groups: severe infection (50 metacercariae/hamster), mild infection (15 metacercariae/hamster) and uninfected (vehicle-PBS) groups. Each group consisted of equal number of male and female animals. Plasma samples were collected one day before the infection and then every two weeks up to week 22 after infection. The samples were subjected to <sup>1</sup>H Nuclear Magnetic Resonance (NMR) spectroscopy and multivariate statistical modelling.

### Principal findings

The time-resolved study of the metabolic response to *Opisthorchis* infection in plasma in the main lines agrees with our previous report on urine data. The response reaches its peak around the 4<sup>th</sup> week of infection and stabilizes after the 10<sup>th</sup> week. Yet, unlike the urinary data there is no strong effect of the gender in the data and the intensity of infection is presented in the first two principal components of the PCA model. The main trends of the metabolic response to the infection in blood plasma are the transient depletion of essential amino acids and an increase in lipoprotein and cholesterol concentrations.

### Conclusions

The time resolved metabolic signature of *Opisthorchis* infection in the hamster's plasma shows a coherent shift in amino acids and lipid metabolism. Our work provides insight into the metabolic basis of the host response on the helminth infection.

## Author summary

Opisthorchiasis is a parasitic infection caused by liver flukes of the *Opisthorchiidae* family. The liver fluke infection triggers development of hepatobiliary pathologies such as chronic forms of cholecystitis, cholangitis, pancreatitis, and cholelithiasis and increases the risk of intrahepatic cholangiocarcinoma. This manuscript is the second part of our outgoing project dedicated to a comprehensive description of the metabolic response to opisthorchiasis (more specifically *Opisthorchis felineus*) in an animal model. We show that the metabolic response in blood plasma is unfolding according to the same scenario as in urine, reaching its peak at the 4<sup>th</sup> week and stabilizing after the 10<sup>th</sup> week post-infection. Yet, unlike the response described in urine, the observed metabolic response in plasma is less gender specific. Moreover, the biochemical basis of the detected response in blood plasma is restricted to the remodeling of the lipid metabolism and the transient depletion of essential amino acids. Together with our first manuscript this report forms the first systematic description of the metabolic response on opisthorchiasis in an animal model using two easily accessible biofluids. Thus, this contribution provides novel results and fills an information gap still existing in the analytically driven characterization of the “Siberian liver fluke”, *Opisthorchis felineus*.

## Introduction

Opisthorchiasis is a hepatobiliary disease caused by flukes of the trematode family *Opisthorchiidae*: *Opisthorchis felineus* (*O. felineus*), *Opisthorchis viverrini* (*O. viverrini*) and *Clonorchis sinensis* (*C. sinensis*). Together they affect more than 45 million people and 600–750 million people are at risk in the endemic regions of Eurasia [1]. The clinical manifestations of acute opisthorchiasis are non-specific and its chronic stages are often asymptomatic [2, 3]. Yet, not only does the chronic opisthorchiasis leads to severe hepatobiliary morbidities [2, 4], but also *O. viverrini* and *C. sinensis* were classified as carcinogenic agents by the International Agency for Research on Cancer (IARC) [5]. Consequently, the application of modern analytical technologies to the study of the parasite and its interaction with the host are becoming an essential element in the search for the mechanisms of the hepatobiliary morbidity.

Over the last three decades each of four key levels of biological regulations, namely genome, transcriptome, proteome and metabolome were strengthened by the corresponding “omics” disciplines. To date, a draft of the genome of the *O. viverrini* has been published [6, 7], the transcriptome data have been available for some time [8] and despite a rather critical assessment of the proteome data [9] there are 160 tegumental and 43 excreted proteins described [10]. The data on metabolomics of the *Opisthorchiidae* and host responses to the infection are still very limited. For an overview of the current status, advantages and limitations of metabolomics in helminthology we refer to our recent critical review of the topic [11]. Here we only would like to mention two factors that contribute to a slower growth of available helminth related metabolomics data: the chemical diversity of the metabolites leading to an increased complexity of the analytical workflows and the difficulties with a straight-forward mechanistic interpretation of the data (especially data on body fluids). Yet, as a post-genomic discipline, metabolomics bids a strong alternative to conventional biochemical experimentation by combining advanced analytical techniques capable of simultaneously detecting multiple compounds with multivariate modeling and/or machine learning al-

gorithms. This way the physiological status of an organism can be represented as a combination of metabolites concentrations/abundances in biofluids.

The present study is the second part of our work on the metabolomics of the host response to the *O. felineus* infection. The “Siberian liver fluke”, *O. felineus* [12] forms a health risk for a population that is similar in size to the population in the endemic region of *O. viverrini* [13]. It is also known for its cancerogenic properties but remains far less studied. Of the four levels of biological regulation (genome, transcriptome, proteome, and metabolome) only a single report on the transcriptome of the different life stages of the parasite has been published so far [14].

To fill the existing data gap, we concentrate on a comprehensive description of the time-resolved response of the host on the *O. felineus* infection using metabolomics. The first part was dedicated to the metabolic changes detected in the urine samples [15], the current work covers the infection-dependent changes in the blood plasma samples. The study was designed as a longitudinal study with two degrees of the infection intensity. Both sets of samples (urine and plasma) were collected from the same animal models.

## Methods

### Ethics statement

All procedures with animals were carried out according to the recommendations of the national guidelines for animal caring: 12.08.1977 N 755 "On measures to further improve the organizational forms of work using experimental animals" and approved by the Siberian State Medical University (license number 3296 issued on 29.04.2013).

### Experimental opisthorchiasis model

The study design was described in detail the previously published urinary NMR (Nuclear Magnetic Resonance) based metabolomics study of experimental opisthorchiasis in the golden hamster (*Mesocricetus auratus*). Briefly, hamsters were divided in 3 groups: severe infection (50 metacercariae/hamster), mild infection (15 metacercariae/hamster) and uninfected (vehicle-PBS) groups. Each group consisted of 10 animals - five males and five females. The hamsters were approximately five weeks old at the time of infection.

The blood samples were collected from anesthetized hamsters one day before infection and then every two weeks, specifically at the weeks 2, 4, 6, 8, 10, 12, 14, 16, 18, 20 and 22 after infection according to the previously described protocol [16]. In brief, at each time point the hamsters were lightly restrained by gentle handling, the gingival vein was pierced with a 26-gauge needle, and blood was collected into test tubes pre-coated with sodium heparin. The hamsters were observed after each blood collection. The total volume of collected blood was selected to represent the maximal blood volume that can be withdrawn in accordance with ethical recommendations [17].

After collection into individually labelled Eppendorf tubes, all samples were transferred to a freezer (-80°C) for long term storage. The worm burden and egg output were described in details in the first part of the exploratory metabolomics of the experimental opisthorchiasis in a golden hamster [15].

### Eggs and worms counts

The method of calculation of the number of eggs per gram of

feces and the estimation of the worm burden were described in the urinary NMR-based metabolomics study of experimental opisthorchiasis in the golden hamster (*Mesocricetus auratus*) [15].

### **Blood plasma sample preparation and NMR data acquisition**

All chemicals used for the buffer solution were purchased from Sigma-Aldrich except for the  ${}^2\text{H}_2\text{O}$  which was purchased from Cortecnet and the 3-(trimethylsilyl)propionic-2,2,3,3-d4acid sodium salt (TSP) which was obtained from Cambridge Isotope Laboratories Inc. 96-well plates and NMR tubes were purchased from Bruker Biospin Ltd. (Germany).

The 33  $\mu\text{l}$  of each plasma sample were mixed with 77  $\mu\text{l}$  milli-Q water, then 110  $\mu\text{l}$  buffer solution in  $\text{H}_2\text{O}/\text{D}_2\text{O}$  (80/20) with a pH of 7.4 containing 6.15 mM  $\text{NaN}_3$  and 4.64 mM TSP were added using a Gilson 215 liquid handler in combination with a Bruker SampleTrack system. Finally, 190  $\mu\text{l}$  of each plasma-buffer mixture were transferred to 3 mm SampleJet NMR tubes and placed in refrigerated racks ( $6^\circ\text{C}$ ) in a Bruker SampleJet system until the NMR measurement.

NMR data were recorded using a Bruker 14.1T AVANCE II spectrometer ( ${}^1\text{H}$  Larmor frequency 600 MHz), equipped with a triple resonance inverse cryoprobe with Z-gradient system and automatic tuning and matching. All NMR experiments were performed as described elsewhere [18] with some minor modifications: for the 1D nuclear Overhauser enhancement Spectroscopy (NOESY) and 1D Carr-Purcell-Meiboom-Gill pulse sequence (CPMG) experiments were collected with 32 scans; J-resolved spectra (JRES) were recorded with a total 2 scans for each increment in the indirect dimension. In addition, to achieve more information about the lipoprotein profile, a 1D diffusion-edited pulse sequence with diffusion time of 120 ms was performed [19]. After applying 4 dummy scans, a total of 98,304 data points covering a spectral width of 18,029 Hz and an exponential window function was applied with a line broadening factor of 1.0 Hz before Fourier transformation were accumulated using 16 scans for each sample.

### **Spectral data processing and data analysis**

Pre-processing of NMR data was performed in the KIMBLE workflow [20]. All  ${}^1\text{H}$  1D NMR spectra were baseline-corrected using a polynomial fit of degree 5.

For exploratory analysis, the 1D NOESY spectra were binned from 0.5 to 9.5 ppm using adaptive intelligent binning [21]. Initial bin width was set to 0.02 ppm and final variable bins sizes were calculated based on the peaks edges in the spectra by using a lowest standard deviation criterion. The spectral region that is dominated by the residual water signal (4.35–5.0 ppm) was excluded from the data. The final data consisted of 469 bins of variable size  $\times$  343 observations (samples), which were normalized by PQN normalization to correct for dilution differences from sample to sample [22].

Principal component analysis (PCA) was performed on the univariate scaled NOESY binned dataset in the R statistical environment (<http://www.r-project.org/>, R versions 3.4.4), “Rcpm”, “pcaMethods” packages were used. The visualizations were made using “ggplot2”, “cowplot”, “caret” and “gridExtra” packages.

For supervised statistical modelling ANOVA-simultaneous component analysis (ASCA) was chosen. This method is based on the assumption that every variable is a function of all factors included in a study and uses analysis of variance for the analysis of the individual experiment factors and their interactions [23]. ASCA is specifically suited for time-resolved multigroup, multisubject and multivariate data. However, it is very sensitive to unbalanced design. 4.7% of all samples were lost during NMR acquisition because the spectra did not satisfy the quality inspection. Unfortunately, this resulted in unbalanced data. In order to apply ASCA to the data, imputation was performed. The nonparametric missing value imputation was performed using the Random Forest approach in the “missForest” package in the R environment [24].

ASCA was performed on the centered imputed dataset of NOESY experiment in Matlab R2016a (The MathWorks) [23]. The model quality was estimated by running a permutation test (number of permutations = 1000).

For selected small metabolites a quantification approach was applied which combines the superior signal-to-noise ratio of the CPMG pulse sequence with the superior resolution of the 2D JRES experiment [18, 20].

The multivariate analysis of variance was performed in R statistical environment (<http://www.r-project.org/>, R versions 3.4.4) using standard commands.

Diffusion-edited spectra were used for definition of the lipopro-

tein profile of plasma samples. For this aim, selected regions of the spectra were integrated after local baseline correction.

### **Identification of the metabolites**

Identification of metabolites was performed by exhausting search of the total 1D and 2D JRES data using the proprietary Bbiforecode (Bruker Biospin Ltd.) database. Lipoproteins were identified using information performed R. Mallol at el [25].

## Results

### The exploratory analysis of plasma metabolic profiles

The worm burden and egg output were described in detail in the first part of the exploratory metabolomics of opisthorchiasis in the golden hamster [15]. To get an overview of the main sources of variance in the data we used principal component analysis (PCA). Figure 1 shows a PCA model built on the unit variance-scaled 1D NOESY data from all time points. The ten principal components (PCs) of the model cover 80% of the variance, with the first two components explaining more than 60% of the total variance. Contrary to our results reported for the urine samples, a clear trend related to intensity of the infection is visible already in the first two PCs (Figure 1A). No strong gender effect is observed (Figure 1B) and the influence of the sampling time appears surprisingly weak (Figure 1C). However, a geometric trajectory visualization approach [16] reveals the group-specific trends (Figure 2). The samples of both infection intensity groups and the controls collected at time point 0 (1 day before infection) are located close to each other. At the second and fourth weeks of infection, the difference between the experimental groups becomes maximal before gradually reducing towards the tenth week (Figure 2). From the tenth to the twenty second week the trajectories are somewhat random and remain within their own clusters.

### ANOVA-simultaneous component analysis

One of the main questions of our study is finding the metabolic features describing infection unfolding in time. There is only a limited number of statistical approaches for modeling a time-resolved metabolomics study design with several experimental groups [26]. One of them is ASCA (ANOVA-simultaneous component analysis)-a method based on the assumption that every variable is a function of all factors included in a study and uses analysis of variance for the analysis of the individual experiment factors and their interactions [23]. Thus, ASCA modelling estimates the contribution of every factor to the data variability. The ASCA analysis of our dataset shows that infection explains 33% of the variance in the data and as such is the most

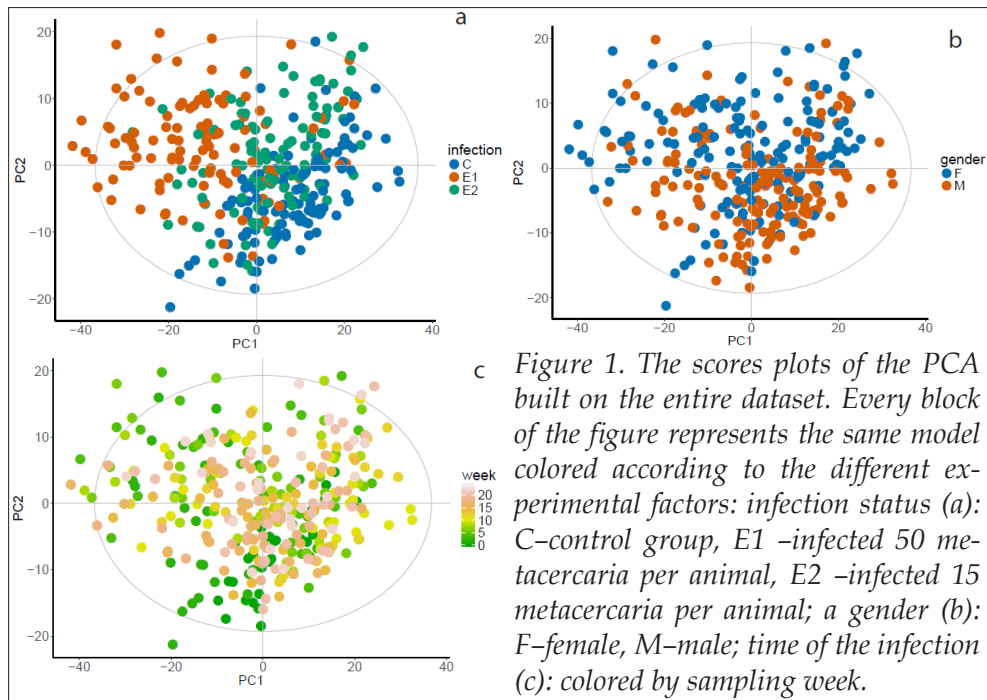


Figure 2. The geometric trajectory visualization of the PCA scores. Control group (blue); infected animals with 15 metacercaria per animal (orange); infected animals with 50 metacercaria per animal (green).

dominant factor, followed by time (18%); the interaction between the experimental factors (time and infection) explains 12% of the variance in the data. All factors and their interactions were significantly altered: the p-values for the infection and the time both were 0.001, while the p-value for them interaction was 0.0140.

Figure 3 shows the score plots for a time\*infection interaction submodel. The two components of the model explain 72% of the variance. The first component (56% of the variance) shows that the strongest metabolic changes are observed up to the tenth week (Figure 3A); in the second component (16%), the clear difference between the groups is seen only at the second week of infection (Figure 3B). Thus, the strongest metabolic response to the *O. felineus* infection is observed from 2 to 10 weeks post-infection, which is in agreement with the results of the study on urinary metabolomics of the *O. felineus* infected animals [15].

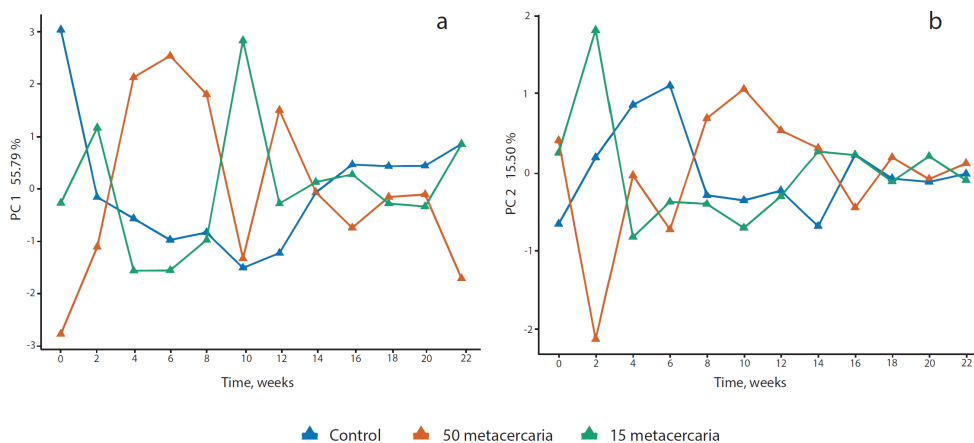


Figure 3. Scores plots of the first (a) and second (b) components of the ASCA model for the "Infection\*time" interaction.

S1 Figure gives a visual summary of the relative contribution of the individual variables to the model explaining both infection and the time factors of the experiment. The variable importance is proportional to the value of its loading (Y axis); this way we can select a subset of influential variables and annotate them. Table 1 summarizes the annotated metabolites.

Table 1. Annotated variables selected on the basis of the ASCA model loadings

$\delta$ , ppm	Annotation	Principal component
0.64-0.68	Cholesterol	PC2
0.82-0.88	Lipids $\text{CH}_3$	PC1, PC2
0.96-1.00	Valine, Leucine, Isoleucine	PC2
1.08-1.12	Unknown	PC2
1.22-1.36	Lipids $\text{CH}_2$ , Lactate	PC1, PC2
1.30-1.36	Lactate	PC2
1.94-2.02	Lipids $(\text{CH}_2)_n\text{-CH}_2\text{-CH=}$	PC1, PC2
2.20-2.24	Lipids $\text{CH}_2\text{-CH}_2\text{-COOC}$	PC2
3.182-3.237	Lipids $\text{-N}(\text{CH}_3)_3$	PC1, PC2
4.081-4.117	Lactate	PC2
4.24-4.28	Threonine	PC2
5.26-5.32	Lipids $\text{CH=CH}$	PC1

### Time trajectories of the significant metabolites

One of the most frequently used strategies of NMR data pre-processing is data reduction by binning, or more recently, adaptive binning. This approach was used for the current study as well. A bin is a narrow spectral region containing signals of zero, one, or only a few metabolites. On the other hand, a single metabolite can generate multiple signals or exceptionally broad signals that contribute intensity to multiple bins. Lipoproteins are an example of a plasma component with wide signals that cover several neighboring bins (see Table 1). Therefore, to obtain an additional validation of our findings and make practical use of the quantitative nature of the NMR we quantified the metabolites reported in Table 1. Amino acids and lactate were quantified using the 1D Carr-Purcell-Meiboom-Gill pulse sequence (CPMG) and the 2D J-resolved spectra (JRES) data [20]. For the lipoproteins and lipids, the corresponding regions of the diffusion-edited spectra were integrated. The 1D diffusion-edited experiment was developed especially for analysis of macromolecular assemblies without interference of the small molecules [25]. The integration of the relevant regions in the diffusion-edited experiment is probably the best possible alternative in absence of a true lipoprotein quantification model for hamster blood plasma. Figure 4 shows the time trajectories for the individual

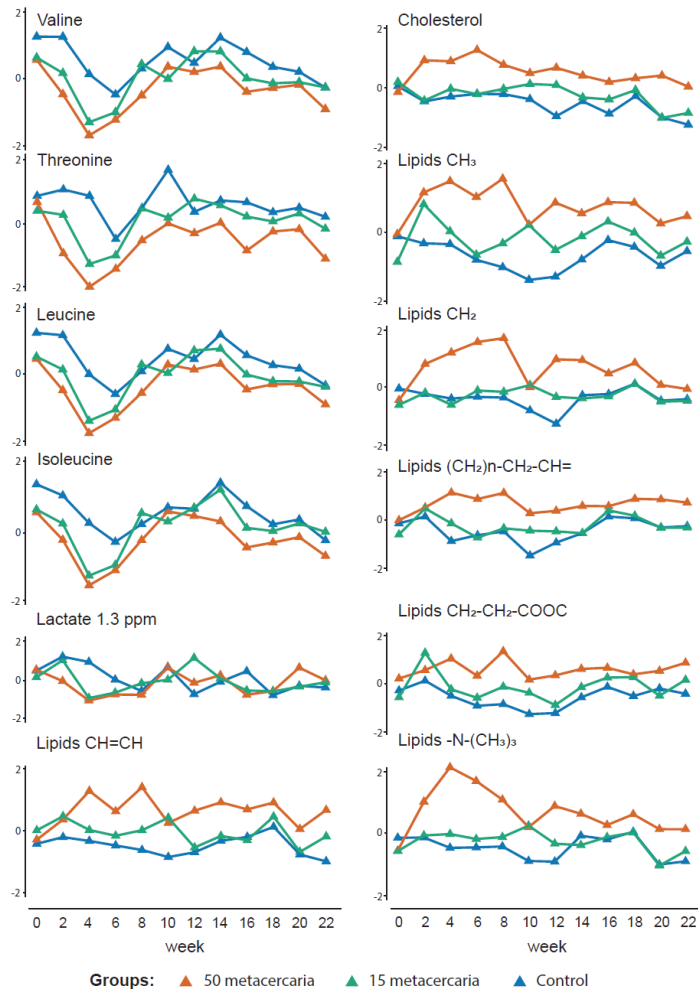


Figure 4. Spaghetti plots of the quantified metabolites selected on the basis of the two first PCs of the ASCA model, using the "infection\*time" interaction. Blue-control group; orange- 50 metacercaria; green -15 metacercaria.

metabolites. In general, the trends are in agreement with the results of the ASCA time\*infection submodel. To support the visual presentation with a statistical description we applied the multivariate analysis of variance (MANOVA) method to our quantitative data. The results summarized in Table 2 show that both the MANOVA model and its individual predictors (with an expedition of an unknown metabolite) indicated a statistically significant trend for time\*infection interaction term.

Table 2. Results of the MANOVA analysis performed on the quantified metabolites

MANOVA model metrics		Wilks $\lambda$	F	Pr(>F)
		0.474	6.640	2.2*10 <sup>-16</sup>
<b>Individual terms for interaction infection*time</b>				
ID	Sum sq	Mean sq	F	Pr(>F)
Cholesterol	103.97	34.66	49.23	2.2*10 <sup>-16</sup>
Lipids CH <sub>3</sub>	103.38	34.46	48.83	2.2*10 <sup>-16</sup>
Valine	20.45	6.82	7.18	1.09*10 <sup>-4</sup>
Leucine	20.34	6.78	7.14	1.15*10 <sup>-4</sup>
Isoleucine	20.17	6.72	7.08	1.26*10 <sup>-4</sup>
Unknown	7.71	2.57	2.61	0.05161
Lipids CH <sub>2</sub>	49.49	16.50	19.10	1.79*10 <sup>-11</sup>
Lactate (1.3 ppm)	10.48	3.49	3.57	0.01435
Lipids (CH <sub>2</sub> ) <sub>n</sub> -CH <sub>2</sub> -CH=	76.35	25.45	32.43	2.2*10 <sup>-16</sup>
Lipids CH <sub>2</sub> -CH <sub>2</sub> -COOC	53.08	17.70	20.74	2.29*10 <sup>-12</sup>
Lipids -N-(CH <sub>3</sub> ) <sub>3</sub>	84.48	28.16	37.00	2.2*10 <sup>-16</sup>
Lactate (4.1 ppm)	9.80	3.27	3.33	0.01971
Threonine	46.05	15.35	17.57	1.25*10 <sup>-10</sup>
Lipids CH=CH	75.87	25.29	32.16	2.2*10 <sup>-16</sup>

The resonances for quantification were selected on basis of the ASCA model

## Discussion

The current manuscript is our second work dedicated to the description of the time resolved metabolic response to *Opisthorchis* infection in an animal model. The first part was focused on the metabolic changes detected in urine samples, the current one covers the infection dependent changes in the plasma samples. Both sets of samples (urine and plasma) were collected within the same study which was designed as a longitudinal study with two degrees of infection intensity (mild – 15 and severe – 50 metacercariae per animal) and a control group. The plasma samples were collected every second week until 22 weeks of post-infection; this time interval includes both infection response phases: the acute phase and the phase which roughly corresponds to a chronic stage. Our data show that the strongest metabolic response was observed between the 2<sup>nd</sup> and 10<sup>th</sup> weeks after the experiment: a time when the worms are reaching the bile duct where they are transforming into the adult form and starting the egg production [27]. It has been shown that the acute phase of *O. felineus* infection in humans is more pronounced than in *O. viverrini* and *C. clonorchis* infection and often is accompanied by diarrhea, abdominal pain, nausea, and vomiting [28, 29]. Thus, it is important to mention that between the 2<sup>nd</sup> and 10<sup>th</sup> week of the experiment no diarrhea, loss of appetite, or loss of body mass was registered in the infected animals.

On a metabolic level the first ten weeks are characterized by rapid changes of amino acids and lipids which is in agreement with our report on urinary metabolomics [15]. The ASCA loadings plot (Figure 3) shows that the 4<sup>th</sup> week of the infection is the point where metabolic differences between the experimental groups are most pronounced. The egg production was recorded for the first time in the same week. One of the characteristic features of the metabolic response at this time point is a decrease of the blood plasma levels of the essential amino acids in the infected animals (Figure 4). It is worth mentioning that the observed decrease of the plasma levels of two essential amino acids isoleucine and leucine is associated with their increase in urine at 2<sup>nd</sup> and 4<sup>th</sup> weeks of infection [15]. The depletion of the essential amino acids (valine, isoleucine and leucine) during the acute stage of the in-

fection was also described for *Echinostoma caproni* infection [30, 31]; the parasite-induced malabsorption is one of the possible physiological explanations of the effect [32]. A similar, but not identical trend (no data on isoleucine were reported) was observed in a co-infection model of *Necator americanus* and *Schistosoma mansoni* [33]. In the case of opisthorchiasis an interpretation based entirely on malabsorption is not applicable; the parasite is more likely to change the pool of the free amino acids in the circulation by affecting the liver function [34]. Threonine, another essential amino acid which plays an important role in protein and lipid metabolism, is also depleted in the infected animal by the fourth week (Figure 4). Interestingly, an increase of threonine was found in feces in a human study of *O. felineus* [35]. However, a confirmation of malabsorption and mechanism of influence on essential amino acids in case of *O. felineus* requires an additional study. Apart from the amino acids a short-time decrease of lactate in plasma samples of both infected groups (S1 Figure) was detected. However, the quantified data does not show clear trends beyond the 4<sup>th</sup> week post-infection (Figure 4).

Lipid metabolism also shows a clear response to the infection. However, it has to be mentioned that for hamster lipids NMR spectroscopy remains a sub-optimal technique. For instance, while cholesterol can be annotated and quantified from NMR data without a problem, the spectral regions of the physiologically important lipoprotein particles such as low density lipoproteins (LDL), very low density lipoproteins (VLDL), high density lipoproteins (HDL) are strongly overlapped. Recently an elegant solution for an accurate quantitative analysis of the serum lipo-particles by NMR was introduced [36, 37], sadly this platform is only available for human serum. For animal material we can only indirectly estimate their contribution to the lipid profile using the NMR peaks corresponding to the various chemical functional groups. Our data shows that for all lipid-related spectral areas which were selected on basis of the ASCA analysis ( $\text{CH}_2$ ,  $\text{CH}_3$  and  $\text{CH}=\text{CH}$  chemical groups and cholesterol) a very distinct time trend is observed for the severe infection group at the early weeks of the infection (Figure 4). From the 10<sup>th</sup> week of infection onward the trends for both infected groups become more alike but as a rule the group with the severe infection consistently shows the higher values.

Despite the fact that a shift in the lipid homeostasis during the acute phase of infection is well-documented for helminthiases, it is

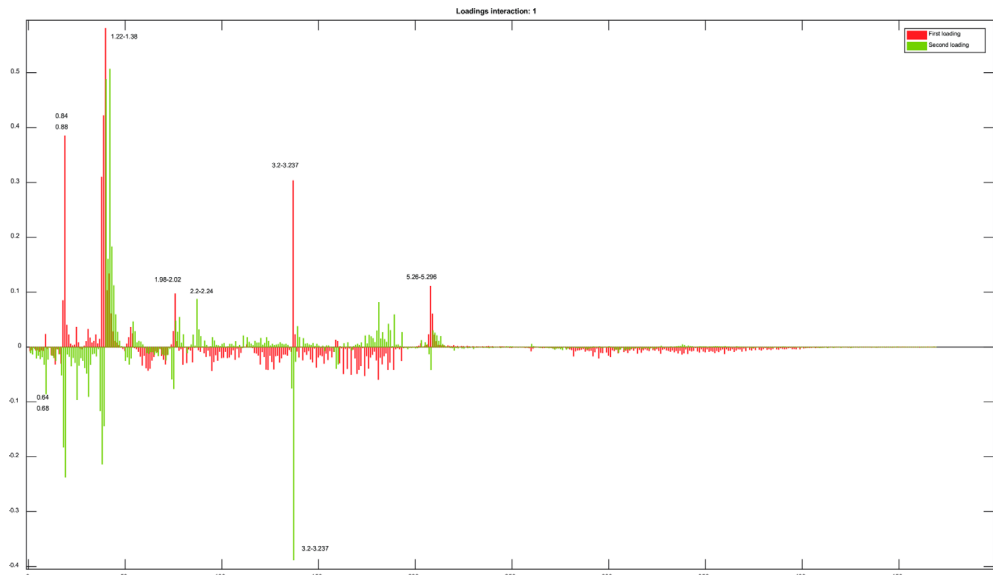
not easy to put our findings into the context of the existing reports. The main problem is the limited number of relevant reports, and the reports that exist use a variety of methodologies and experimental models. For instance, an NMR study on a mouse model of the *Echinostoma caproni* infection shows an increase of the lipid fraction related resonances in the infected animals. However, the maximum lipid increase was observed already at the 12<sup>th</sup> day of the experiment, which is much earlier than in our model (4 to 6 weeks) [30, 31]. At the same time, a mouse model of *Schistosoma japonicum* infection is characterized by a decrease of the lipoproteins from three weeks after infection [38]. There is no NMR-based study on *Opisthorchiidae*, but a report of Laothong et al. [39] where the cholesterol and lipoprotein particles in hamster's plasma were measured using the standard clinical chemistry methods is mostly in agreement with our data. Authors report an increase in cholesterol around one month after infections and a strong increase of LDL up to twelve weeks after infection. In the discussion they explain an increase in the LDL concentration as a reaction to leakage of vitamin E (alpha-tocopherol) from a damaged liver; a plausible interpretation which could be applied to our observations as well.

Even more difficult is to fit the observations obtained on the animal models to the data available on human material. The only clinical study on the lipids and lipoproteins in *O. viverrini* infection known to us [40] reports a significant decrease in cholesterol concentration for the group of the infected patients. It is very tempting to explain the differences in the observed trends as a result of the different technological approaches: colorimetric quantification of the cholesterol and NMR. Yet, we do not believe that this is the case. It has been shown that during the acute phase of an infection, the cholesterol level increases in the serum of the animals with low baseline values of LDL cholesterol (rodents) but remains stable in primates where the baseline values are higher [41–43]. Thus, the mechanisms controlling the lipid homeostasis in rodents and primates can explain the differences in the trends of cholesterol and lipoproteins between our data and the human studies.

## Conclusions

The time resolved study of the metabolic response to opisthorchiasis in blood plasma in the main lines agrees with our report on urine data. The response reaches its peak around the 4<sup>th</sup> week of infection and stabilizes after the 10<sup>th</sup> week. Yet, unlike the urinary data there is no strong effect of the gender in the data and the intensity of infection is presented in the first two principal components. The main trends of the metabolic response to infection in plasma are the transient depletion of the essential amino acids and an increase in lipoprotein and cholesterol concentrations.

## Supplementary information



**S1 Figure.** A visual summary of the relative contribution of the individual variables to the model explaining both infection and the time factors of the experiment. The variable importance is proportional to the value of its loading (Y axis); this way we can select a subset of the influential variables and annotate them

## References

1. Petney TN, Andrews RH, Sajjuntha W, Wenz-Mucke A, Sithithaworn P. The zoonotic, fish-borne liver flukes *Clonorchis sinensis*, *Opisthorchis felineus* and *Opisthorchis viverrini*. *Int J Parasitol*. 2013;43(12-13):1031-46.
2. Mairiang E, Mairiang P. Clinical manifestation of opisthorchiasis and treatment. *Acta Tropica*. 2003;88(3):221-7.
3. Pungpak S, Chalermrut K, Harinasuta T, Viravan C, Schelp PF, Hempfling A, et al. *Opisthorchis viverrini* infection in Thailand: symptoms and signs of infection--a population-based study. *Trans R Soc Trop Med Hyg*. 1994;88(5):561-4.
4. Liu LX, Harinasuta KT. Liver and intestinal flukes. *Gastroenterol Clin North Am*. 1996;25(3):627-36.
5. Humans IWGOrEoCRt. Biological agents. Volume 100 B. A review of human carcinogens. IARC Monogr Eval Carcinog Risks Hum. 2012;100(Pt B):1-441.
6. Young ND, Nagarajan N, Lin SLJ, Korhonen PK, Jex AR, Hall RS, et al. The *Opisthorchis viverrini* genome provides insights into life in the bile duct. *Nature Communications*. 2014;5.
7. Young ND, Gasser RB. *Opisthorchis viverrini* Draft Genome - Biomedical Implications and Future Avenues. *Asiatic Liver Fluke - from Basic Science to Public Health*, Pt A. 2018;101:125-+.
8. Young ND, Campbell BE, Hall RS, Jex AR, Cantacessi C, Laha T, et al. Unlocking the Transcriptomes of Two Carcinogenic Parasites, *Clonorchis sinensis* and *Opisthorchis viverrini*. *Plos Neglected Tropical Diseases*. 2010;4(6).
9. Suttiprapa S, Sotillo J, Smout M, Suyapoh W, Chaiyadet S, Tripathi T, et al. *Opisthorchis viverrini* Proteome and Host-Parasite Interactions. *Asiatic Liver Fluke - from Basic Science to Public Health*, Pt B. 2018;102:45-72.
10. Mulvenna J, Sripa B, Brindley PJ, Gorman J, Jones MK, Colgrave ML, et al. The secreted and surface proteomes of the adult stage of the carcinogenic human liver fluke *Opisthorchis viverrini*. *Proteomics*.

2010;10(5):1063-78.

11. Kokova D, Mayboroda OA. Twenty Years on: Metabolomics in Helminth Research. *Trends Parasitol.* 2019.

12. Fedorova OS, Fedotova MM, Sokolova TS, Golovach EA, Kovshirina YV, Ageeva TS, et al. *Opisthorchis felineus* infection prevalence in Western Siberia: A review of Russian literature. *Acta Tropica.* 2018;178:196-204.

13. Keiser J, Utzinger J. Food-borne trematodiases. *Clin Microbiol Rev.* 2009;22(3):466-83.

14. Pomaznay MY, Logacheva MD, Young ND, Penin AA, Ershov NI, Katokhin AV, et al. Whole transcriptome profiling of adult and infective stages of the trematode *Opisthorchis felineus*. *Parasitology International.* 2016;65(1):12-9.

15. Kokova DA, Kostidis S, Morello J, Dementeva N, Perina EA, Ivanov VV, et al. Exploratory metabolomics study of the experimental opisthorchiasis in a laboratory animal model (golden hamster, *Mesocricetus auratus*). *PLoS Negl Trop Dis.* 2017;11(10):e0006044.

16. Rodrigues MV, de Castro SO, de Albuquerque CZ, Mattaraia VGD, Santoro ML. The gingival vein as a minimally traumatic site for multiple blood sampling in guinea pigs and hamsters. *Plos One.* 2017;12(5).

17. Diehl KH, Hull R, Morton D, Pfister R, Rabemampianina Y, Smith D, et al. A good practice guide to the administration of substances and removal of blood, including routes and volumes. *J Appl Toxicol.* 2001;21(1):15-23.

18. Verhoeven A, Slagboom E, Wuhrer M, Giera M, Mayboroda OA. Automated quantification of metabolites in blood-derived samples by NMR. *Analytica Chimica Acta.* 2017;976:52-62.

19. Wu DH, Chen AD, Johnson CS. An Improved Diffusion-Ordered Spectroscopy Experiment Incorporating Bipolar-Gradient Pulses. *Journal of Magnetic Resonance Series A.* 1995;115(2):260-4.

20. Verhoeven A, Giera M, Mayboroda OA. KIMBLE: A versatile visual NMR metabolomics workbench in KNIME. *Analytica Chimica Acta.* 2018;1044:66-76.

21. De Meyer T, Sinnaeve D, Van Gasse B, Tsioporkova E, Rietzschel ER, De Buyzere ML, et al. NMR-based characterization of metabolic alterations in hypertension using an adaptive, intelligent binning algorithm. *Analytical Chemistry.* 2008;80(10):3783-90.

22. Dieterle F, Ross A, Schlot-

terbeck G, Senn H. Probabilistic quotient normalization as robust method to account for dilution of complex biological mixtures. Application in  $^1\text{H}$ -NMR metabonomics. *Analytical Chemistry*. 2006;78(13):4281-90.

23. Smilde AK, Jansen JJ, Hoefsloot HCJ, Lamers RJAN, van der Greef J, Timmerman ME. ANOVA-simultaneous component analysis (ASCA): a new tool for analyzing designed metabolomics data. *Bioinformatics*. 2005;21(13):3043-8.

24. Stekhoven DJ, Buhlmann P. MissForest--non-parametric missing value imputation for mixed-type data. *Bioinformatics*. 2012;28(1):112-8.

25. Mallol R, Rodriguez MA, Brezmes J, Masana L, Correig X. Human serum/plasma lipoprotein analysis by NMR: Application to the study of diabetic dyslipidemia. *Progress in Nuclear Magnetic Resonance Spectroscopy*. 2013;70:1-24.

26. Smilde AK, Westerhuis JA, Hoefsloot HCJ, Bijlsma S, Rubingh CM, Vis DJ, et al. Dynamic metabolomic data analysis: a tutorial review. *Metabolomics*. 2010;6(1):3-17.

27. Kaewpitoon N, Kaewpitoon SJ, Pengsaa P, Sripa B. *Opisthorchis viverrini*: The carcinogenic human liver fluke. *World J Gastroentero*. 2008;14(5):666-74.

28. Mel'nikov V, Skarednov NI. Clinical aspects of acute opisthorchiasis in the nonnative population of the northern Ob region. *Med Parazitol (Mosk)*. 1979;48(5):12-6.

29. WHO. Opisthorchiasis felinea [Available from: [https://www.who.int/foodborne\\_trematode\\_infections/opisthorchiasis/Opisthorchiasis\\_felinea/en/](https://www.who.int/foodborne_trematode_infections/opisthorchiasis/Opisthorchiasis_felinea/en/)].

30. Saric J, Li JV, Wang Y, Keiser J, Veselkov K, Dirnhofer S, et al. Panorganismal metabolic response modeling of an experimental *Echinostoma caproni* infection in the mouse. *J Proteome Res*. 2009;8(8):3899-911.

31. Saric J, Li JV, Wang Y, Keiser J, Bundy JG, Holmes E, et al. Metabolic profiling of an *Echinostoma caproni* infection in the mouse for biomarker discovery. *PLoS Negl Trop Dis*. 2008;2(7):e254.

32. Weinstein MS, Fried B. The Expulsion of *Echinostoma-Trivolvis* and Retention of *Echinostoma-Caproni* in the Icr Mouse - Pathological Effects. *International Journal for Parasitology*. 1991;21(2):255-7.

33. Wu JF, Holmes E, Xue J, Xiao SH, Singer BH, Tang HR, et al. Metabolic alterations in the hamster co-infected with

Schistosoma japonicum and Necator americanus. *Int J Parasitol.* 2010;40(6):695-703.

34. Pershina AG, Ivanov VV, Efimova LV, Shevelev OB, Vtorushin SV, Perevozchikova TV, et al. Magnetic resonance imaging and spectroscopy for differential assessment of liver abnormalities induced by *Opisthorchis felineus* in an animal model. *Plos Neglected Tropical Diseases.* 2017;11(7).

35. Kostidis S, Kokova D, Dementeva N, Saltykova IV, Kim HK, Choi YH, et al. (1)H-NMR analysis of feces: new possibilities in the helminthes infections research. *BMC Infect Dis.* 2017;17(1):275.

36. Jimenez B, Holmes E, Heude C, Tolson RF, Harvey N, Lodge SL, et al. Quantitative Lipoprotein Subclass and Low Molecular Weight Metabolite Analysis in Human Serum and Plasma by (1)H NMR Spectroscopy in a Multilaboratory Trial. *Anal Chem.* 2018;90(20):11962-71.

37. Barrilero R, Gil M, Amigo N, Dias CB, Wood LG, Garg ML, et al. LipSpin: A New Bioinformatics Tool for Quantitative (1)H NMR Lipid Profiling. *Anal Chem.* 2018;90(3):2031-40.

38. Wu J, Xu W, Ming Z, Dong H, Tang H, Wang Y. Metabolic changes reveal the development of schistosomiasis in mice. *PLoS Negl Trop Dis.* 2010;4(8).

39. Laothong U, Pinlaor P, Boonsiri P, Hiraku Y, Khoontawad J, Hongsrichan N, et al. alpha-Tocopherol and lipid profiles in plasma and the expression of alpha-tocopherol-related molecules in the liver of *Opisthorchis viverrini*-infected hamsters. *Parasitology International.* 2013;62(2):127-33.

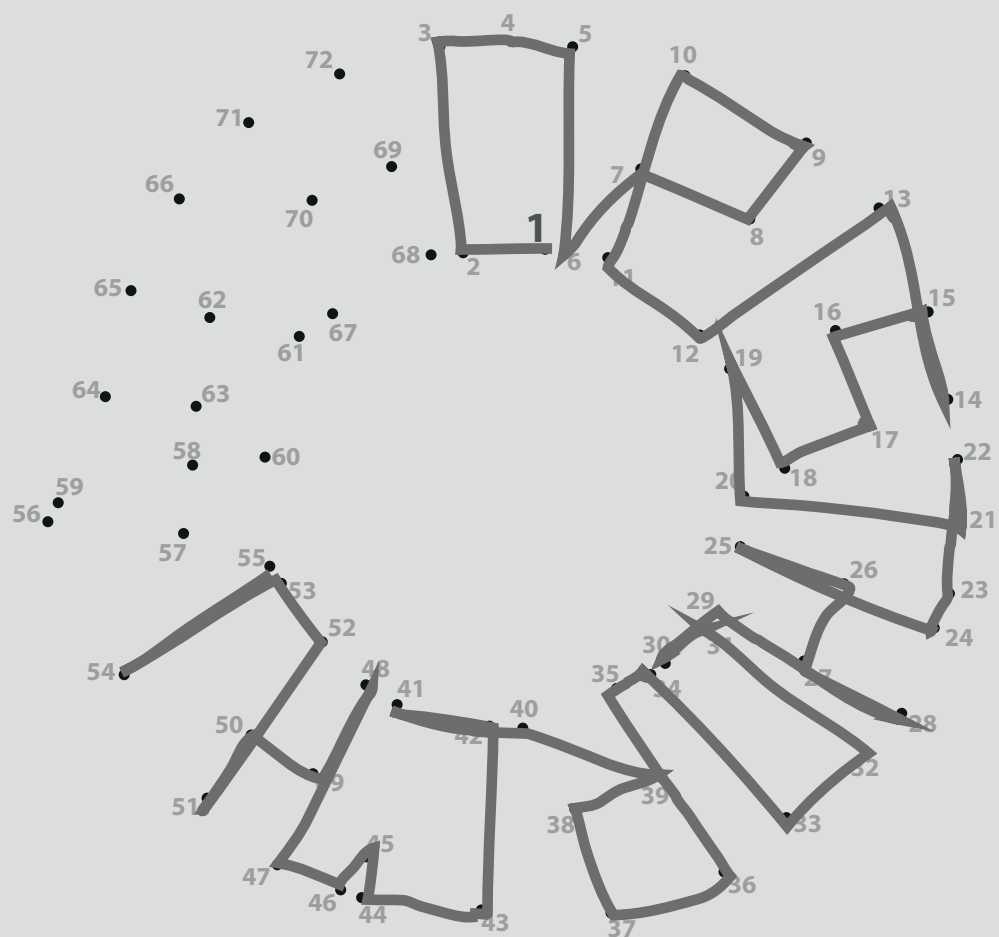
40. Changbumrung S, Ratarasarn S, Hongtong K, Migasena P, Vutikes S, Migasena S. Lipid-Composition of Serum Lipoprotein in Opisthorchiasis. *Annals of Tropical Medicine and Parasitology.* 1988;82(3):263-9.

41. Hardardottir I, Grunfeld C, Feingold KR. Effects of endotoxin and cytokines on lipid metabolism. *Curr Opin Lipidol.* 1994;5(3):207-15.

42. Kitagawa S, Yamaguchi Y, Imazumi N, Kunitomo M, Fujiwara M. A uniform alteration in serum lipid metabolism occurring during inflammation in mice. *Jpn J Pharmacol.* 1992;58(1):37-46.

43. Sherman DR, Guinn B, Perdok MM, Goldberg DE. Components of sterol biosynthesis assembled on the oxygen-avid hemoglobin of *Ascaris*. *Science.* 1992;258(5090):1930-2.





# 5

## $^1\text{H}$ -NMR analysis of feces: new possibilities in the helminthes infections research

S. Kostidis  
**D. Kokova**  
N. Dementeva  
I.V. Saltykova

H.K. Kim  
Y.H. Choi  
O.A. Mayboroda

BMC Infectious Diseases. 17:275 (2017)  
DOI 10.1186/s12879-017-2351-7

## Abstract

### Background

Analysis of the stool samples is an essential part of routine diagnostics of the helminthes infections. However, the standard methods such Kato and Kato-Katz utilize only a fraction of the information available. Here we present a method based on the nuclear magnetic resonance spectroscopy (NMR) which could be auxiliary to the standard procedures by evaluating the complex metabolic profiles (or phenotypes) of the samples.

### Method

The samples were collected over the period of June-July 2015, frozen at -20°C at the site of collection and transferred within four hours for the permanent storage at -80°C. Fecal metabolites were extracted by mixing aliquots of about 100 mg thawed stool material with 0.5 mL phosphate buffer saline, followed by the homogenization and centrifugations steps. All NMR data were recorded using a Bruker 600 MHz AVANCE II spectrometer equipped with a 5 mm triple resonance inverse cryoprobe and a z-gradient system.

### Results

Here we report an optimized method for NMR based metabolic profiling/phenotyping of the stool samples. Overall, 62 metabolites were annotated in the pool sample using the 2D NMR spectra and the Bruker Biorefcode database. The compounds cover a wide range of the metabolome including amino acids and their derivatives, short chain fatty acids (SCFAs), carboxylic acids and their derivatives, amines, carbohydrates, purines, alcohols, and others. An exploratory analysis of the metabolic profiles reveals no strong trends associated with the infectionstatus of the patients. However, using the penalized regression as a variable selection method we succeeded in finding a subset of eleven variables which enables to discriminate the patients on basis of their infections status.

### Conclusions

A simple method for metabolic profiling/phenotyping of the stools samples is reported and tested on a pilot opisthorchiasis cohort. To our knowledge this is the first report of a NMR-based feces analysis in the context of the helminthic infections.

## Background

Analysis of stool samples is an essential part of routine diagnostics of the helminthes infections. For years, despite a consistent background of criticism and occasional new developments, the direct smear and Kato-Katz techniques remain the gold standard diagnostic tests for schistosomiasis, opisthorchiasis and the soil-transmitted helminthiasis [1]. However, here we introduce a method based on nuclear magnetic resonance spectroscopy (NMR), which could be auxiliary to the standard methodologies. In contrast to the Kato and Kato-Katz tests which use only the eggs count as a measure, we examine the complex metabolic profile of the sample. In other words, we are applying the metabolomics approach. Metabolomics is a discipline studying the metabolome – a totality of the metabolites that can be measured in a biological sample. The metabolites are defined as the end products and the intermediates of the metabolism. In the clinical setting the metabolomics studies are commonly based on the analysis of the body fluids. Urine and blood (serum or plasma) are being the most common sample types due to the minimally invasive procedures of sample collection. Feces as a material for metabolomics studies has only recently started to gain the deserved attention [2, 3]. Over recent years few metabolomics studies in such areas as e.g. dietary interventions [4], inflammatory bowel disease [5, 6] and colorectal cancer [7] have been published.

Indeed, the fecal masses are the physiological product of the gastrointestinal tract, one of the key metabolic systems of the human body. Thus, it is logical to assume that their composition should reflect current metabolic status of the digestive tract or its metabolic phenotype [8]. The human gut represents a complex ecosystem and harbors gut bacteria outnumbering the cells in our organism [9] and the analysis of the fecal masses or/ and their derivatives (e.g. extracts or fecal waters) offers the most direct access to the physiological processes controlling the gastrointestinal system homeostasis, gut bacteria-host interactions and interaction between the hosts and parasitic helminthes. For example, the helminth infections are often accompanied by such symptoms as diarrhea, abdominal pain and blood in the stool. The given exam-

ples represent the extreme cases, but they provide a clear illustration of the parasite's ability changing the metabolic homeostasis of the host and the host's digestive system in particular. This, in turn, makes metabolic analysis of the fecal masses an interesting, non-invasive way to monitor such changes.

Here we present a simple NMR based metabolomics workflow for the analysis of fecal samples. For this pilot study we used stool samples of patients diagnosed with opisthorchiasis and a group of matched controls. Opisthorchiasis is parasitic disease caused by trematodes belonging to the family *Opisthorchiidae* (*Opisthorchis felineus*, *Opisthorchis viverrini*) [10]. According to WHO there are about 17 million infected people and approximately 112 million people exposed or at risk of infection. The workflow presented here is only a proof of principle, but it can be easily scaled, tuned towards a quantitative analysis and implemented into other case studies or in future routine screening without fundamental modification of the sample collection or the exiting diagnostic routines.

# Methods

## Sample collection

The study was reviewed and approved by the local ethics committee of the Siberian State Medical University (Tomsk, Russia). The samples were collected over the period of June-July 2015. The samples were frozen at -20°C at the site of collection and transferred within four hours for the permanent storage at -80°C. The diagnosis of opisthorchiasis was confirmed by the Kato-Katz test [1]. Table 1 summarizes the demographic data of the patients. In total the samples of 30 patients (16 infected and 14 uninfected) were used.

Table 1. Characteristics of participants

Parameter	Summary	Opisthorchiasis (n=16)	Control (n=14)
Age (year)	range	(21, 64)	(24, 63)
	mean	45	60
Gender	male	0	0
	female	16	14
Height (cm)	range	(153, 168)	(155, 169)
	mean	162	160.9
Weight (kg)	range	(50, 106)	(53, 83)
	mean	70.3	70.3
BMI	range	(18.4, 43.6)	(21.7, 32.5)
	mean	26.6	27.1
the presence of allergies	positive	3	1
	negative	9	12
	unknown	4	1

## Fecal metabolites extraction

Fecal metabolites were extracted as described elsewhere [11] with some minor modifications. Briefly, the aliquots of about 100 mg thawed stool material were mixed with 0.5 mL phosphate buffer saline (1.9 mM Na<sub>2</sub>HPO<sub>4</sub>, 8.1 mM NaH<sub>2</sub>PO<sub>4</sub>, 150 mM NaCl, pH 7.4; Sigma-Aldrich, Germany) containing 10% deuterated water (D<sub>2</sub>O 99.8%;

Cortecnet, France) and 0.05 mM sodium 3-trimethylsilyl-propionate-d4 (TMSP-2,2,3,3-d4; Cambridge Isotope Laboratories Inc., UK) as chemical shift reference. The mixtures were homogenized by bead beating with zirconium oxide beads of 1 mm diameter for 30 s at 4°C in a Bullet Blender 24 (Next Advance Inc., USA). The fecal slurry was then centrifuged at 16100×g for 15 min at 4°C. Supernatants were collected and centrifugation was repeated. Finally, the resulting fecal extracts were transferred to a 96 well plate (Bruker, Germany) and 190 µL of each sample was transferred to a 3 mm NMR tube in SampleJet 96 tube rack (Bruker, Germany) using 215 Gilson liquid handler. The samples were then placed in a SampleJet system and kept cooled at 6 °C while queued for NMR measurements.

Alternative protocols for fecal extraction, as described elsewhere [5, 12, 13] were also applied using technical replicates and the same equipment and chemicals described above. For filtration we used the Whatman filters with 0.2 µm diameter pores (GE Healthcare, UK). An ultracentrifugation step with filtration was also tested using Amicon Ultra cellulose centrifugal filters with a cut-off MW of 3000 Da (Millipore Ireland, Ltd). The filters were washed with doubly distilled water before use and tested for impurities and presence of additives using a blank PBS buffer sample and acquisition of NMR spectra with the same parameters as those used for fecal extracts measurements (see below).

### NMR spectroscopy

All NMR data were recorded using a Bruker 600 MHz AVANCE II spectrometer equipped with a 5mm triple resonance inverse cryo-probe and a z-gradient system. The temperature of the samples was controlled at 27°C during measurement. Prior to data acquisition, tuning and matching of the probe head followed by shimming and proton pulse calibration were performed automatically for each sample. One-dimensional (1D) <sup>1</sup>H NMR spectra were recorded using the first increment of a NOESY pulse sequence with presaturation ( $\gamma$ B1 = 50 Hz) for water suppression during a relaxation delay of 4 s and a mixing time of 10 ms [14, 15] 64 scans of 65,536 points covering 12,335 Hz were recorded and zero filled to 65,536 complex points prior to Fourier transformation, an exponential window function was applied with a line-broadening factor of 1.0 Hz. The spectra were automatically phase and baseline corrected and referenced to the internal standard

(TMSP;  $\delta$  0.0 ppm).

After tube filling, 30  $\mu$ L from the leftovers of each sample were combined to form a pool sample mix. The pool sample was aliquoted and used for acquisition of two-dimensional (2D) NMR spectra to aid the assignment of fecal metabolites. The set of 2D experiments included a J-resolve (J-res),  $^1\text{H}$ - $^1\text{H}$  correlation spectroscopy (COSY),  $^1\text{H}$ - $^1\text{H}$  total correlation spectroscopy (TOCSY),  $^1\text{H}$ - $^{13}\text{C}$  heteronuclear single quantum correlation (HSQC) and  $^1\text{H}$ - $^{13}\text{C}$  heteronuclear multiple bond correlation spectroscopy (HMBC) using the standard parameters implemented in Topspin 3.0 (Bruker Biospin, Germany).

### NMR data processing

NMR data were further processed using in house routines written in Matlab 2014a (The Mathworks, Inc., USA) and Python 2.7 (Python Software Foundation, [www.python.org](http://www.python.org)). Briefly, the obtained  $^1\text{H}$  spectra were re-evaluated for incorrect baselines and corrected using a polynomial fit of degree 5. The spectral region from 0.5 to 9.7 ppm was binned using an in-house algorithm for adaptive intelligent binning, which is based on the original paper of De Meyer et al. [16]. Initial bin width was set to 0.02 ppm and final variable bins sizes were calculated based on the peaks position and width in the spectra. The spectral region with the residual water peak (4.5 – 5.1 ppm) was excluded from the data. The final data consisted of 429 bins that were normalized by the Probabilistic Quotients Normalization method [17] to correct for dilution differences from sample to sample. Data were first normalized to unit total area and subsequently, the variables of each sample were divided by those of a reference sample, in this case the median spectrum. Each sample was subsequently scaled by its median quotient, which represents the most probable dilution factor. Finally, the normalized data was autoscaled prior to statistical analysis.

### Data analysis

All the analysis was performed in the R statistical software environment (<http://www.r-project.org/>, R version 3.2.3.). Exploratory data analysis was performed using the package “pcaMethods” [18]. Variable selection was performed with the “glmnet” package [19]. For data visualization the “ggplot2”, “GGally” and “gridExtra” packages were used.

## Results

### Optimization of the sample preparation

In contrast to other body fluids like urine and blood for which the well-established standard operating procedures (SOP) exist, no consensus for feces handling has been reached yet. Thus, to get an optimal extraction of the feces samples several protocols described in the literature [11–13] were tested. A detailed overview of the available methods can be found in recent review by Deda et al. [2]. In our case, a minimally modified protocol of the one recently suggested by Lamichhane et al. [11] provided an optimal outcome in terms of spectra quality and the number of the metabolites detected. In the original manuscript, the authors suggested mixing the fecal material with 2 volumes of PBS (Wf:Vb; mg of feces  $\times$   $\mu$ L $^{-1}$  of PBS buffer), which according to them provides better signal to noise ratios and minimal compromise for peak shifting due to small inter-sample pH differences. They also used a freeze-thaw cycle with centrifugation of the fresh fecal slurry, storage at -80°C and thawing at the day of analysis followed by a second centrifugation. Since, the samples used in our study were already frozen and stored at -80°C at the site of collection we opted to avoid the extra freeze-thaw step. Therefore, after thawing the frozen fecal aliquots and the homogenization of the fecal slurry, we performed two

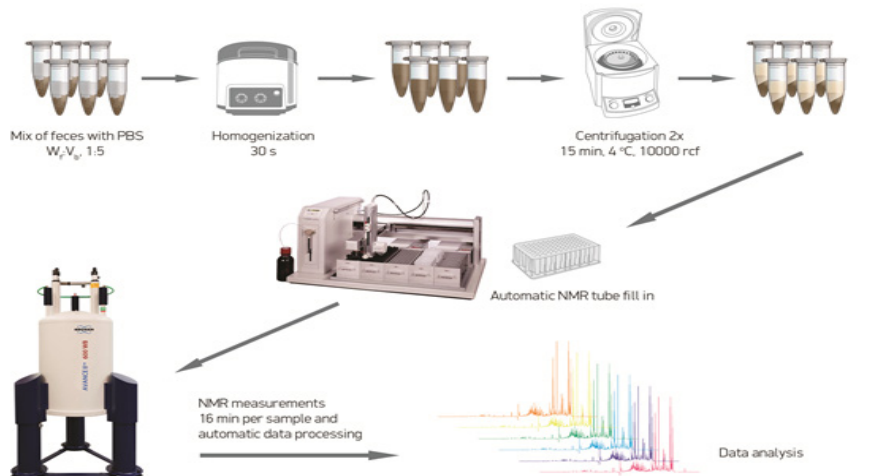


Figure 1. A schematic outline of the sample preparation workflow

consecutive centrifugation steps at 4°C. The suggested 1:2 Wf:Vb ratio did not work well in our case as the supernatants could not be easily separated from the precipitated material even after extending the centrifugation time. An obvious solution would be to include a filtration step but this would require an extra step to wash the filters, which increases the time and costs of the protocol. On the other hand, we found that by using the 1:5 Wf:Vb and 7 min 1D 1H-NMR acquisition method (64 scans per sample) the losses in the signal to noise ration were minimal even for the weak signal of formic acid (SNR 36.3 and 29.8 for 1:2 and 1:5 Wf:Vb, respectively) while the peak shifting of pH sensitive protons was reduced comparing to 1:2 Wf:Vb as an effect of better pH control. We therefore decided to follow the 1:5 Wf:Vb mixing with PBS for all the samples analyzed in this study. Figure 1 shows a schematic representation of the entire workflow.

Figure 2 shows the 1H spectrum of a pooled sample with annotations of the identified metabolites. Overall, 62 metabolites were annotated in the pool sample using the 2D NMR spectra and the Bruker Biorefcode database (Bruker Biospin, Germany). The detected compounds cover a wide range of the metabolites including amino acids and their derivatives, short chain fatty acids (SCFAs), carboxylic acids and their derivatives, amines, carbohydrates, purines, alcohols and others. The complete list of metabolites is enumerated in the legend of Figure 2.

### Exploratory analysis of the data

The main purpose of an exploratory data analysis is to reveal the major trends in the data as well as the possible analytical and/or biological confounders if any. Principal Component Analysis (PCA) is commonly used method for such analysis. Figure 3 shows a combined score plot of the first three principal components of the PCA model. The first three components cover almost 50% (~ 49) of the total variance in the data but apparently the infection status does not represent a visible trend in the data. Since initial PCA model failed to describe any tendencies in the data associated with the study design we built a two-class Partial Least Squares Discriminant Analysis (PLS-DA) model with infections status as a class ID. The model proved to be a statistically poor and described the data narrowly better than a random one (data not shown). One could interpret the results as a lack of association between infection status and metabolic composition of the feces.

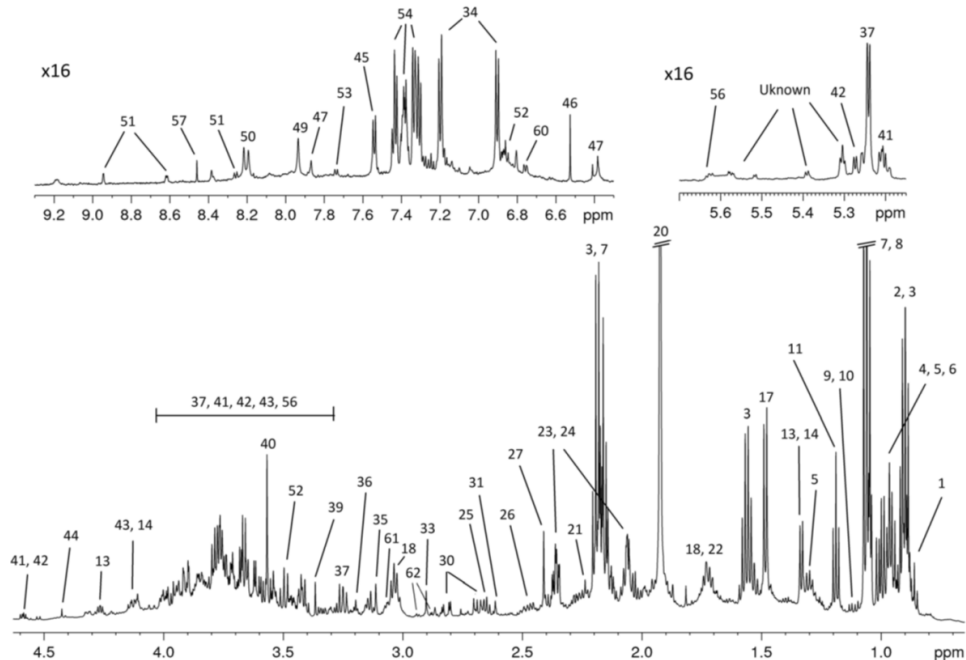


Figure 2. Regions of the 600 MHz 1D 1H NMR spectrum of the pool sample mix of all fecal extracts used in this study. The regions on top are multiplied 16 times for better visualization. 60 fecal metabolites were identified with most of them annotated on the spectrum. Metabolites and their numbering as displayed in figure: 1: 2-methylbutyrate; 2: Valerate; 3: *n*-butyrate; 4: Leucine; 5: Isoleucine; 6: Valine; 7: Propionate; 8: Isobutyrate; 9: 3-methyl-2-oxoisovalerate; 10: 2-oxoisovalerate; 11: Ethanol; 12: 3-hydroxybutyrate; 13: Threonine; 14: Lactate; 15: 2-hydroxyisobutyrate; 16: 3-hydroxy-2-butanone; 17: Alanine; 18: Lysine; 19: Thymine; 20: Acetate; 21: 5-aminopentanoate; 22: Ornithine; 23: Proline; 24: Glutamate; 25: Methionine; 26: Glutamine; 27: Succinate; 28: 2-oxoglutarate; 29: 3-phenylpropionate; 30: Aspartate; 31: Methylamine; 32: Malate; 33: Trimethylamine; 34: Tyrosine; 35: Malonate; 36: Choline; 37: D-glucose; 38: Taurine; 39: Methanol; 40: Glycine; 41: D-xylose; 42: D-galactose; 43: Fructose; 44: Dihydroxyacetone; 45: Uracil; 46: Fumarate; 47: Urocanate; 48: Ethanolamine; 49: Xanthine; 50: Hypoxanthine; 51: Nicotinate; 52: 3-hydroxyphenylacetate; 53: Tryptophan; 54: Phenylalanine; 55: Orotate; 56: UDP-glucuronate; 57: Formate; 58: Benzoate; 59: 4-aminohippurate; 60: Homovanillate; 61: Putrescine; 62: Asparagine

The performance of the PLS-DA model clearly supports such interpretation. However, the structure of our data set (30 observations and 429 variables) is such that the number of predictive variables ( $p$ ) is much larger than the number of samples ( $n$ ). The PLS-DA method, despite being one of the most popular classification methods in metabolomics analysis, is a suboptimal choice for the  $p > n$  data sets [20]. Thus, we decided to employ an alternative data analysis strategy including a variable selection step which could identify a subset of predictors relevant to the study design.

### Variable selection and validation of the selected subset

The analysis of high dimensional datasets has progressed enormously since the beginning of “omics” era. Several methods specifically addressing  $p \gg n$  problem are described and tested in practice, but the area of application for the methods is mainly restricted to the genomics data [21, 22]. We decided to use the penalized regression approach based on its “track record” in solving comparable problems, namely a high number of the variables and the limited number of the observations [22, 23]. A penalized variable section belongs to the class of the regulations methods: the methods which improve the estimates “for over-parameterized problems through the use of additional assumptions, prior information or penalties” [24]. A subset of eleven variables was selected using a lasso type of penalty. Before subjecting the set of selected variables to the next statistical test we have also made an inventory of the selection trying to estimate whether the feature selecting routine has picked the NMR spectral areas influenced by the noise and/or any baseline effect. Figure 4 shows the box plots for all eleven predictors selected by this method. Table 2 summarizes all the selected bins showing their corresponding spectral regions, identity and Benjamini-Hochberg corrected p-values. Finally, we have included the selected variables into a logistic regression model. The resulting model is characterized by the chi square 27.74 and chi square probability of 1.05E-4.

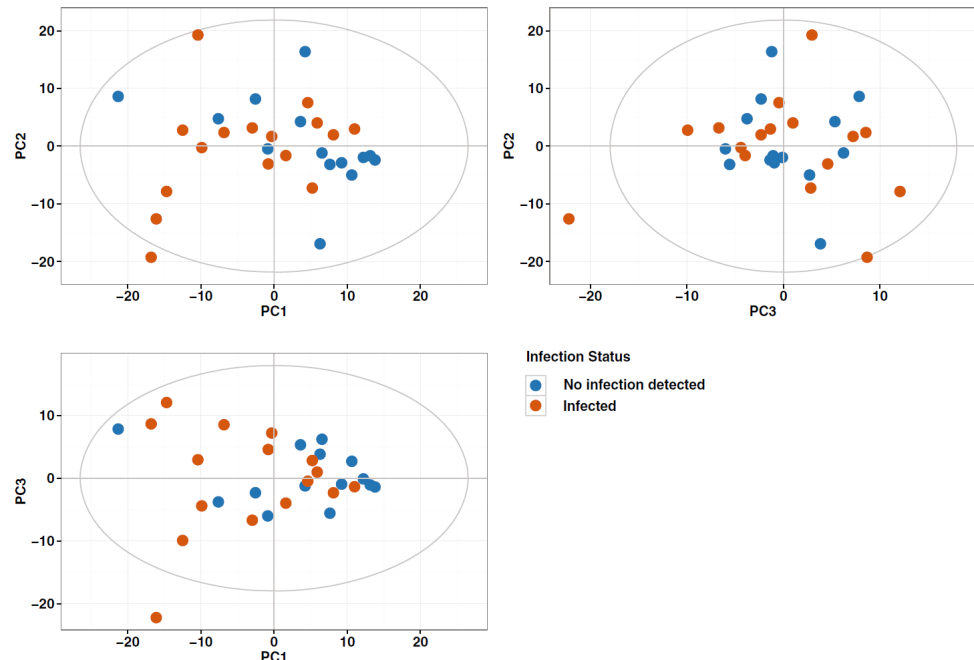


Figure 3. PCA score plots for the first three components

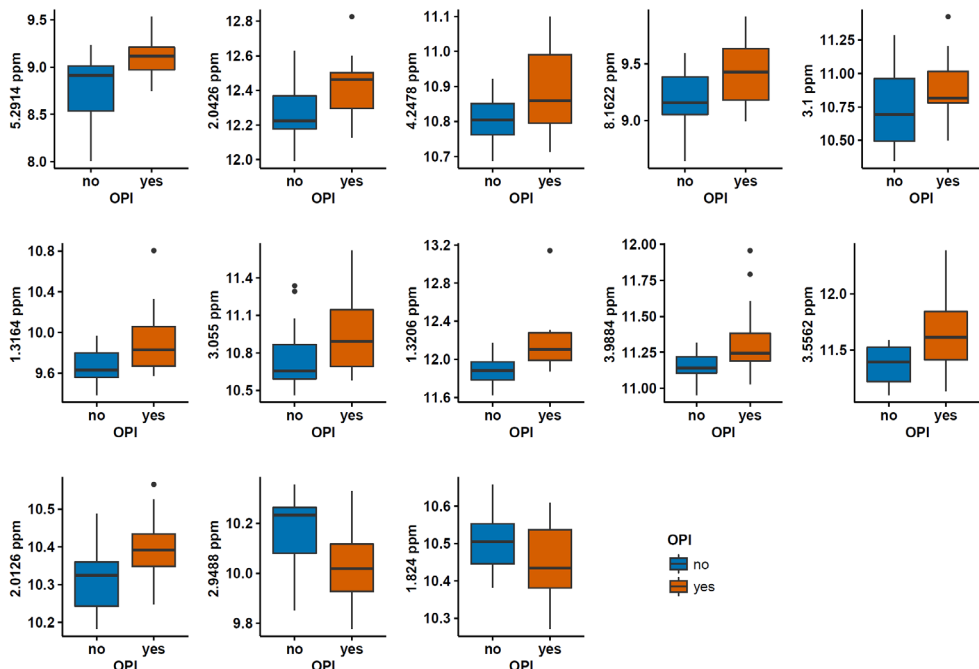


Figure 4. Box-plots for the variables selected with the lasso regression. The variable assignments and corresponding p-values are shown in the Table 2

Table 2. The selected variable assignments and corresponding p-values

Spectral region (ppm)	p-value	ID
5.2914	0.0378	Unknown triplet/4.12/1.99/1.80
4.2478	0.0942	Threonine
2.0426	0.0601	Glutamate/Proline
1.3164	0.0378	Threonine and lactate
3.1	0.1661	Malonate
8.1622	0.0378	Hypoxanthine
3.9884	0.0601	Phenylalanine/ d-Galactose
3.055	0.0942	Tyrosine/Putrescine/Ornithine
1.3206	0.0031	Threonine and Lactate
1.824	0.1322	Ornithine/2-Aminoadopate
2.9488	0.0378	Asparagine

## Discussion

Here we present an analytical workflow for  $^1\text{H}$ -NMR analysis of feces with special emphasis on application in the field of the helminthes infections. The described procedure resulted in rich spectra where 62 metabolites are annotated (Figure 2). Using our set of the samples selection we were able to dissect a subset of the metabolites (Figure 4) which may be discriminative for the infection's status. This subset includes such common constituents of human biofluids as threonine, asparagine, lactate and hypoxanthine. Asparagine is higher in the samples of the control patients while the other selected compounds have higher levels in the infected samples. The limited number of samples is a clear limitation of this study and therefore we restrain ourselves from the discussion of the possible physiological models based on the selected markers or the attempts to deconvolute the metabolic profiles into the infection predictive patterns. On the other hand, the proposed method clearly stresses out the potential for a new window of information that can be used in such case studies. In principle, the fact that a subset of the discriminative metabolites can be dissected gives a clear illustration of the method's potential. A combination of a simple, commonly accepted diagnostic method and such advanced analytical method as NMR provides a powerful research tool which enables the collection of a wealth of information without interference or in parallel with the routine diagnostics or epidemiological studies. Taking advantage of the robustness and quantitative nature of this technology, obtaining the metabolic profiles of fecal material is rather straightforward and provides both an insight into biochemistry/physiology of the host-pathogen interaction and the possibility of accessing the morbidity and eventually play an auxiliary role in the diagnostics. The main limitations of this approach arise mainly from the absence of standard procedures in stool collection rather than the technology itself. However, taking into account the increasing interest in using the NMR (as well as mass spectrometry) based metabolomics approaches in fecal samples, we envisage that more established routines and practices in sample collection will be developed in the near future which will reveal the underlying potential of this type of analysis.

## Conclusions

In summary, a simple method for metabolic profiling/phenotyping of the stools samples is reported and tested on a pilot opisthorchiasis cohort. To our knowledge this is the first report of a NMR-based feces analysis in the context of the helminthic infections. With this study, an attempt was made to extend a conventional way of the stool analysis adding an extra dimension which can be used for metabolic phenotyping of the patients, in depth exploration of the host-parasite interaction and search for metabolic morbidity or/and infection markers. To extend and take full advantage of the possibilities offered by NMR based metabolic profiling much larger cohorts than the one used in this study are needed, preferably, even collected in the different endemic areas. With this report however, we provide a simple proof of concept aiming to introduce a well-established technology in the field of infectious diseases and fecal material analysis and with this, trigger future studies in this direction.

## Acknowledgments

This study was supported by the Tomsk State University Academic D.I. Mendeleev Fund Program (grant № 8.1.52.2015). We thank Dr. Eugenie Semichev for facilitation of the sample collection.

## References

1. McCarthy JS, Lustigman S, Yang GJ, Barakat RM, Garcia HH, Sripa B, Willingham AL, Prichard RK, Basanez MG. A research agenda for Helminth diseases of humans: diagnostics for control and elimination Programmes. *PLoS Negl Trop Dis.* 2012;6(4):e1601.
2. Deda O, Gika HG, Wilson ID, Theodoridis GA. An overview of fecal sample preparation for global metabolic profiling. *J Pharmaceut Biomed.* 2015;113:137–50.
3. Gratton J, Phetcharaburadin J, Mullish BH, Williams HR, Thursz M, Nicholson JK, Holmes E, Marchesi JR, Li JV. Optimized Sample Handling Strategy for Metabolic Profiling of Human Feces. *Anal Chem.* 2016;88(9):4661–668.
4. Lamichhane S, Yde CC, Forssten S, Ouwehand AC, Saarinen M, Jensen HM, Gibson GR, Rastall R, Fava F, Bertram HC. Impact of dietary Polydextrose fiber on the human gut Metabolome. *J Agr Food Chem.* 2014;62(40):9944–51.
5. Le Gall G, Noor SO, Ridgway K, Scovell L, Jamieson C, John-  
son IT, Colquhoun IJ, Kemsley EK, Narbad A. Metabolomics of fecal extracts detects altered metabolic activity of gut Microbiota in ulcerative colitis and irritable bowel syndrome. *J Proteome Res.* 2011;10(9):4208–18.
6. Marchesi JR, Holmes E, Khan F, Kochhar S, Scanlan P, Shanahan F, Wilson ID, Wang YL. Rapid and noninvasive metabonomic characterization of inflammatory bowel disease. *J Proteome Res.* 2007;6(2):546–51.
7. Monleon D, Morales JM, Barrasa A, Lopez JA, Vazquez C, Celda B. Metabolite profiling of fecal water extracts from human colorectal cancer. *NMR Biomed.* 2009;22(3):342–8.
8. Holmes E, Loo RL, Stamler J, Bictash M, Yap IKS, Chan Q, Ebbels T, De Iorio M, Brown IJ, Veselkov KA, et al. Human metabolic phenotype diversity and its association with diet and blood pressure. *Nature.* 2008; 453(7193):396–U350.
9. Goodman AL, McNulty NP, Zhao Y, Leip D, Mitra RD, Lozupone CA, Knight R, Gordon JI. Identifying genetic determinants needed to estab-

lish a human gut Symbiont in its habitat. *Cell Host Microbe*. 2009;6(3):279-89.

10. Sripa B, Bethony JM, Sithithaworn P, Kaewkes S, Mairiang E, Loukas A, Mullen J, Laha T, Hotez PJ, Brindley PJ. Opisthorchiasis and Opisthorchis-associated cholangiocarcinoma in Thailand and Laos. *Acta Trop*. 2011;120:S158-68.

11. Lamichhane S, Yde CC, Schmedes MS, Jensen HM, Meier S, Bertram HC. Strategy for nuclear-magnetic-resonance-based Metabolomics of human feces. *Anal Chem*. 2015;87(12):5930-7.

12. Wu JF, An YP, Yao JW, Wang YL, Tang HR. An optimised sample preparation method for NMR-based faecal metabonomic analysis. *Analyst*. 2010;135(5):1023-30.

13. Saric J, Wang Y, Li J, Coen M, Utzinger J, Marchesi JR, Keiser J, Veselkov K, Lindon JC, Nicholson JK, et al. Species variation in the fecal metabolome gives insight into differential gastrointestinal function. *J Proteome Res*. 2008;7(1):352-60.

14. Kumar A, Ernst RR, Wuthrich K. A two-dimensional nuclear Overhauser enhancement (2d Noe) experiment for the elucidation of complete proton-proton cross-relaxation networks in biological macromolecules. *Biochem Biophys Res Co*. 1980;95(1):1-6.

15. Price WS. Water signal suppression in NMR spectroscopy. *Ann R Nmr S*. 1999;38:289-354.

16. De Meyer T, Sinnaeve D, Van Gasse B, Tsiporkova E, Rietzschel ER, De Buyzere ML, Gillebert TC, Bekaert S, Martins JC, Van Criekinge W. NMR-based characterization of metabolic alterations in hypertension using an adaptive, intelligent binning algorithm. *Anal Chem*. 2008;80(10):3783-90.

17. Dieterle F, Ross A, Schlotterbeck G, Senn H. Probabilistic quotient normalization as robust method to account for dilution of complex biological mixtures. Application in H-1 NMR metabonomics. *Anal Chem*. 2006;78(13):4281-90.

18. Stacklies W, Redestig H, Scholz M, Walther D, Selbig J. pcaMethods - a bioconductor package providing PCA methods for incomplete data. *Bioinformatics*. 2007;23(9):1164-7.

19. Friedman J, Hastie T, Tibshirani R. Regularization paths for generalized linear models via coordinate descent. *J Stat Softw*. 2010;33(1):1-22.

20. Westerhuis JA, Hoefsloot HCJ, Smit S, Vis DJ, Smilde AK, van Velzen EJJ, van Duijn-

hoven JPM, van Dorsten FA. Assessment of PLSDA cross validation. *Metabolomics*. 2008;4(1):81–9.

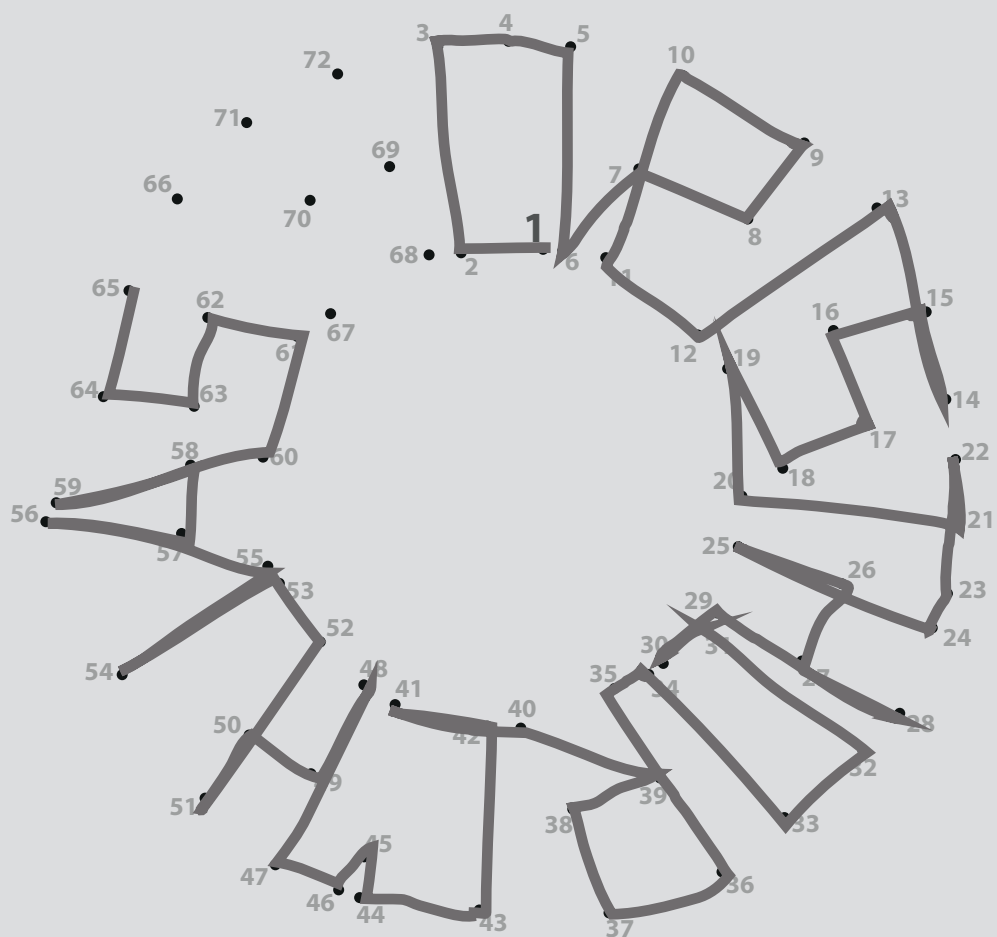
21. Saeys Y, Inza I, Larrañaga P. A review of feature selection techniques in bioinformatics. *Bioinformatics*. 2007;23(19):2507–17.

22. Golub TR, Slonim DK, Tamayo P, Huard C, Gaasenbeek M, Mesirov JP, Coller H, Loh ML, Downing JR, Caligiuri MA, et al. Molecular classification of cancer: class discovery and class prediction by gene expression monitoring. *Science*. 1999;286(5439):531–7.

23. Liu C, Shi T, Lee Y. Two Tales of variable selection for high dimensional regression: screening and model building. *Stat Anal Data Min*. 2014;7(2):140–59.

24. Zhao Q, Shi XJ, Huang J, Liu J, Li Y, Ma SG. Integrative analysis of ‘-omics’ data using penalty functions. *Wiley Interdiscip Re*. 2015;7(1):99–108.





# 6

## Metabolic homeostasis in chronic helminth infection is sustained by organ specific metabolic rewiring

D. Kokova  
A. Verhoeven  
E.A. Perina  
V.V. Ivanov

M. Heijink  
M. Yazdanbakhsh  
O.A. Mayboroda

ACS Infect. Dis. 7:4 (2021)  
<https://doi.org/10.1021/acsinfecdis.1c00026>

## Abstract

Opisthorchiasis, is a hepatobiliary disease caused by flukes of the trematode family *Opisthorchiidae*. A chronic form of the disease implies a prolonged coexistence of a host and the parasite. The pathological changes inflicted by the worm to the host's hepatobiliary system are well documented. Yet, the response to the infection also triggers a deep remodeling of the host systemic metabolism reaching a new homeostasis and affecting the organs beyond the worm location. Understanding the metabolic alternation in chronic opisthorchiasis, could help us pinpoint pathways that underlie infection opening possibilities for the development of more selective treatment strategies. Here, with this report we apply an integrative, multicompartiment metabolomics analysis, using multiple biofluids, stool samples and tissue extracts to describe metabolic changes in *O. felineus* infected animals at the chronic stage. We show that the shift in lipid metabolism in the serum, a depletion of the amino acids pool, an alteration of the ketogenic pathways in the jejunum and a suppressed metabolic activity of the spleen are the key features of the metabolic host adaptation at the chronic stage of *O. felineus* infection. We describe this combination of the metabolic changes as a "metabolically mediated immunosuppressive status of organism" which develops during a chronic infection. A prolonged status of the immuno-hibernation might be one of the factors which increases risk of the infection related malignancy.

## Significance Statement

A chronic helminths infection triggers a deep remodeling of the host systemic metabolism reaching a new homeostasis. Applying an integrative, multicompartment metabolomics analysis we show that the key features of the metabolic host adaptation at the chronic stage of *O. felineus* infection are the shift in lipid metabolism in the serum, a depletion of the amino acids pool, an alteration of the ketogenic pathways in the jejunum and most importantly a suppressed metabolic activity of the spleen. The metabolic patterns described here give a new insight into the host-parasite interaction. Finally, a simultaneous profiling of the metabolic signatures in the body fluids and the key metabolic organs helps spotting the potential metabolic vulnerabilities that might be targeted therapeutically.

## Introduction

Opisthorchiasis a hepatobiliary disease is caused by flukes of the trematode family *Opisthorchiidae*: *Opisthorchis felineus* (*O. felineus*), *Opisthorchis viverrini* (*O. viverrini*) and *Clonorchis sinensis* (*C. sinensis*). Together, these three species affect more than 45 million people in endemic regions [1, 2]. The clinical manifestations of acute opisthorchiasis are non-specific and its chronic form usually appears asymptomatic [3, 4]. Yet, at chronic stage of infection, there is progressive accumulation of pathological changes in the host due to egg induced fibrosis and the local damage inflicted to the biliary epithelium by the worms. Moreover, a long-term coexistence with a parasite leads to a remodeling of the host systemic metabolism. How and at what cost this new homeostasis is sustained is still poorly understood, but a current theoretical framework [5] implies that metabolic shift has a profound influence on the host immune status and eventually affects the organs that are not directly involved in the immune response. Understanding the metabolic alternation in opisthorchiasis, could help us understand pathways that underlie infection and disease progression that might be targets of therapeutics.

Metabolomics technology offers a method for exploring of the systemic metabolism. Today, metabolomics of helminth infections is an area of active research. It has been shown that metabolic response of the host usually leads to changes in the pattern of amino acids in the body fluids, remodeling of the lipid metabolism and changes in composition of the microbiota-related metabolites [6]. Yet, while metabolic responses to helminth infections in animal models are rather strong and easily detectable, the field studies with human participants have shown that these infections are not one of the strongest factors that can influence the metabolic composition of body fluids. The traditional confounding factors such as age, gender, BMI, and lifestyle mask the infection related metabolic adaptations [7]. Of course, one of the main differences of the field studies with the animal experiments is the degree of control over the sources of the unwanted variance. Another difference is that animal studies often report only the effects observed at the early stage of the infection, while in the “real life” situation, it is

the chronic stages of infection that we are likely to encounter.

Recently, using an experimental infection system with a liver fluke *O. felineus* we have shown that in urine and blood the metabolic response stabilizes after the 12<sup>th</sup> week of infection and hardly any statistically significant changes can be found between infected and uninfected animals [8, 9]. Here to emulate the chronic stage of infection data are generated over twenty weeks post infection. Moreover, the systemic changes in the metabolism are not expected to be limited to the serum or urine but could affect multiple organs and functional systems of an organism. Therefore, for the first time a multicompartment approach were used for a detailed description of the metabolic phenotype of the chronic helminth infection, beyond the conventionally used biofluids (blood, urine). The choice of compartments was guided by the current views on parasite biology and published studies on the morbidities associated with opisthorchiasis. To this end we analyzed serum, urine, and stool samples in addition to the organs, liver, spleen, gut (jejunum, ileum, and colon) and the kidneys. The liver, where the flukes reside, the three segments of intestine: jejunum, ileum, and colon where the eggs of the flukes are usually pass and can get trapped in granulomas, as well as the spleen, the largest part of the lymphatic system involved in the immune response of a host to a parasite infection [10, 11]. It has been shown that opisthorchiasis leads to nephropathy, thus the kidney – one of the key metabolic organs was also included in our analysis [12, 13]. Finally, not only have we looked at the metabolomics using NMR but we have also used the quantitative gas chromatography-mass spectrometric profiling of fatty acids in peripheral blood with the view to the role that lipid metabolism plays in a host response to an infection. Every compartment delivers an independent set of the data, which we refer to as “data blocks”. In total, eleven data blocks corresponding to each of the sample types were generated and analyzed (Figure 1).

Thus, with this report we for the first time apply an integrative analysis, using multiple biofluids and tissue extracts to describe metabolic changes in *O. felineus* infected animals at the chronic stage. We show that the shift in lipid metabolism in the serum and the changes in the spleen metabolism are the key features of the metabolic host adaptation at the chronic stage of *O. felineus* infection.

## Results

### Outline of the experiment, basic animal characteristics, histology, and metabolite quantification

Figure 1 summarizes our experimental design: an observational study with two (infected vs. non-infected) experimental equally sized experimental groups. One animal deceased before the end of the experiment, thus our final sample consists of 19 animals: 10 controls (5 females and 5 males) and 9 infected animals (4 females and 5 males). At the end of the experiment, the median body weight of the animals in the control and infected group was 133.85 and 118.20 grams, respectively, with no statistically significant difference. However, a gender specific comparison shows that body weight of the infected female animals is significantly lower than non-infected ones ( $p$ -value = 0.04). Similarly, liver weight shows no significant difference between the infected and non-infected group, while a gender specific comparison shows an increase in the liver weight for the infected male animals ( $p$ -value < 0.0001) (Supplementary Figure 1).

To obtain a representative overview of the metabolic differences between the infected and non-infected animals at twenty weeks post infection we collected the main biofluids (blood and urine), feces, the main metabolic organs (liver and kidney), three segments of the digestive tract (colon, ileum and jejunum) and the spleen. The histological analysis shows no difference between the segments of the digestive tract or the kidney of infected and uninfected groups. The liver samples of *O. felineus* infected animals had areas of inflammatory cell infiltration occurring around the bile ducts. The histological analysis of the liver samples of the control group showed no evidence of pathological changes in the liver or the bile ducts (Supplementary Figure 2).

For metabolomics analysis we took a quantitative targeted approach. Using the Chenomx NMR suite we quantified 22 metabolites in urine, 45 in liver, 39 in kidney, 37 in spleen and ileum, 33 in jejunum, 28 in colon samples, 24 in feces and 24 in the serum samples. Moreover, for serum nine resonances corresponding to the different parts of the serum lipoproteins were integrated (SI file data) and 38 short-, long- and very long-chain fatty acids in serum samples were

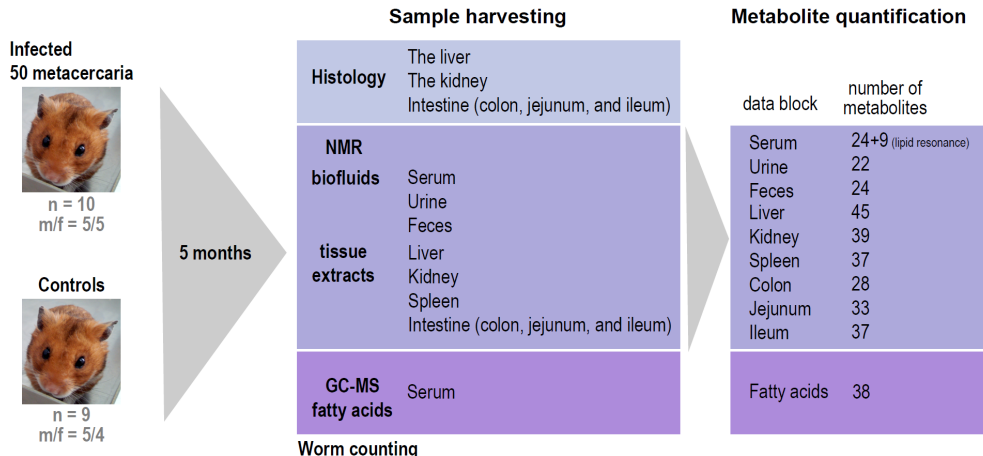


**Figure 1. Study design.** Twenty golden Syrian Hamsters (*Mesocricetus auratus*) of both genders were divided for two groups. Ten animals (five males and five females) were infected orally with 50 *O. felineus* metacercariae (Infected group). The remaining ten hamsters (five males and five females) were kept as a control group. During the experiment one female animal of the infected group died. Blood serum, urine, feces, liver, kidney, spleen, and intestine samples were collected in the 20th week post-infection from the animals of both groups for NMR, GC-MS and morphological analysis.

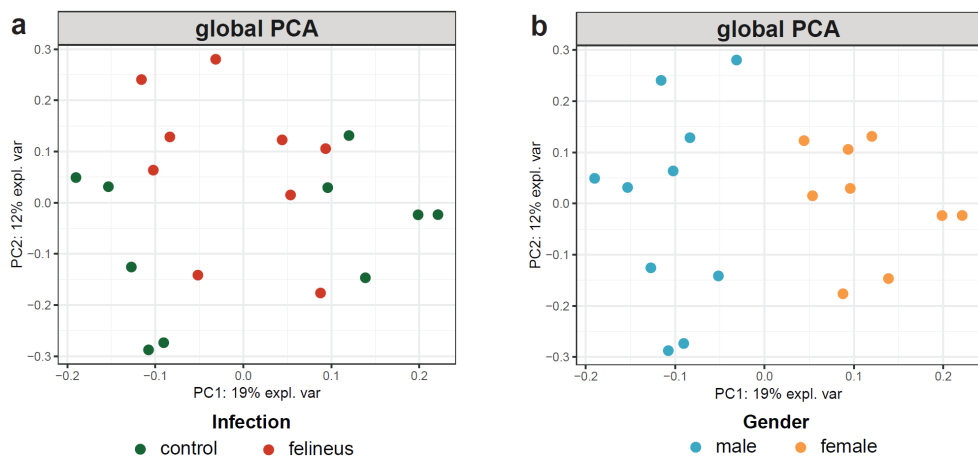


**Figure 2. The scores plot of the observations on the first two kernel principal components (PCs) in global PCA model built on all datasets; a: colored by the infection status; b: colored by gender of an animal. The model shows that not the infection, but gender is the main source of variance in the combined model.**

quantified using mass spectrometry. Only alanine and lactate were detected in all studied samples; tyrosine, valine, choline, phenylalanine, isoleucine, and leucine were found almost in all samples apart from urine. Creatine, glutamine, glutamate, uracil, fumarate, and glucose were quantified in all tissue samples. Supplementary Figure 3 summarizes the quantified metabolites across the samples.

### Multi-block analysis and selection of the relevant data blocks

Figure 2 shows a score plot of the global PCA model built on all 11 data blocks using an unsupervised multiple kernel method [14]. The method enables an integrated overview of the major trends in the data. The model required 5 principal components (PC) to explain 56 % of the variance with 31% covered by the first two components. The score plot of the model shows that not the infection (Figure 2a) but gender (Figure 2b) is the main source of variance in the combined model. The gender-related clustering is associated with the strongest component of the combined model which explains 19% of the total variance (Figure 2). To estimate the relative contribution of each individual block to the variance associated with infection, we applied an unsupervised multi-block modeling approach with correction for the gender effect. A practical realization of such analysis is the Multi-Omics Factor Analysis (MOFA) algorithm [15]. The MOFA can be viewed as a generalization of PCA for multi-block problems, which obtains a set of latent factors capturing the major variation across multiple data sets. Figure 3 summarizes the MOFA model built on 11 available blocks of data. The model converged to 10 factors, which cumulatively explain 77% of variation in the colon samples, 56% in the ileum, 56% in the jejunum, 70% in the liver, 77% in the spleen, 50% in the kidney, 71% in the urine samples, 65% in the stool, 69% in the serum, 70% in serum fatty acids, and only 8% in the lipoprotein block (Figure 3a). An overview of all factors (Supplementary Figure 4 and Figure 3b) shows that the latent factor 6 is aligned with the status of infection. Figure 3c shows the contribution of the individual data blocks to latent factor 6. It is evident that four blocks, namely the serum fatty acids (15% of the variance), the jejunum (13%), liver (12%) and spleen (12%) have strongest influence on the factor. Supplementary Figures 5-8 show the heat maps for the four selected blocks visualizing the weights of the individual metabolites on latent factor 6. However, even though the changes between the infected and non-infected animals can be identi-

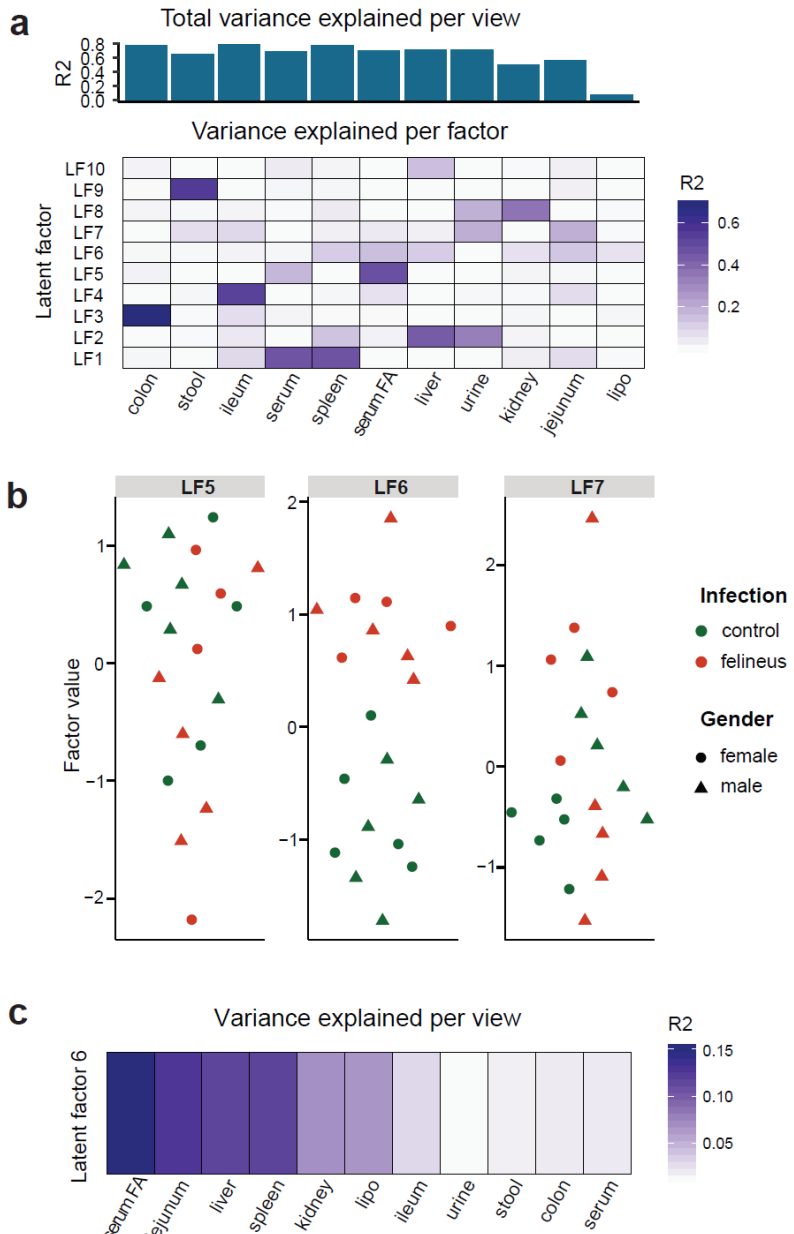


*Figure 3. Multi-Omics Factor Analysis (MOFA) modeling. The model built on the 11 available blocks of data. a: cumulative proportion of total variance ( $R^2$ ) per block of the data and variance explained per factor in each data block; b: the swarm plots showing the sample clustering along the factors values for the latent factors 5, 6 and 7; color shows infection status and shape – gender. c: representation of decomposition of variance ( $R^2$ ) in the latent factor 6 in each data block.*

fied visually, a selection of the most relevant metabolites which could compose an “infection signature” requires a regression-based strategy.

### Metabolic signature of chronic opisthorchiasis

Figure 4a shows the distribution of the individual samples along the first two component of the multiblock regression model. All datasets show clear clustering of two sample groups on the first component (covers 41.3% of variance in spleen data, 31.3% in liver, 27.8% in serum fatty acids, and 17.6% in jejunum). Figure 4b presents the variables in a clustered image map (Fig 4b) based on the Euclidean distance and complete linkage. It displays an unsupervised clustering between selected metabolites of spleen, liver, jejunum and serum fatty acids and the animals. Figure 4b presents all significantly increasing serum fatty acids in the infected animals; concentrations of inosine, lactate, myo-inositol, proline, sarcosine, theophylline, maltose, and carnitine are suppressed in the infected group, while liver uracil is increased; levels of methyl-histidine, leucine, citrate, in jejunum of *O. felineus* group are increased, while jejunum lactate and xanthine are decreased; and in spleen, the level of glutamine is lifted in presence of opisthorchiasis, when most metabolites are suppressed: ascorbate, alanine, myo-inositol, methionine, creatine, glutamate, fumarate, o-phosphocholine, and threonine. Figure 5 shows the correlation between the selected variables of the different blocks (correlation cut-off  $|0.7|$ ). Remarkably, all serum fatty acids show negative correlations with the metabolites of the tissues. The liver metabolites, namely inosine, lactate, carnitine, sarcosine, proline, and maltose positively correlate with the spleen and jejunum. With exception of glutamine, all spleen metabolites show positive correlations with liver and jejunum and negative one with the fatty acids; yet ascorbate correlates only with jejunum xanthine and serum DGLA. Of the jejunum metabolites, only lactate and xanthine show correlation with other data blocks.

To access our model performance, we applied 5-fold cross-validation. Supplementary Table 1 summarizes the cross-validated AUC values and their respective p-values for each block. Finally, we used an unsupervised clustering approach to test the selected subset of metabolites. The Supplementary Figure 9 shows the results of a PCA plot of the K-means clusters built on the selected variables; the samples are clustered according to the infection status, which implies that the

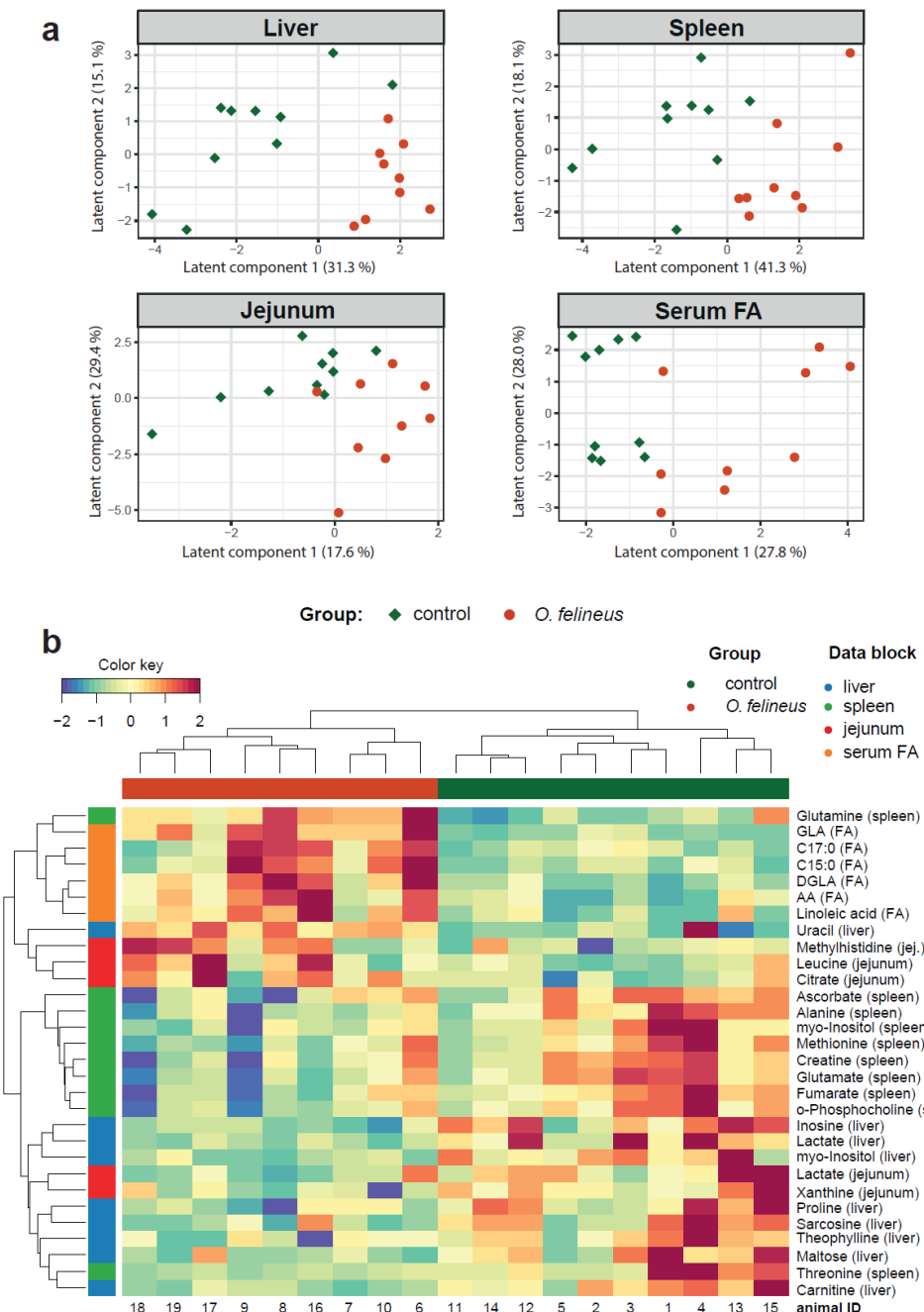


**Figure 4. DIABLO modelling.** *a:* Scores plots of each data blocks based on the first and the second components from the DIABLO model. *b:* A heat map built on the subset of the variables selected by a DIABLO model; the columns present the observations, the rows – the discriminating metabolites.

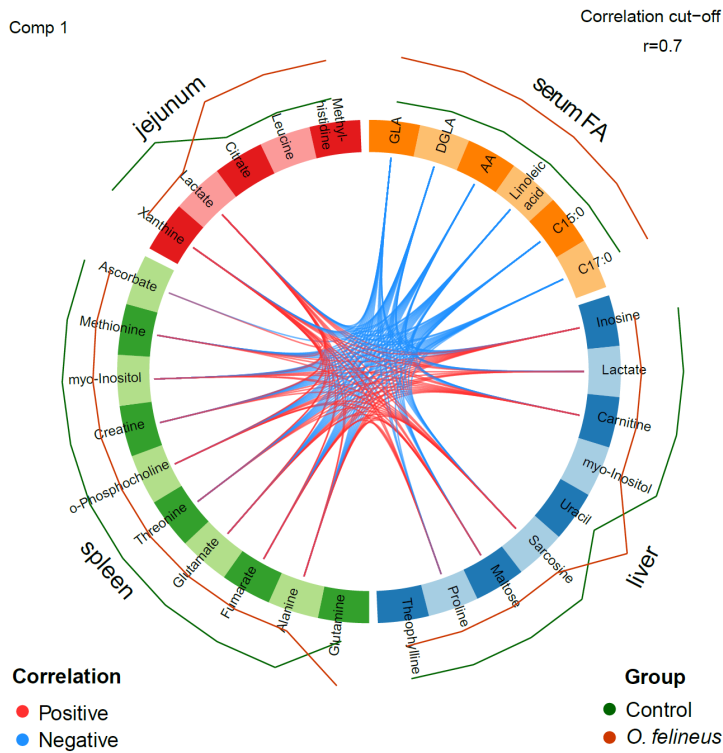


Figure 5. Plot represents the correlations (cut-off is 0.7) between variables of different blocks. All serum fatty acids show negative correlations with the metabolites of the tissues. With exception of glutamine, all spleen metabolites show positive correlations with liver and jejunum and negative one with the fatty acids. Of the jejunum metabolites, only lactate and xanthine show correlation with other data blocks.

samples within the clusters have similar metabolic characteristics.

### Pathway enrichment analysis on the metabolic signature of chronic *O. felineus*-infection

To get insight into the metabolic networks which could be associated with the infection we used the MetExplore environment. MetExplore can map the selected subsets of the metabolites into the pathways using organism specific databases. To this end, we used for mapping a subset of the spleen metabolites: ascorbate, methionine, myo-inositol, creatine, o-phosphocholine, threonine, glutamate, fumarate, alanine, and glutamine. Seven significant pathways involving were 30 reactions (Table 1) were chosen based on the Bonferroni-corrected p-values. All metabolites, except o-phosphocholine,

were mapped into the sub-networks (Supplementary Figure 10). The mapping of the liver metabolites did not result in any significantly enriched pathways ( $p$ -value  $\geq 0.05$ ). For jejunum only leucine and citrate were significantly associated with 2-oxocarboxylic acid metabolism. Thus, a limited number of the metabolites included in the analysis certainly restricts the possibilities for interpretation. Yet, spleen data clearly point towards a dis-regulation in the glutathione, glutamate, and alanine balance.

*Table 1. The result of the pathway enrichment analysis run on the metabolites selected by DIABLO multi-block modeling*

Significant pathway	KEGG identifier	Number of metabolites	Corrected p-value
<b>Spleen</b>			
Biosynthesis of amino acids	cge01230	6	2.4*10 <sup>-5</sup>
Aminoacyl-tRNA biosynthesis	cge00970	5	1.7*10 <sup>-4</sup>
Alanine, aspartate, and glutamate metabolism	cge00250	4	7.9*10 <sup>-4</sup>
Arginine and proline metabolism	cge00330	4	5.9*10 <sup>-3</sup>
Glutamine and glutamate metabolism	cge00471	2	0.017
Nitrogen metabolism	cge00910	2	0.023
Ascorbate and aldarate metabolism	cge00053	2	0.049
<b>Jejunum</b>			
2-Oxocarboxylic acid	cge01210	2	0.02

### Systemic balance of glutamine

It has been shown that an active infection process increases the catabolism of glutamine by the immune cells and as such changes the balance of glutamine, glutamine/glutamate and therefore the glutamine/alanine ratios [16]. The Figure 6 shows a comparative overview of glutamine balance for serum and all analyzed tissue samples. In agreement with existing data on the glutamine distribution its concentration in serum was higher than in the tissues, but there is no significant difference between serum concentrations of glutamine of the infected and non-infected animals. The glutamine/glutamate ratio is significantly lower in the liver of the infected animals ( $p$ -value = 0.02). The most consistent changes are observed in the spleen: the

concentration of glutamine (p-value = 0.0007) and corresponding glutamine/ glutamate (p-value < 0.00001) and glutamine/ alanine (p-value < 0.00001) ratios are higher in the spleen of the infected animals.

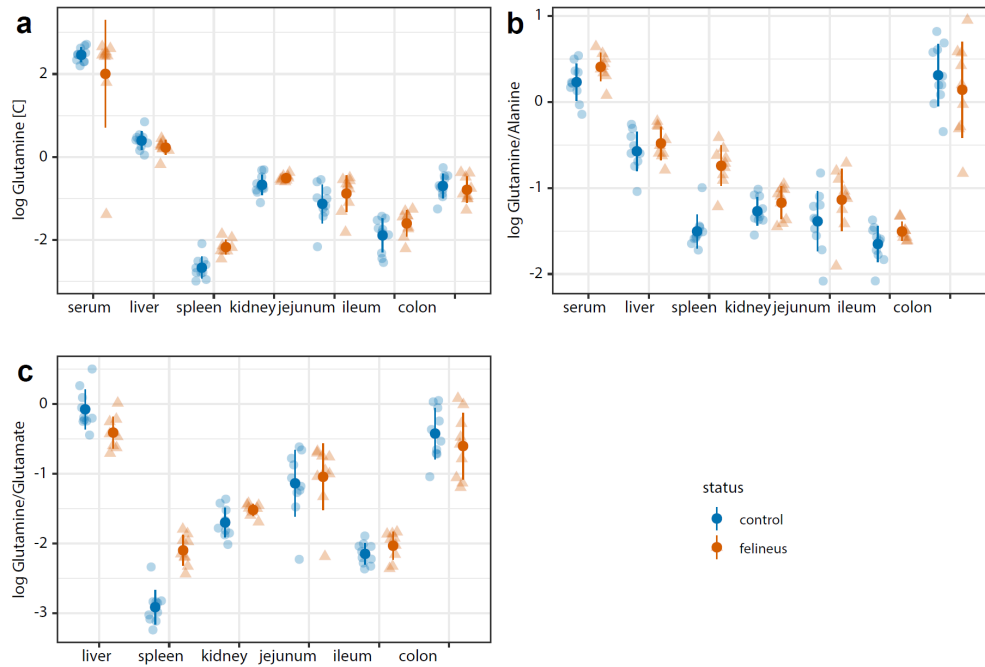


Figure 6. An overview of glutamine balance; a: glutamine. The glutamine concentration in serum was higher than in the tissues, but there is no significant difference of serum glutamine concentrations between the infected and non-infected animals. The most consistent changes are observed in the spleen (p-value = 0.0007). b: glutamine/alanine ratio. The glutamine/alanine ratio is higher in the spleen of the infected animals (p-value < 0.00001). c: glutamine/glutamate ratio. The glutamine/glutamate ratio is significantly lower in the liver tissue (p-value = 0.02) and higher in spleen tissue (p-value < 0.00001) for the infected animals. glutamine/glutamate (p-value < 0.00001).

## Discussion

Metabolic phenotyping of the pathological conditions is often restricted to the most accessible types of biological samples such as urine, serum, and feces. Yet, the systemic changes in the metabolism are not limited to the serum or urine but affect multiple organs and functional systems of an organism. Thus, aiming for an extended study of the metabolic phenotype of the chronic *O. felineus* infection we analyzed the samples from the most relevant compartments in the body. We have generated eleven data blocks, each corresponding to the samples analyzed. A set of four - liver, spleen, jejunum, and serum fatty acids were needed to, as a whole, explain the variance of the data related to chronic infection with *O. felineus*. (Figure 3). Thus, we can conclude that with the exception of the serum fatty acids at the chronic stage of the infection metabolic composition of the biofluids in the infected and non-infected animals remains rather similar. This observation is in an agreement both with the reports on the human material [7] and our recent publication on the animal model [8, 9]. Indeed, the field studies on the human body fluids show that the traditional confounding factors such as age, gender, BMI, and lifestyle affect their metabolic composition more strongly than the infection and simply override the effect of infection. In our report of the animal model we have shown that the infection related metabolomic changes in urine are the most pronounced from the fourth week up to the 12th weeks post-infection. At later time points no significant differences between the infected and control animals were detected [8]. The same applies to serum metabolites, and serum lipoprotein clusters: the statistically significant changes in amino acids and lipid clusters were observed in the first weeks after the infection [9]. Only few metabolites remained marginally different beyond the tenth week of infection. Thus, the current results and our previous reports show that after initial state of the “metabolic stress” [8, 9] organism reaches a state of metabolic homeostasis. This homeostasis, however, is sustained by a shift in the systemic lipid metabolism and local, organ specific metabolic rewiring.

Indeed, here we indicate that the circulating serum fatty acids, liver, spleen, jejunum show the strongest contribution to the systemic

metabolic changes associated with chronic opisthorchiasis. While our analysis does not exclude a possibility that other body compartments may contribute, the ones we identified here appear essential for the description of the metabolic changes triggered by chronic *O. felineus* infection. Our results show that “integrated metabolic signature” of chronic opisthorchiasis consists of 30 structures associated with lipid, amino acid, and energy metabolism. Moreover, six serum fatty acids, glutamine in the spleen, uracil in the liver and methyl-histidine, leucine and citrate in jejunum form a cluster of compounds that are increased in the chronically infected animals. The remaining 22 metabolites are depleted in the chronically infected group. Thus, the most important metabolic features of the chronic *O. felineus* infection are the increase in the circulating serum fatty acids, depletion of the amino acids pool in liver, spleen and jejunum. We believe that the given pattern points towards a specific type of systemic metabolic adaptation.

Indeed, a subset of the free fatty acids contributing to the infection signature contains two odd-chain fatty acids (pentadecanoic and heptadecanoic acids) and a group of the functionally linked structures, namely LA, GLA, DGLA and AA. All those structures were reported having a reverse association with a risk of type 2 diabetes [17-19]. Moreover, all mentioned fatty acids are either essential or conditionally essential which implies their dietary origin, or as the recent report on C15:0 and C17:0 fatty acids showing, they can be produced by gut microbiota [20, 21] and therefore the characterization of the microbiome at the chronic stage of opisthorchiasis should shed light on this. This, in turn, makes it possible to suggest involvement of the microbiota in regulation of metabolic homeostasis during the chronic infection. Furthermore, a recently published meta-analysis of the metabolic markers of the pre-diabetic and diabetic subjects show that the increased concentrations of the BCAs, aromatic amino acids, alanine, lactate and the glutamine/ glutamate ratio in the blood is characteristic for these conditions [22]. In our report on the time-resolved metabolomics of serum samples during *O. felineus* infection, we observed the strong decrease of the BCAs during the first weeks of infection [9]. Although the depletion of the circulating BCAs stabilizes around the tenth week, their levels remain lower than controls for the 22 weeks of the entire experiment [9]. In the current report, the concentration of alanine in the infected animals was lower not only in the liver and spleen, the organs which contribute to the infection signature but also

in serum (Figure 6). Considering the data on a negative association between helminth infections and a risk of metabolic syndrome [23], one might be tempted to focus on the similarities between the changes in the systemic metabolism triggered by the chronic *O. felineus* infection and the “protective” metabolic patterns. Yet, the chronic infection with *O. felineus* increases the risk of liver pathologies and even cancer [24]; thus, we believe that the prolonged changes in the utilization of the main metabolic fuel components and the local depletion of the amino acids pool leads gradually to a physiological condition which can be labeled as a “metabolically driven immunosuppression”. For instance, we show that metabolic activity of the spleen is suppressed in the infected animals; our data show the increased concentrations of glutamine/glutamate and glutamine/alanine ratios in the spleen of the infected animals. This, in turn, implies a reduced conversion of glutamine to glutamate by glutaminase. The glutamine/glutamate ratio is often used for a rough assessment of the cell proliferation activity: a high ratio indicates a reduced consumption of glutamine and consequently lower proliferation rates within an organ [25]. It is worth of mentioning that in liver the glutamine/glutamate ratio is shifted in the opposite way, thus suggesting a higher metabolic activity of the liver of the infected animals. This is in agreement with the liver responses to the presence of the parasite, the adaptations to the mechanical damage of the biliary system, and the processes controlling the inflammation, eosinophilia and periductal fibrosis [26]. All those factors are probably responsible for the increased weight of the organ in the infected animals (Supplementary Figure 1). Finally, the pathway enrichment analysis suggests an alteration in the keto-acids pathways (2-oxocarboxylic acids metabolism) in jejunum, which is in agreement with the reported increased concentration of leucine (Supplementary Figure 11). Leucine is a strictly ketogenic amino acid, which implies that it is converted to the fat rather than glucose. Moreover, an active catabolism of leucine is essential for regulation of intestinal immune function [27] and regulation of the entire mTOR signaling system [28]. Thus, although the limited number of the metabolites that change upon chronic opisthorchiasis restricts our ability to draw firm mechanistic insights, they do indicate a local depletion of the amino acids pool, an alteration of the ketogenic pathways in the jejunum and last but not least a suppressed metabolic activity of the spleen. We can tentatively describe this combination of the metabolic changes a “met-

abolically mediated immunosuppressive status of organism" which develops during a chronic infection. A prolonged status of the immuno-hibernation might be one of the factors which increases risk of the infection related malignancy.

# Materials and Methods

## Ethics statement

All procedures with animals were carried out according to the recommendations of the national guidelines for animal caring: 12.08.1977 N 755 "On measures to further improve the organizational forms of work using experimental animals" and approved by the Siberian State Medical University (license number 5786 issued on 26.02.2018).

## Parasites, experimental opisthorchiasis model and experimental design

Twenty golden Syrian Hamsters (*Mesocricetus auratus*) of both genders were purchased from the animal facility of the Institute of Bioorganic Chemistry Academicians M.M. Shemyakin and U. A. Ovchinnikov. The hamsters were housed in groups of five with provided food and water ad libitum for the duration of the experiment. After one week of acclimatization, ten animals (five males and five females) were infected orally with 50 *O. felineus* metacercariae in phosphate-buffered saline (PBS) of each hamster (Infected group). *O. felineus* metacercariae were obtained from naturally infected fishes captured from the Ob river in endemic areas of Tomsk, Russian Federation. The viable metacercariae were collected and identified by microscopy from the pepsin-HCl-digested muscular and subcutaneous tissues. The remaining ten hamsters (five males and five females) were subjected to the same procedures with PBS (control group). During the experiment one female animal of the infected group died.

## Sample collection and assessment of the infection

Blood serum, urine, feces samples were collected in the 20th week post-infection from the animals of both groups. The hamsters were placed individually into sterile empty glass crates for collecting urine and feces, where separation of stool from urine was facilitated. The urine samples were collected into labeled cryotubes over ice and stored frozen at -80°C. 2-3 pellets of animal feces were collected into labeled cryotubes over ice and stored frozen at -80°C until NMR analysis.

On the day after collecting the biofluid samples, the animals were sacrificed, and tissue samples and serum were collected for NMR and morphological analysis. The blood samples were collected into vacutainer tubes (no additive), left on ice for coagulation, and centrifuged at 3500 g for 10 min. The provided serum was transferred into cryotubes and stored at -80°C. Small samples of the 3 intestinal parts (colon, jejunum and ileum), part of the liver, and the right kidney were transferred into 5 mL tubes containing a solution of 4% buffered formalin for subsequent histological analysis via hematoxylin and eosin staining. The left kidney and the spleen were harvested and transferred into a 2 mL cryotube, immediately immersed in liquid nitrogen and stored at -80 °C for NMR analysis. Small portions (~0.5 cm) of intestinal tissue (colon, jejunum and ileum) were cut from the middle of each section. Then, the intestinal tissue portions were washed with PBS, transferred into cryotubes, immersed in liquid nitrogen, and stored at -80 °C for NMR analysis. The rest of the liver from infected animals after collecting histological material, was treated over ice to remove flukes from the bile ducts. The liver then was collected into the cryotubes, immersed in liquid nitrogen, and stored at -80 °C. The liver from control group of animals was treated by the same procedure as the liver of infected animals.

Assessment of the infection intensity was performed by counting worms in the liver and bile ducts for each infected hamster.

### **Sample preparation for NMR data acquisition**

All chemicals used for the buffer solutions were purchased from Sigma-Aldrich except for the 2H2O (Cortecnet) and the 3-(trimethylsilyl)propionic-2,2,3,3-d4acid sodium salt (TSP) (Cambridge Isotope Laboratories Inc). Two buffer solutions were prepared. Buffer solution A was a disodium phosphate buffer in H2O/D2O (80/20) with pH of 7.4 containing 6.15 mM NaN3 and 4.64 mM TSP. Buffer solution B was a disodium phosphate buffer in D2O (pH = 7.4) containing 1.5 M K2H-PO4, 2 mM NaN3 and 4 mM of TSP. 96-well Ritter Deepwell plates were acquired from Novaveth B.V. and NMR tubes were purchased from Bruker Biospin Ltd.

The serum samples were thawed at 4°C and were mixed by inverting the tubes 10 times. Next, the samples (120 µL) were mixed with 120 µL of buffer solution A using a Gilson 215 liquid handler in combination with a Bruker SampleTrack system. For each sample,

190  $\mu$ L of buffer-serum mixture was transferred into 3-mm SampleJet NMR tubes in 96 tube racks using a modified Gilson 215 tube filling station and kept at 6°C on a SampleJet sample changer while queued for acquisition.

The sample preparation of urine samples was performed using the method as described elsewhere [8, 9] with minor changes in the sample preparation step: 630  $\mu$ L of urine from each sample were mixed with 70  $\mu$ L buffer solution B; 565  $\mu$ L of urine-buffer mixture were transferred to 5 mm SampleJet NMR tubes.

2-3 fecal pellets from each animal were weighed and mixed with milli-Q water at a ratio of ratio 1:5. The mixtures were homogenized by bead beating with zirconium oxide beads of 1 mm diameter for 3 min in a Bullet Blender 24 (Next Advance Inc., USA). The homogenized mixtures were centrifuged at 16100  $\times$  g for 20 min at 4 °C. The supernatants were carefully collected, and centrifugation was repeated under the same conditions. After the second centrifugation, 500  $\mu$ L supernatant of each sample was taken for filtration.

The filters used for the filtration step were molecular weight cut-off (MWCO) filters Vivaspin 500 3kDa (GE Healthcare, UK). These filters need to be carefully washed prior to use in order to remove the significant glycerol contamination that was present in the unused filters. The washing procedure was as follows: the filters were centrifuged twice with 0.5 mL milli-Q water at 15000  $\times$  g for 20 min at 20°C. Every time residual water was removed from the filters by allowing it to drain out properly. Eppendorf tubes were filled with 1 mL milli-Q water, after which the rinsed filters were inserted. 0.5 mL milli-Q water was added into the filter and the Eppendorf tubes were stored overnight at 4°C. Then water was removed by centrifugation at 15000  $\times$  g for 20 min at 20°C and the filters were rinsed again at the same conditions then residual water was removed from a filter by letting it drain. The filters were used immediately to avoid destroying of the membrane.

Using the washed filters, the supernatant of the second centrifugation of the feces-water mixture was then filtrated at 15000  $\times$  g for 20 min at 20 °C four times. Subsequently 150  $\mu$ L filtrate was mixed with 30  $\mu$ L milli-Q water and 20  $\mu$ L buffer solution B. 190  $\mu$ L of the mixture of each sample were transferred into 3 mm SampleJet NMR tubes.

The frozen liver, the spleen, the left kidney and samples of the three parts of the intestine (colon, jejunum and ileum) were weighed

and mixed with a 70 % methanol: 30 % milli-Q water mixture with the tissue:solvent ratio = 1:3. The mixtures were homogenized by applying 6 cycles of 1 min of bead beating and 1 min cooling on ice. For bead beating zirconium oxide beads of 1 mm diameter were used. The homogenized mixtures were centrifuged at 16100 x g for 20 min at 4 °C. The supernatants were collected and dried under a stream of nitrogen. Then, the dry residues were resuspended with D2O and then centrifuged at 16100 x g for 10 min at 4°C. Buffer B was added to the supernatant for a final buffer concentration of 10%. The sample/buffer mixtures of liver, kidney, spleen, jejunum and ileum were transferred into 3mm SampleJet NMR tubes and colon samples were transferred into 1.7 mm SampleJet NMR tubes.

### **NMR data acquisition and spectral data processing**

<sup>1</sup>H NMR data were collected using a Bruker 600 MHz AVANCE II spectrometer equipped with a 5 mm TCI cryogenic probe head and a z-gradient system. A Bruker SampleJet sample changer was used for sample insertion and removal. Two NMR protocols were used, one for the serum samples and one for all the others.

All experiments were recorded at 300 K, except the serum samples, which were recorded at 310K. A fresh sample of 99.8% methanol-d4 was used for temperature calibration [31]. The axial shims were optimized automatically before every measurement. Duration of 90° pulses were automatically calibrated for each individual sample using a homonuclear-gated mutation experiment [32] on the locked and shimmed samples after automatic tuning and matching of the probe head.

Four NMR experiments were performed on each serum sample: NOESY1D, CPMG, diffusion edited, and 2D JRES. The NOESY1D experiment was recorded using the first increment of a NOESY pulse sequence [33] with presaturation ( $\gamma B_1 = 25$  Hz) during a relaxation delay of 4 s and a mixing time of 10 ms for efficient water suppression [34]. 64 scans of 65,536 points covering a sweepwidth of 18,029 Hz were recorded and zero-filled to 65,536 complex points prior to Fourier transformation. A standard 1D Carr-Purcell-Meiboom-Gill (CPMG) pulse sequence with presaturation was used to for the acquisition of T2-filtered spectra. A pulse train of 128 refocusing pulses with individual spin echo delays of 0.6 ms was applied resulting in a total T2 filtering delay of 78 ms. After applying 4 dummy scans, a

total of 73,728 data points covering a spectral width of 12,019 Hz were collected. Otherwise the parameters were similar to the 1DNOESY experiment. The diffusion-edited spectrum was recorded with presaturation. The pulse sequence parameters were similar to those of the 1DNOESY experiment. An exponential window function was applied with a line-broadening factor of 1.0 Hz. After Fourier transformation, the spectra were automatically phase and baseline corrected and automatically referenced to the internal standard (TSP = 0.0 ppm). Afterwards, the spectra were referenced to the anomeric glucose doublet (5.23 ppm).

J-resolved spectra (JRES) were recorded with a relaxation delay of 2 s with presaturation ( $\gamma B_1 = 25$  Hz) and 8 scans for each increment in the indirect dimension. A data matrix of  $40 \times 12,288$  data points was collected covering a sweep width of  $78 \times 10,000$  Hz. A sine-shaped window function was applied to both dimensions and the data was zero-filled to  $256 \times 16,384$  complex data points prior to Fourier transformation. In order to remove the skew, the resulting data matrix was tilted along the rows by shifting each row ( $k$ ) by  $0.4992 \cdot (128-k)$  points and symmetrised about the central horizontal lines.

The NMR parameters were similar as for serum, except for the use of a stronger presaturation field ( $\gamma B_1 = 50$  Hz). For the 1D experiments, 16 scans of 65536 points covering a sweepwidth of 12,336 Hz were accumulated, except for the colon and ileum samples, where 64 scans were used. Other parameters were similar as to those of the serum NOESY1D experiments. The 2D JRES experiments were also recorded with similar settings as to those of serum, with 2 scans per increment in the indirect dimension, and 8 scans per increment for colon and ileum.

### **Identification and quantification of the metabolites**

Identification of small metabolites (< 1000 Da) was performed by exhausting search of the total 1D and 2D JRES data using the proprietary Bbiorfcode (Bruker Biospin Ltd.).

Quantification of the small metabolites and glycogen in liver samples was performed manually with the Chenomx NMR suite 8.1 software (Chenomx Inc.). Concentrations were extracted using the known TSP concentration (0.4 mM).

Serum lipoproteins and cholesterol were identified and quantified as described elsewhere [9].

### GS-MS analysis of serum fatty acids

GC-MS quantitate analysis of medium- and long-chain fatty acids in serum samples was performed accordingly the protocol [30]. GC-MS quantitate analysis of serum short-chain fatty acids was performed accordingly the protocol [29].

### Data analysis

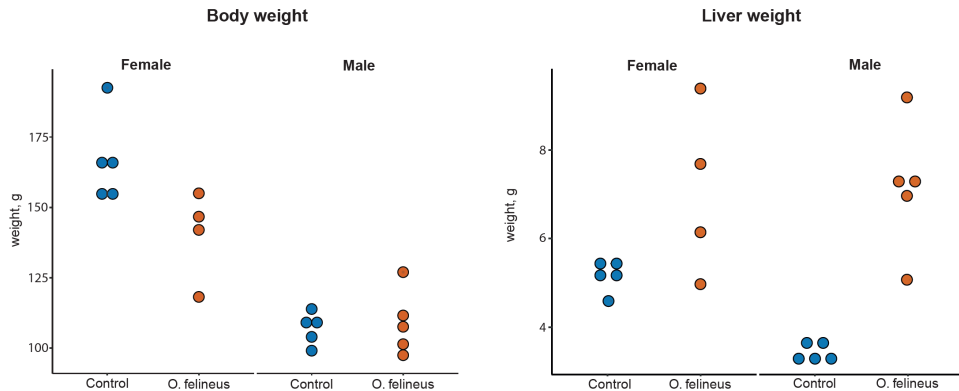
All data analysis was performed with the R statistical environment (<http://www.r-project.org/>, R versions 3.6.0, 3.6.1). Basic data table handling was performed with a help of the tidyverse package (version 1.1.2); the data.Normalization function of the clusterSim (version 0.48-1) package was used for the data normalization before the modelling. For the evaluation of the principle source of variance on multi-block data and selection of the most relevant data blocks the Multi-Omics Factor Analysis (MOFA) package 1.2.0 and mixKernel (version 0.3) were used. To dissect an optimal subset of metabolites we used a regression approach, namely the DIABLO (Data Integration Analysis for Biomarker discovery using Latent variable approaches for 'Omics studies) tool of the mixOmics package (version 6.10.1). DIABLO combines a surprised multi-block modeling with variable selection. K-means clustering was computed using the standard of R command. For data visualization the ggplot2 package (version 3.2.1) was used.

Metabolic network enrichment analysis was performed in the MetExplore v2.23.15 environment, using the KEGG global network for a Chinese hamster (*Cricetulus griseus*) (a network for a golden Syrian hamster (*Mesocricetus auratus*) is not available currently) [35, 36]. The metabolites selected by the multi-block regression modeling were used for the pathway enrichment on each block separately. Only the pathways with  $p < 0.05$  after Bonferroni correction were included in the resulting graphs.

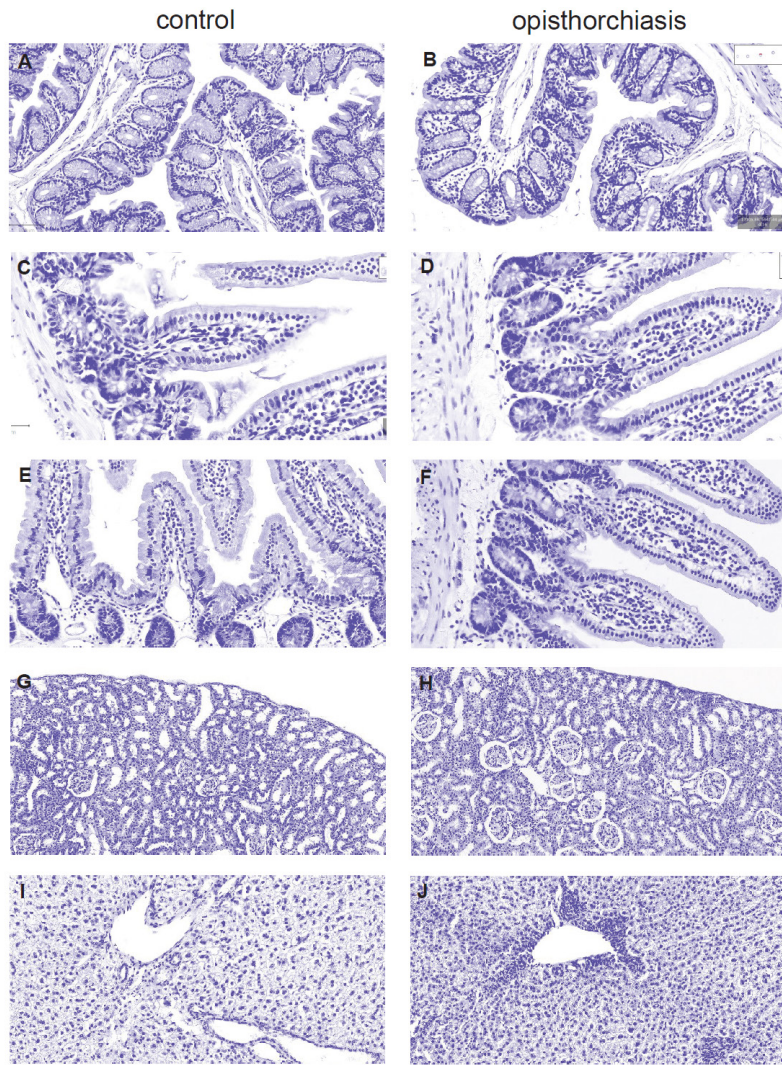
## Acknowledgments

The research was supported by The Tomsk State University competitiveness improvement programme.

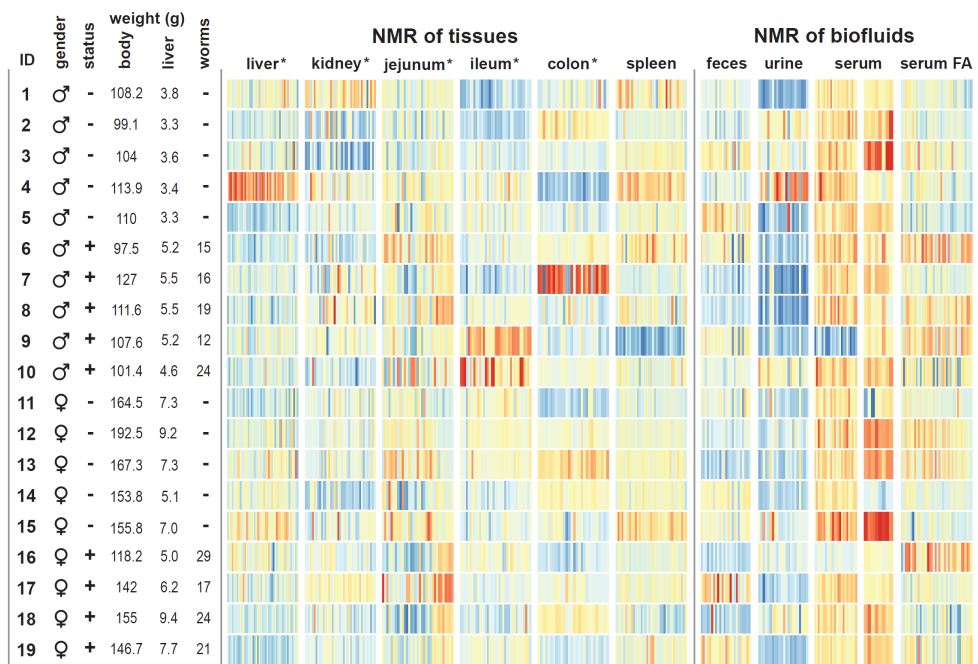
## Supplementary information



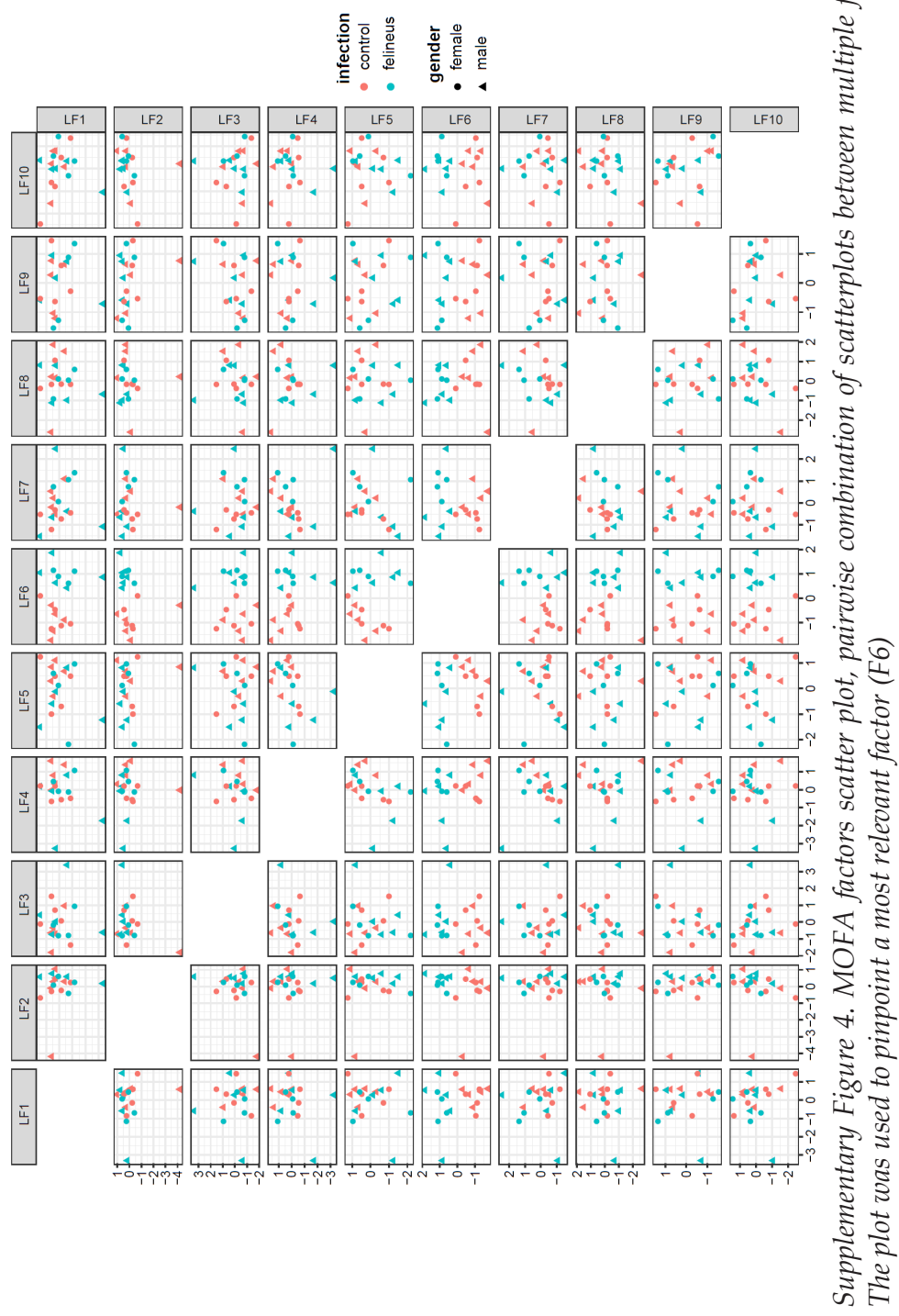
*Supplementary Figure 1. The body and liver weights in the experimental animals. The values are presented separately for the female and male animals. A gender specific comparison shows that body weight of the infected female animals is significantly lower than non-infected ones ( $p$ -value = 0.04); liver weight of infected male animals is higher ( $p$ -value < 0.0001)*

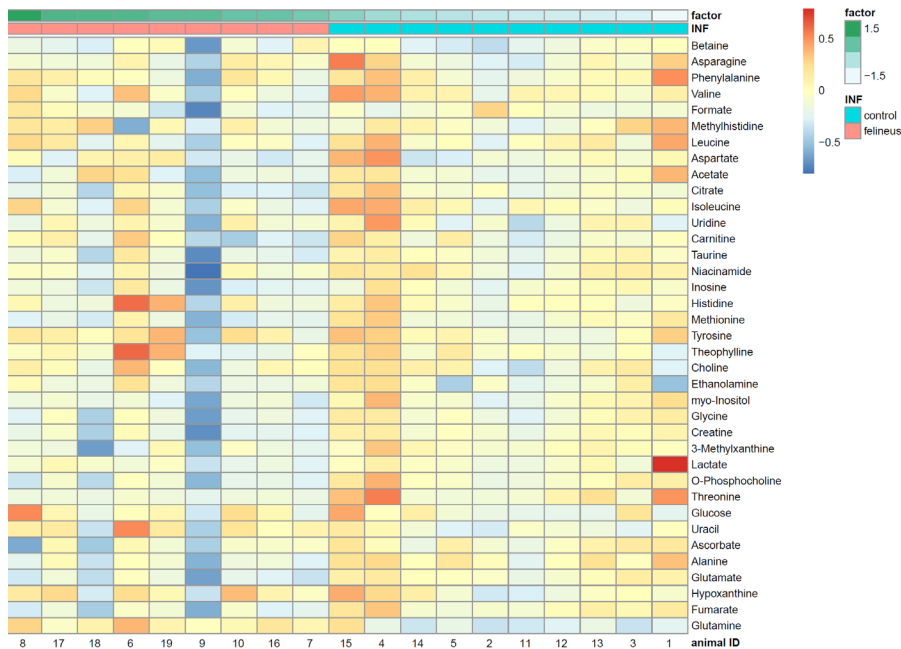


*Supplementary Figure 2. Representative images of histological changes (hematoxylin and eosin staining) in investigated compartments. A: colon of the control animal, B: colon of the infected animal; C: ileum of the control animal, D: ileum of the infected animal; E: jejunum of the control animal, F: jejunum of the infected animal; G: kidney of the control animal, H: kidney of the infected animal; I: liver of the control animal, J: liver of the infected animal. There is no apparent difference between the segments of the digestive tract or the kidney of infected and uninfected groups. The liver samples of *O. felineus* infected animals had areas of inflammatory cell infiltration occurring around the bile ducts. The histological analysis of the liver samples of the control group showed no evidence of pathological changes in the liver or the bile ducts.*

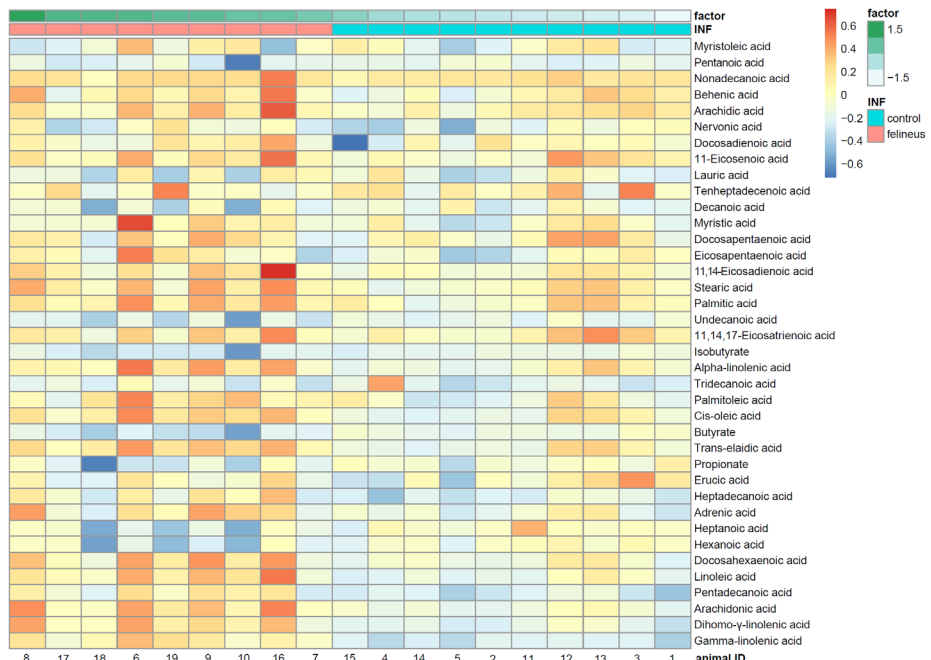


Supplementary Figure 3. A graphical summary of the entire data set.

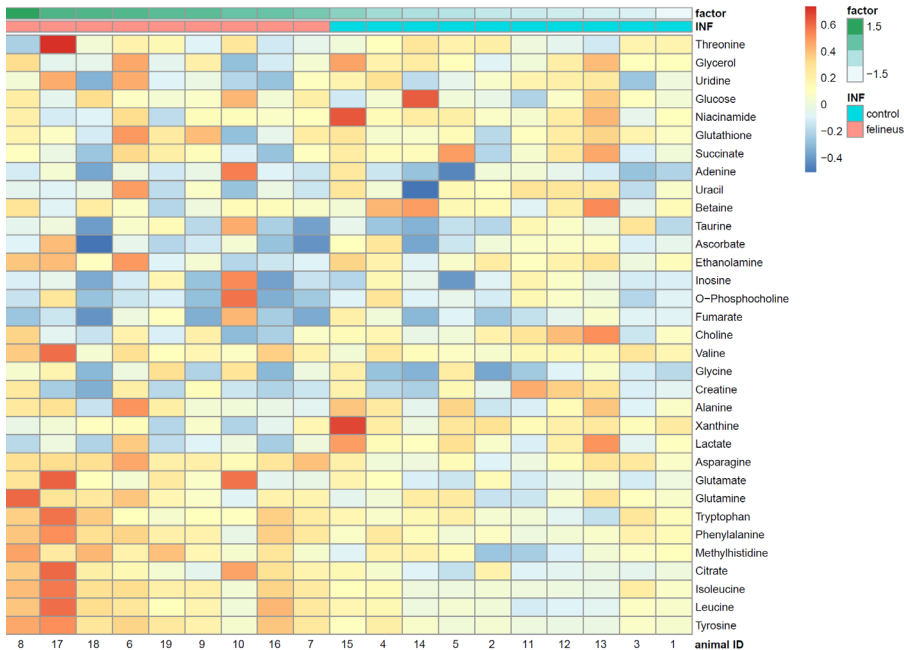




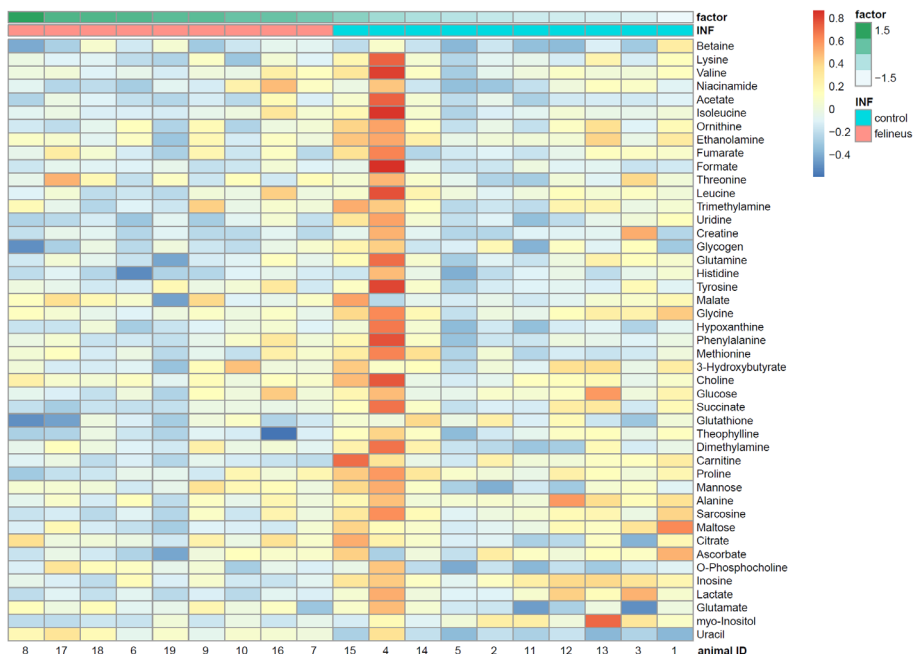
Supplementary Figure 5. Spleen. Heatmap of the normalized metabolites values. Samples are ordered by their factor values.



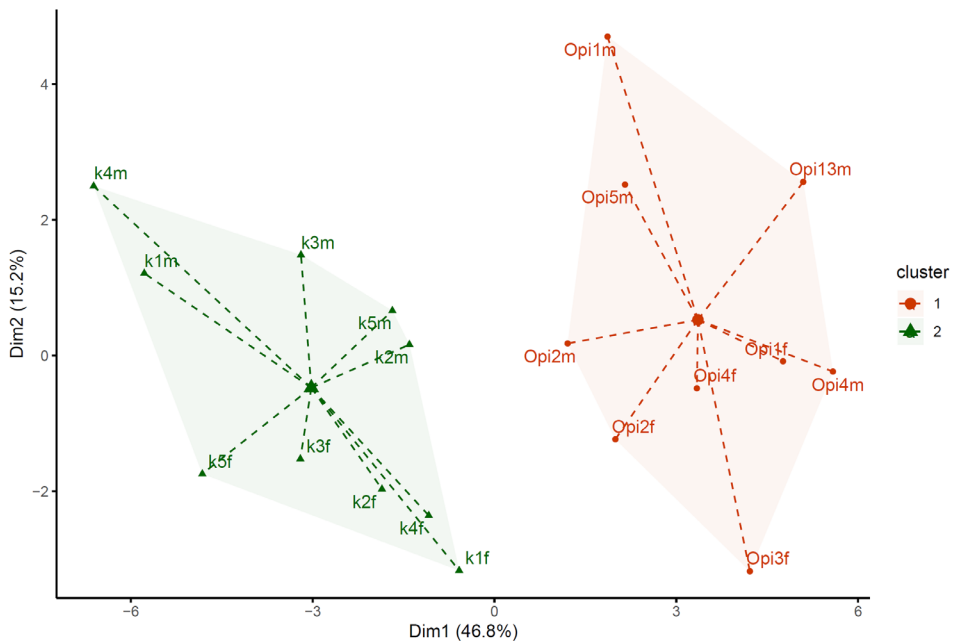
Supplementary Figure 6. Serum Fatty Acids. Heatmap of the normalized metabolites values. Samples are ordered by their factor values.



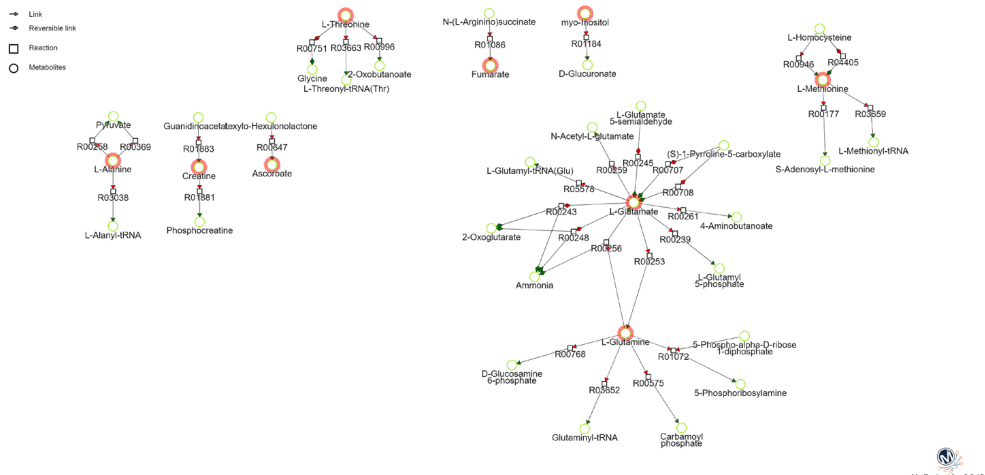
Supplementary Figure 7. Jejunum. Heatmap of the normalized metabolites values. Samples are ordered by their factor values.



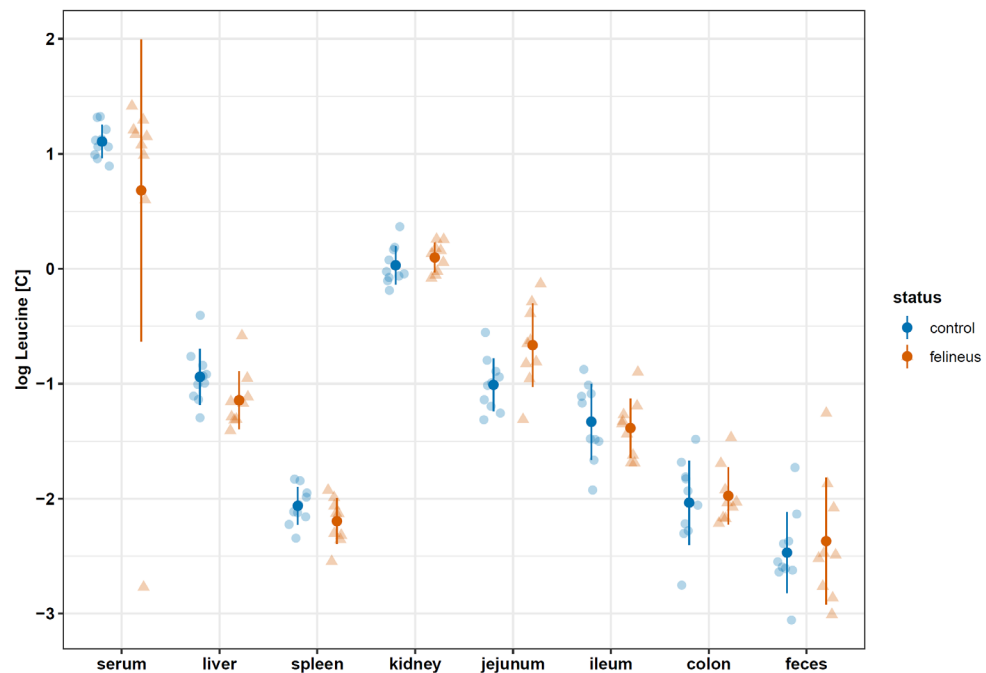
Supplementary Figure 8. Liver. Heatmap of the normalized metabolites values. Samples are ordered by their factor values.



*Supplementary Figure 9. K-means clustering solution built on the subset of the metabolites selected with a DIABLO (mixOmics) model.*



*Supplementary Figure 10. The map of the metabolic networks of the spleen which could be associated with the *O. felineus* infection. MetExplore was used for mapping selected subsets of the metabolites into the pathways using organism specific database. Seven significant pathways involving were 30 reactions were chosen based on the Bonferroni-corrected p-values.*



Supplementary Figure 11. Overview of the Leucine balance

Supplementary Table 1. 5-fold cross-validation AUC values and their respective p-values for each data block.

Block	cross-validated AUC	p-value
liver	0.922	0.0019
spleen	0.967	0.0002
jejunum	0.900	0.0033
serum fatty acids	1.000	0.0002

## References

1. Petney TN, Andrews RH, Sajjuntha W, Wenz-Mucke A, Sithithaworn P. The zoonotic, fish-borne liver flukes *Clonorchis sinensis*, *Opisthorchis felineus* and *Opisthorchis viverrini*. *Int J Parasitol*. 2013;43(12-13):1031-46.
2. Mairiang E, Mairiang P. Clinical manifestation of opisthorchiasis and treatment. *Acta Tropica*. 2003;88(3):221-7.
3. Pungpak S, Chalermrut K, Harinasuta T, Viravan C, Schelp PF, Hempfling A, et al. *Opisthorchis viverrini* infection in Thailand: symptoms and signs of infection--a population-based study. *Trans R Soc Trop Med Hyg*. 1994;88(5):561-4.
4. Liu LX, Harinasuta KT. Liver and intestinal flukes. *Gastroenterol Clin North Am*. 1996;25(3):627-36.
5. Humans IWGOrEoCRt. Biological agents. Volume 100 B. A review of human carcinogens. IARC Monogr Eval Carcinog Risks Hum. 2012;100(Pt B):1-441.
6. Young ND, Nagarajan N, Lin SLJ, Korhonen PK, Jex AR, Hall RS, et al. The *Opisthorchis viverrini* genome provides insights into life in the bile duct. *Nature Communications*. 2014;5.
7. Young ND, Gasser RB. *Opisthorchis viverrini* Draft Genome - Biomedical Implications and Future Avenues. *Asiatic Liver Fluke - from Basic Science to Public Health*, Pt A. 2018;101:125-+.
8. Young ND, Campbell BE, Hall RS, Jex AR, Cantacessi C, Laha T, et al. Unlocking the Transcriptomes of Two Carcinogenic Parasites, *Clonorchis sinensis* and *Opisthorchis viverrini*. *Plos Neglected Tropical Diseases*. 2010;4(6).
9. Suttiprapa S, Sotillo J, Smout M, Suyapoh W, Chaiyadet S, Tripathi T, et al. *Opisthorchis viverrini* Proteome and Host-Parasite Interactions. *Asiatic Liver Fluke - from Basic Science to Public Health*, Pt B. 2018;102:45-72.
10. Mulvenna J, Sripa B, Brindley PJ, Gorman J, Jones MK, Colgrave ML, et al. The secreted and surface proteomes of the adult stage of the carcinogenic human liver fluke *Opisthorchis viverrini*. *Proteomics*.

2010;10(5):1063-78.

11. Kokova D, Mayboroda OA. Twenty Years on: Metabolomics in Helminth Research. *Trends Parasitol.* 2019.

12. Fedorova OS, Fedotova MM, Sokolova TS, Golovach EA, Kovshirina YV, Ageeva TS, et al. *Opisthorchis felineus* infection prevalence in Western Siberia: A review of Russian literature. *Acta Tropica.* 2018;178:196-204.

13. Keiser J, Utzinger J. Food-borne trematodiases. *Clin Microbiol Rev.* 2009;22(3):466-83.

14. Pomaznay MY, Logacheva MD, Young ND, Penin AA, Ershov NI, Katokhin AV, et al. Whole transcriptome profiling of adult and infective stages of the trematode *Opisthorchis felineus*. *Parasitology International.* 2016;65(1):12-9.

15. Kokova DA, Kostidis S, Morello J, Dementeva N, Perina EA, Ivanov VV, et al. Exploratory metabolomics study of the experimental opisthorchiasis in a laboratory animal model (golden hamster, *Mesocricetus auratus*). *PLoS Negl Trop Dis.* 2017;11(10):e0006044.

16. Rodrigues MV, de Castro SO, de Albuquerque CZ, Mattaraia VGD, Santoro ML. The gingival vein as a minimally traumatic site for multiple blood sampling in guinea pigs and hamsters. *Plos One.* 2017;12(5).

17. Diehl KH, Hull R, Morton D, Pfister R, Rabemampianina Y, Smith D, et al. A good practice guide to the administration of substances and removal of blood, including routes and volumes. *J Appl Toxicol.* 2001;21(1):15-23.

18. Verhoeven A, Slagboom E, Wuhrer M, Giera M, Mayboroda OA. Automated quantification of metabolites in blood-derived samples by NMR. *Analytica Chimica Acta.* 2017;976:52-62.

19. Wu DH, Chen AD, Johnson CS. An Improved Diffusion-Ordered Spectroscopy Experiment Incorporating Bipolar-Gradient Pulses. *Journal of Magnetic Resonance Series A.* 1995;115(2):260-4.

20. Verhoeven A, Giera M, Mayboroda OA. KIMBLE: A versatile visual NMR metabolomics workbench in KNIME. *Analytica Chimica Acta.* 2018;1044:66-76.

21. De Meyer T, Sinnaeve D, Van Gasse B, Tsioporkova E, Rietzschel ER, De Buyzere ML, et al. NMR-based characterization of metabolic alterations in hypertension using an adaptive, intelligent binning algorithm. *Analytical Chemistry.* 2008;80(10):3783-90.

22. Dieterle F, Ross A, Schlot-

terbeck G, Senn H. Probabilistic quotient normalization as robust method to account for dilution of complex biological mixtures. Application in  $^1\text{H}$ -NMR metabonomics. *Analytical Chemistry*. 2006;78(13):4281-90.

23. Smilde AK, Jansen JJ, Hoefsloot HCJ, Lamers RJAN, van der Greef J, Timmerman ME. ANOVA-simultaneous component analysis (ASCA): a new tool for analyzing designed metabolomics data. *Bioinformatics*. 2005;21(13):3043-8.

24. Stekhoven DJ, Buhlmann P. MissForest--non-parametric missing value imputation for mixed-type data. *Bioinformatics*. 2012;28(1):112-8.

25. Mallol R, Rodriguez MA, Brezmes J, Masana L, Correig X. Human serum/plasma lipoprotein analysis by NMR: Application to the study of diabetic dyslipidemia. *Progress in Nuclear Magnetic Resonance Spectroscopy*. 2013;70:1-24.

26. Smilde AK, Westerhuis JA, Hoefsloot HCJ, Bijlsma S, Rubingh CM, Vis DJ, et al. Dynamic metabolomic data analysis: a tutorial review. *Metabolomics*. 2010;6(1):3-17.

27. Kaewpitoon N, Kaewpitoon SJ, Pengsaa P, Sripa B. *Opisthorchis viverrini*: The carcinogenic human liver fluke. *World J Gastroentero*. 2008;14(5):666-74.

28. Mel'nikov V, Skarednov NI. Clinical aspects of acute opisthorchiasis in the nonnative population of the northern Ob region. *Med Parazitol (Mosk)*. 1979;48(5):12-6.

29. WHO. Opisthorchiasis felinea [Available from: [https://www.who.int/foodborne\\_trematode\\_infections/opisthorchiasis/Opisthorchiasis\\_felinea/en/](https://www.who.int/foodborne_trematode_infections/opisthorchiasis/Opisthorchiasis_felinea/en/)].

30. Saric J, Li JV, Wang Y, Keiser J, Veselkov K, Dirnhofer S, et al. Panorganismal metabolic response modeling of an experimental *Echinostoma caproni* infection in the mouse. *J Proteome Res*. 2009;8(8):3899-911.

31. Saric J, Li JV, Wang Y, Keiser J, Bundy JG, Holmes E, et al. Metabolic profiling of an *Echinostoma caproni* infection in the mouse for biomarker discovery. *PLoS Negl Trop Dis*. 2008;2(7):e254.

32. Weinstein MS, Fried B. The Expulsion of *Echinostoma-Trivolvis* and Retention of *Echinostoma-Caproni* in the Icr Mouse - Pathological Effects. *International Journal for Parasitology*. 1991;21(2):255-7.

33. Wu JF, Holmes E, Xue J, Xiao SH, Singer BH, Tang HR, et al. Metabolic alterations in the hamster co-infected with

Schistosoma japonicum and Necator americanus. *Int J Parasitol.* 2010;40(6):695-703.

34. Pershina AG, Ivanov VV, Efimova LV, Shevelev OB, Vtorushin SV, Perevozchikova TV, et al. Magnetic resonance imaging and spectroscopy for differential assessment of liver abnormalities induced by *Opisthorchis felineus* in an animal model. *Plos Neglected Tropical Diseases.* 2017;11(7).

35. Kostidis S, Kokova D, Dementeva N, Saltykova IV, Kim HK, Choi YH, et al. (1)H-NMR analysis of feces: new possibilities in the helminthes infections research. *BMC Infect Dis.* 2017;17(1):275.

36. Jimenez B, Holmes E, Heude C, Tolson RF, Harvey N, Lodge SL, et al. Quantitative Lipoprotein Subclass and Low Molecular Weight Metabolite Analysis in Human Serum and Plasma by (1)H NMR Spectroscopy in a Multilaboratory Trial. *Anal Chem.* 2018;90(20):11962-71.

37. Barrilero R, Gil M, Amigo N, Dias CB, Wood LG, Garg ML, et al. LipSpin: A New Bioinformatics Tool for Quantitative (1)H NMR Lipid Profiling. *Anal Chem.* 2018;90(3):2031-40.

38. Wu J, Xu W, Ming Z, Dong H, Tang H, Wang Y. Metabolic changes reveal the development of schistosomiasis in mice. *PLoS Negl Trop Dis.* 2010;4(8).

39. Laothong U, Pinlaor P, Boonsiri P, Hiraku Y, Khoontawad J, Hongsrichan N, et al. alpha-Tocopherol and lipid profiles in plasma and the expression of alpha-tocopherol-related molecules in the liver of *Opisthorchis viverrini*-infected hamsters. *Parasitology International.* 2013;62(2):127-33.

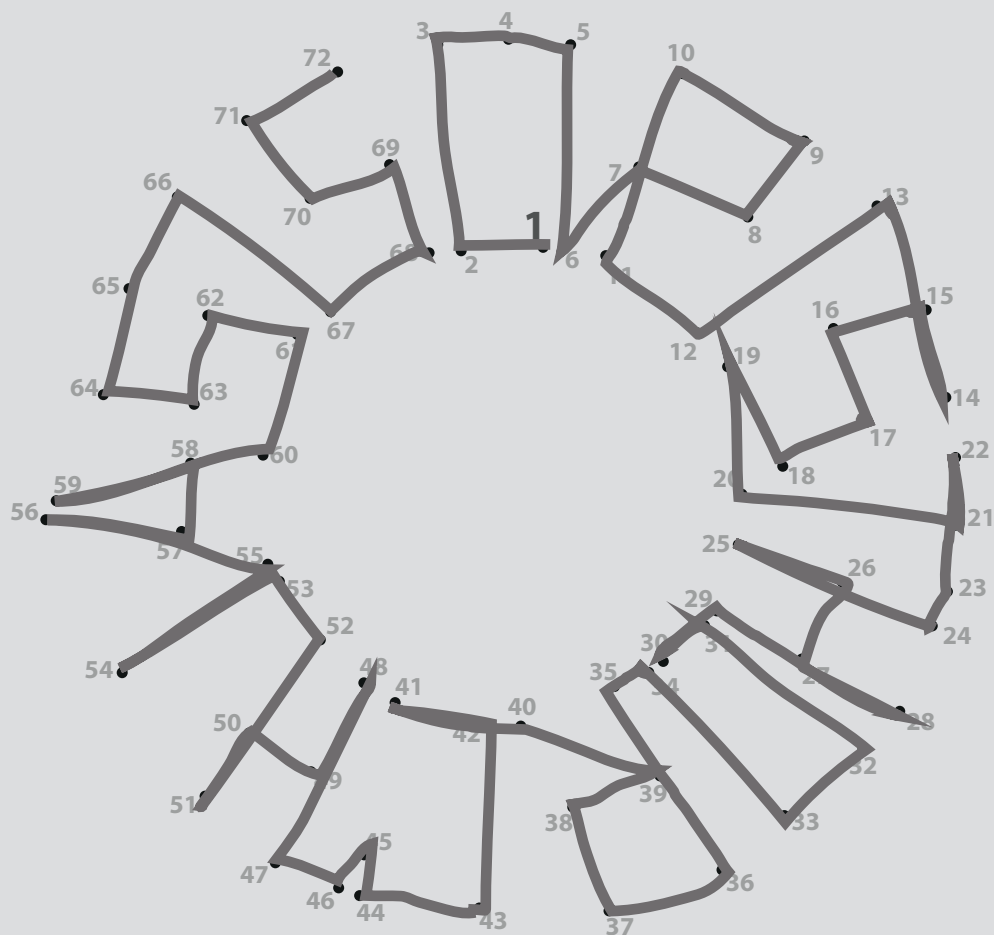
40. Changbumrung S, Ratarasarn S, Hongtong K, Migasena P, Vutikes S, Migasena S. Lipid-Composition of Serum Lipoprotein in Opisthorchiasis. *Annals of Tropical Medicine and Parasitology.* 1988;82(3):263-9.

41. Hardardottir I, Grunfeld C, Feingold KR. Effects of endotoxin and cytokines on lipid metabolism. *Curr Opin Lipidol.* 1994;5(3):207-15.

42. Kitagawa S, Yamaguchi Y, Imazumi N, Kunitomo M, Fujiwara M. A uniform alteration in serum lipid metabolism occurring during inflammation in mice. *Jpn J Pharmacol.* 1992;58(1):37-46.

43. Sherman DR, Guinn B, Perdok MM, Goldberg DE. Components of sterol biosynthesis assembled on the oxygen-avid hemoglobin of *Ascaris*. *Science.* 1992;258(5090):1930-2.





# 7

## General discussion

In this thesis, the systemic host metabolic response to experimental *Opisthorchis felineus* (*O. felineus*) infection using Nuclear Magnetic Resonance (NMR) spectroscopy has been investigated. Overall, the studies examined the experimental model of opisthorchiasis, which included male and female animals, mild and severe infections, acute and chronic (up to 32 weeks) as well as biofluids and organs. Multi-block data analysis was applied to the model of chronic opisthorchiasis to delineate how infection affects the metabolic profile of infected versus uninfected animals at a detailed level, enhancing our understanding of this neglected disease affecting 56 million worldwide.

**Chapter 2** is dedicated to an overview of the metabolomics studies on trematode infections. No relevant publications on *Opisthorchis* sp. were found, however, the review highlights the studies on other trematodes such as *Schistosoma mansoni* (*S. mansoni*) *Schistosoma japonicum* (*S. japonicum*), *Fasciola hepatica* (*F. hepatica*), and *Echinostoma caproni* (*E. caproni*), which are widespread infections worldwide. Focusing on NMR spectroscopy, known for its robustness, we tried to achieve a more reliable comparison of the results from the different laboratories. Likewise, animal studies offer a degree of control for multiple confounding factors, which is almost impossible to reach in human studies. The literature overview led us to the two conclusions relevant for the current work: a) the main features of the hosts metabolic response to the trematode infections can be described as a dysregulation of the amino acid and lipid metabolism, and changes in the microbiota related metabolites; and b) a prevailing case-control design and analysis of a single biofluid type gives only a limited overview of the possible metabolic adaptation of the host to the infection. Therefore, we adapted our experiential design to include the following features: longitudinal data sampling, two body fluids (urine and plasma); two different degrees of *O. felineus* infection (mild and severe) compared with a control group (PBS-vehicle); and the animals of the both genders were included in the experiment. The results of the time-resolved studies are presented in **Chapters 3** (urine data) and **Chapter 4** (blood plasma data).

Our data in these chapters show the strongest metabolic response in both urine and plasma biofluids is observed between the 2<sup>nd</sup> until 10<sup>th</sup> week post-infection, which is related to the acute stage of opisthorchiasis. During this period worms reach the bile duct where they transform into an adult form and start egg production [1]. The

maximal metabolic response to the infection was observed in 4<sup>th</sup> week post-infection; the time point when eggs are first detected in the feces. The metabolic response of the host to acute opisthorchiasis has a few general characteristics. The first one is the changes in the metabolism of the essential amino acids. The acute stage of the infection is characterized by depletion of the branched-chain amino acids (BCAAs) – valine, leucine, isoleucine in blood, but the elevation of isoleucine in urine samples, which could indicate a modulation of liver function [2]. Taurine, another essential amino acid, participating in bile formation, demonstrated a trend for a decrease in urine of the infected group. This, in turn, might relate to overproduction of bile acids as a consequence of blockage of bile ducts by worms or eggs. The increase of bile acids in urine of *O. felineus* infected group may confirm this hypothesis. Therefore, bile acids might be a prospective marker for diagnostics of opisthorchiasis at the acute phase of infection. On the other hand, taurine plays an important part in the regulation of lipid metabolism, and the level of urinary taurine can relate to changes in host lipid metabolism, which can be strongly manifested in blood plasma data [3].

A strong trend of the metabolic response to *O. felineus* infection is a shift in lipid metabolism. At the first 12 weeks of infection, there is an extreme upregulation of lipoproteins for both infected groups (mild and severe). Our results mostly agree with the study of *O. viverrini* infected hamsters, where it had been shown that changes in lipid metabolism are associated with leakage of  $\alpha$ -tocopherol from an injured liver [4]; moreover, changes of lipoproteins were reported for other trematode infections [5].

Changes in lipid metabolism are strongly connected with another metabolic change during acute opisthorchiasis, namely in nicotinic acid metabolism. This change is unique for opisthorchiasis and has not been reported in metabolomics studies on other trematode infections. We hypothesize that in the first weeks of the infection, which is often described as a period of metabolic stress, a consumption of nicotinic acid increases as it is needed for NAD<sup>+</sup> production. This, in turn, leads to the reduced release of its derivatives such as e.g. nicotinuric in urine of the infected group. Even though urine and plasma samples have shown similar trends, urine samples had a gender-specific response – a stronger response is seen in males than in females. The explanation for this phenomenon could be the gender specific difference of the renal system, though blood which reflects the sum of all

processes is less affected by sex.

Taken together, the metabolomics studies have highlighted that *O. felineus* infection modulates lipid, energy, and amino acid metabolism, but the response is not specific for the infection and can be mediated by common metabolic stress. By using a longitudinal study design, it was demonstrated that the strongest metabolic response was observed during the acute stage (until the 12<sup>th</sup> week of infection) with the peak corresponding to when egg production commences.

Feces is the sample routinely used for diagnosis of helminth infections by for example, Kato-Katz tests [6]. However, feces, as a product of the gastrointestinal tract, can have essential information about exogenous metabolites and microbiota. Therefore, it would be useful to be able to analyze feces metabolomics during opisthorchiasis but there are no standardized protocols for measurement of metabolites in feces samples. Therefore, **Chapter 5** was dedicated to the development of the NMR-based metabolomics workflow for feces. Human feces samples were chosen for the development, because the amounts available exceed that from hamsters. After tuning the method, final protocol involved few steps for sample preparation: homogenization, water extraction, and double centrifugation. Using the workflow, 62 fecal metabolites were identified in a pooled human sample. The protocol was tested on a small subset of infected and non-infected samples from *O. felineus*-infected people. The method was used in **Chapter 6**.

As it was indicated above, the differences in the metabolic composition of the body fluids between the infected and non-infected animals are becoming negligible after the 12<sup>th</sup> week of infection. We speculate that after the initial metabolic stress caused by the worm intervention and starting egg production, the host reaches metabolic homeostasis which indicates the beginning of the chronic infection. Yet, the question how and at which cost the host metabolism reaches this condition remains unanswered. **Chapter 6** presents an integrative metabolomics approach which was focused on how different organs and functional systems of a host are affected by the infection and how the host adapts to the chronic infection. Six relevant body compartments, blood serum, urine, and stool samples were included in the study, but 26 metabolites of liver, spleen, and jejunum and 6 serum fatty acids were relevant to a map of metabolic signature for chronic opisthorchiasis. Therefore, the metabolic homeostasis depends on system lipid metabolism and local metabolic changes in the liver, where

the fluke is located; the spleen, which is central to the immune system; and jejunum, the closest intestinal segment to the liver.

The elevated fatty acids belonged to linoleic acid metabolism and odd-chain fatty acids are strong in driving the data. It has been shown that those structures have a reverse association with a risk of type 2 diabetes [7-9]. Furthermore, arachidonic acid (the end product of linoleic acid pathway) is an important mediator of inflammation. It can affect the functioning of several organs and systems either directly or upon its conversion into eicosanoids including prostaglandins, thromboxanes, and leukotrienes [10].

The metabolic changes at the level of the individual organs could be explained from point of view of the regulation of the immune response. For instance, it has been shown that leucine plays a role in regulation of intestinal immunity and the entire mTOR signaling system [11,12]. An activation of the metabolic mechanisms involving leucine was also shown for *Shistosoma mansoni* and *Fasciola hepatica* infection [13,14].

Finally, our analysis shows that metabolically the spleen was the most affected organ, which could be interpreted as an indication of its key role in long-term metabolic response to *O. felineus* infection. The glutamine/glutamate and glutamine/alanine ratios in the spleen of the infected animals indicate lower cell proliferation rates [15]. At the same time, low liver glutamine/glutamate ratio showed a higher metabolic activity of the liver during chronic opisthorchiasis which can be related to adaptations to the presence of the parasite (inflammation, eosinophilia and periductal fibrosis at the chronic stage) [16,17].

To summarize, while the acute infection represents a state of temporary metabolic stress which is resolved in a new homeostasis, the new “status-quo” is achieved at the cost of the prolonged changes in the utilization of the main metabolic fuel components and the local depletion of the amino acids pool. We can tentatively describe this combination of the metabolic changes as a “metabolically mediated hibernative state of the organism” which develops during the chronic infection.

## Conclusions

For the first time, the comprehensive host metabolic response to *Opisthorchis felineus* (*O. felineus*) infection has been explored and is presented in this thesis. Using a longitudinal study design, it was possible to show that the metabolic response to the opisthorchiasis has two clear stages – acute and chronic. The acute stage characterizes the changes in the host metabolism of lipids, energy and essential amino acids which corresponds to common metabolic stress caused by an invasion and onset of egg production. After the period of an adaptation, at the chronic stage, the metabolic changes in the biofluids (blood and urine) are flattened. However, multicompartiment metabolomics study showed that chronic opisthorchiasis suppresses the metabolic activity of jejunum, liver and spleen that can increase the risk of development of the associated pathologies. Thus, acute and chronical opisthorchiasis characterizes different metabolic conditions, at the beginning, *O. felineus* infection provokes metabolic stress which shifts to a metabolic homeostasis which is driven by systemic changes in lipid metabolism and organ-specific amino acid metabolism.

## References

1. Kaewpitoon N, Kaewpitoon SJ, Pengsaa P, Sripa B. *Opisthorchis viverrini*: The carcinogenic human liver fluke. *World J Gastroentero.* 2008;14(5):666- 74
2. Pershina AG, Ivanov VV, Efimova LV, Shevelev OB, Vtorushin SV, Perevozchikova TV, et al. Magnetic resonance imaging and spectroscopy for differential assessment of liver abnormalities induced by *Opisthorchis felineus* in an animal model. *Plos Neglected Tropical Diseases.* 2017;11(7).
3. Ribeiro RA, Bonfleur ML, Batista TM, Borck PC, Carneiro EM. Regulation of glucose and lipid metabolism by the pancreatic and extra-pancreatic actions of taurine. *Amino Acids.* 2018 Nov;50(11):1511-1524
4. Laothong U, Pinlaor P, Boonsiri P, Hiraku Y, Khoontawad J, Hongsrichan N, et al. alpha-Tocopherol and lipid profiles in plasma and the expression of alpha-tocopherol-related molecules in the liver of *Opisthorchis viverrini*-infected hamsters. *Parasitology International.* 2013;62(2):127-33
5. Kokova D, Mayboroda OA. Twenty Years on: Metabolomics in Helminth Research. *Trends Parasitol.* 2019 Apr;35(4):282-288
6. McCarthy JS, Lustigman S, Yang GJ, Barakat RM, Garcia HH, Sripa B, Willingham AL, Prichard RK, Basanez MG. A research agenda for Helminth diseases of humans: diagnostics for control and elimination Programmes. *PLoS Negl Trop Dis.* 2012;6(4):e1601
7. Ahola-Olli AV, Mustelin L, Kalimeri M, Kettunen J, Jokelainen J, Auvinen J, Puukka K, Havulinna AS, Lehtimäki T, Kähönen M, Juonala M, Keinänen-Kiukaanniemi S, Salomaa V, Perola M, Järvelin MR, Ala-Korpela M, Raitakari O, Würtz P. Circulating metabolites and the risk of type 2 diabetes: a prospective study of 11,896 young adults from four Finnish cohorts. *Diabetologia.* 2019 Dec;62(12):2298-2309
8. Wu JHY, Marklund M, Ima-mura F, Tintle N, Ardisson Korat AV, de Goede J, Zhou X, Yang WS, de Oliveira Otto MC, Kröger J, Qureshi W, Virtanen JK, Bassett JK, Frazier-Wood AC, Lankinen M, Murphy RA,

Rajaobelina K, Del Gobbo LC, Forouhi NG, Luben R, Khaw KT, Wareham N, Kalsbeek A, Veenstra J, Luo J, Hu FB, Lin HJ, Siscovick DS, Boeing H, Chen TA, Steffen B, Steffen LM, Hodge A, Eriksdottir G, Smith AV, Gudnason V, Harris TB, Brouwer IA, Berr C, Helmer C, Samieri C, Laakso M, Tsai MY, Giles GG, Nurmi T, Wagenknecht L, Schulze MB, Lemaitre RN, Chien KL, Soedamah-Muthu SS, Geleijnse JM, Sun Q, Harris WS, Lind L, Årnlöv J, Risérus U, Micha R, Mozaffarian D; Cohorts for Heart and Aging Research in Genomic Epidemiology (CHARGE) Fatty Acids and Outcomes Research Consortium (FORCE). Omega-6 fatty acid biomarkers and incident type 2 diabetes: pooled analysis of individual-level data for 39 740 adults from 20 prospective cohort studies. *Lancet Diabetes Endocrinol.* 2017 Dec;5(12):965-974

9. Meikle, P.J.; Wong, G.; Barlow, C.K.; Weir, J.M.; Greeve, M.A.; MacIntosh, G.L.; Almasy, L.; Comuzzie, A.G.; Mahaney, M.C.; Kowalczyk, A.; et al. Plasma lipid profiling shows similar associations with prediabetes and type 2 diabetes. *PLoS One* 2013, 8

10. James MJ, Gibson RA, Cleland LG. Dietary polyunsaturated fatty acids and inflammatory mediator production. *Am J Clin Nutr.* 2000 Jan;71(1 Suppl):343S-8S

11. Ren M, Zhang S, Zeng X, Liu H, Qiao S. Branched-chain amino acids are beneficial to maintain growth performance and intestinal immune-related function in weaned piglets fed protein restricted diet. *Asian-Australas J Anim Sci.* 2015;28:1742

12. Powell JD, Pollizzi KN, Heikamp EB, Horton MR. Regulation of immune responses by mTOR. *Annu Rev Immunol.* 2012;30:39

13. Li JV, Holmes E, Saric J, Keiser J, Dirnhofer S, Utzinger J, Wang Y. Metabolic profiling of a *Schistosoma mansoni* infection in mouse tissues using magic angle spinning-nuclear magnetic resonance spectroscopy. *Int J Parasitol.* 2009 Apr;39(5):547-58

14. Saric J, Li JV, Utzinger J, Wang Y, Keiser J, Dirnhofer S, Beckonert O, Sharabiani MT, Fonville JM, Nicholson JK, Holmes E. Systems parasitology: effects of *Fasciola hepatica* on the neurochemical profile in the rat brain. *Mol Syst Biol.* 2010 Jul;6:396

15. Hall JC, Heel K. Glutamine. *British Journal of Surgery* 1996, 83, 305-312

16. Sripa B. Pathobiology of opist-

horchiasis: an update. *Acta Trop.* 2003 Nov;88(3):209-20

17. Sripa B, Jumnainsong A, Tangkawattana S, Haswell MR. Immune Response to *Opisthorchis viverrini* Infection and Its Role in Pathology. *Adv Parasitol.* 2018;102:73-95



&  
Appendices

## Nederlandse samenvatting

### Opisthorchiasis: een kort overzicht

Ongeveer 46 miljoen mensen zijn geïnfecteerd met de zuigwormen van de familie *Opisthorchiidae* (*Opisthorchis viverrini*, *Opisthorchis felineus*, *Clonorchis sinensis*); 600 miljoen mensen lopen het risico op infectie [1]. *O. felineus* veroorzaakt de meeste besmettingen in Europa, vooral in West-Siberië (Russische Federatie). In het laatste decennium van de 20e eeuw (1990-2000) was in deze Siberische regio tot 80% van de bevolking besmet met *O. felineus* [2]. Ondanks de beschikbaarheid van betaalbare behandelingen en relatief eenvoudige diagnostiek zorgt de infectie vandaag de dag nog steeds voor druk op de Russische gezondheidszorg. Ook worden er gevallen van besmetting met *O. felineus* gemeld in het Verre Oosten, Zuidoost-Azië en Oost-Europa alsook in Noord-Amerika, wat grotendeels kan worden toegeschreven aan de wereldwijde mobiliteit en migratie.

De klinische presentatie van opisthorchiasis is niet erg specifiek, noch voor acute, noch voor chronische vormen van de ziekte. Een chronische infectie met *O. felineus* leidt echter tot talrijke lokale en systemische complicaties van het hepatobiliaire systeem van de gastheer [3]. Epidemiologische en dierstudies tonen aan dat infecties met *O. viverrini* en *C. sinensis* kunnen leiden tot cholangiocarcinoma (galwegkanker), hetgeen heeft geresulteerd in de classificatie, door het International Agency for Research on Cancer, van deze parasieten bij de groep I carcinogenen [3]. Het verband tussen opisthorchiasis en cholangiocarcinoom heeft geleid tot een toename van het aantal publicaties, voornamelijk over parasitologie en epidemiologie en de laatste jaren over diagnose en behandeling. Daarnaast zijn moleculair-gebaseerde benaderingen zoals genomica, transcriptomica en proteomica toegepast om de gastheer-pathogeen-interactie op moleculair niveau te ontrafelen. Het metaboloom is echter in het geheel niet onderzocht. Om deze leemte op te vullen concentreerden wij ons op de mechanismen van de ontwikkeling van *O. felineus*-geassocieerde pathologieën aan de hand van metabolomica.

## Het bepalen van een onderzoeksstrategie

**Hoofdstuk 2** geeft een overzicht van metabolomica-onderzoeken naar infecties met trematoden. Er zijn geen relevante publicaties over *Opisthorchis* sp. gevonden, maar het overzicht belicht de onderzoeken naar andere trematoden zoals *Schistosoma mansoni* (*S. mansoni*), *Schistosoma japonicum* (*S. japonicum*), *Fasciola hepatica* (*F. hepatica*) en *Echinostoma caproni* (*E. caproni*). Dit literatuuronderzoek heeft geleid tot twee conclusies die relevant zijn voor dit onderzoek: a) de belangrijkste kenmerken van de metabolische respons van de gastheer op trematode-infecties kunnen worden beschreven als een ontregeling van het aminozuur- en lipidenmetabolisme, alsook veranderingen in de microbiota-gerelateerde metabolieten; en b) een overwegend case-control opzet en analyse van één enkel type biofluïdum geeft slechts een beperkt overzicht van de mogelijke metabolische aanpassing van de gastheer aan de infectie. Op basis van de informatie uit deze literatuurstudie hebben wij de hiaten opgevuld en hebben we de volgende aspecten in onze studie opgenomen: i) longitudinale gegevensbemonstering; ii) bemonstering van twee verschillende lichaamsvloeistoffen (urine en plasma); iii) twee verschillende *O. felineus*-infecties (mild en ernstig) vergeleken met een controlegroep (PBS-vehikel); en iv) zowel mannelijke als vrouwelijke proefdieren.

## Time-resolved onderzoek van opisthorchiasis

De gegevens in **hoofdstuk 3** en **hoofdstuk 4** tonen aan dat de sterkste metabolische respons op *O. felineus*-infectie in zowel urine- als plasmabiovloeistoffen wordt waargenomen tussen de 2e en 10e week na infectie, wat gerelateerd is aan de acute fase van opisthorchiasis. Tijdens deze periode bereiken de wormen de galbuis, waar ze uitgroeien tot volwassen wormen en eieren gaan produceren. De maximale metabolische respons op *O. felineus*-infectie werd waargenomen in de 4e week na infectie, het moment waarop de eerste eieren kunnen worden gedetecteerd in faecesmonsters van de gastheer. De metabolische reactie van de gastheer op acute opisthorchiasis heeft een paar algemene kenmerken: veranderingen in het metabolisme van aminozuren, een verhoogde hoeveelheid urinegalzuren en een verschuiving in het vet- en energiemetabolisme van de gastheer. Maar de reactie is niet specifiek voor *O. felineus*-infectie en kan door gewone metabolische stress worden veroorzaakt.

## Weefselspecifiek onderzoek van opisthorchiasis

**Hoofdstuk 6** presenteert een integratieve metabolomische benadering die zich richt op de vraag hoe verschillende organen en functionele systemen van de gastheer door de infectie worden beïnvloed, en hoe de gastheer zich aan een chronische infectie aanpast. Zes delen van het lichaam (lever, milt, nier en drie delen van de darmen), bloedserum, urine en ontlasting zijn in deze studie opgenomen. Omdat er voor faecesmonsters geen gestandaardiseerd protocol is om metabolomica-analyses uit te voeren, is **hoofdstuk 5** gewijd aan de ontwikkeling van een NMR-gebaseerde metabolomic workflow voor faeces.

Het onderzoek dat in hoofdstuk 6 wordt beschreven, toont aan dat met 26 metabolieten van lever, milt en jejunum en zes serumvetzuren een metabole handtekening voor chronische opisthorchiasis kon worden opgesteld. De verhoogde serumvetzuren behoren tot het linolzuurmetabolisme; onevenketenvetzuren hebben een sterke invloed op de gegevens. De metabolische veranderingen binnen de individuele organen kunnen worden verklaard als een immuunregulatiereactie. Onze analyse toont aan dat de milt metabolismisch sterk beïnvloed wordt, wat een indicatie kan zijn van zijn sleutelrol in de metabolische respons op lange termijn op *O. felineus*-infectie.

## Conclusies

Dit is de eerste keer dat de metabolische respons van de gastheer op *O. felineus*-infectie uitgebreid is bestudeerd. Door een longitudinale onderzoeksopzet konden we aantonen dat de metabole respons op opisthorchiasis twee duidelijke stadia kent: acuut en chronisch. Het acute stadium wordt gekenmerkt door veranderingen in het metabolisme van lipiden, energie en essentiële aminozuren bij de gastheer. Dit komt overeen met gewone metabolische stress en wordt veroorzaakt door het binnendringen van de parasiet en het begin van eiproduktie. In het chronische stadium lijkt er een aanpassing plaats te vinden wanneer de metabolische veranderingen in de biofluïden (bloed en urine) afvlakken. Bijgevolg worden acute en chronische opisthorchiasis gekenmerkt door verschillende metabolische omstandigheden. In het begin veroorzaakt de infectie met *O. felineus* metabolische stress, waarna een overgang plaatsvindt naar een metabole homeostase die wordt aangedreven door systemische veranderingen in het vetmetabolisme en het orgaanspecifieke aminozuurmetabolisme. Het multi-compartimentele metabolomica-onderzoek toont aan dat chronische

opisthorchiasis de metabolisme activiteit van het jejunum, de lever en de milt onderdrukt, wat het risico van het ontwikkelen van geassocieerde pathologieën kan verhogen.

### **Referenties**

1. Fürst T, Keiser J, Utzinger J. Global burden of human food-borne trematodiasis: A systematic review and meta-analysis. *Lancet Infect Dis.* 2012;12: 210–221. doi:10.1016/S1473-3099(11)70294-8
2. Fedorova OS, Kovshirina Y V., Kovshirina AE, Fedotova MM, Deev IA, Petrovskiy FI, et al. Opisthorchis felineus infection and cholangiocarcinoma in the Russian Federation: A review of medical statistics. *Parasitol Int.* 2017;66: 365–371. doi:10.1016/j.parint.2016.07.010
3. Mairiang E, Mairiang P. Clinical manifestation of opisthorchiasis and treatment. *Acta Tropica.* Elsevier; 2003. pp. 221–227. doi:10.1016/j.actatropica.2003.03.001
4. Bouvard V, Baan R, Straif K, Grosse Y, Secretan B, El Ghissassi F, et al. A review of human carcinogens--Part B: biological agents. *The lancet oncology.* *Lancet Oncol;* 2009. pp. 321–322. doi:10.1016/s1470-2045(09)70096-8

## Acknowledgements

I would like to thank all who contributed directly or indirectly to the completion of this thesis.

Firstly, I would like to thank my promotor, Maria for giving me the opportunity to join your department and opening possibilities to study metabolomics of opisthorchiasis. Thank you, Oleg, my co-promoter, for your guidance and encouragement along the way.

Thank you to all my colleagues in the Department of Parasitology and Center of Proteomics and Metabolomics, I was proud to be a part of such great teams. I would like to say thank you to Suzanne, Gerdien, and Jantien, management assistants of the Parasitology department, for your help with documents, appointments, and many other organizing matters. Dear Aswin and Sarantos, I was grateful to be working with you in the NMR laboratory, you are Jedi of NMR.

Dear Siberian State Medical University collaborators and co-authors, especially Vladimir Vladimirovich, Ekaterina, and Irina, I would like to thank you for contributing to the study. All the animal parts of the study were on your shoulders.

I am thankful to the committee for the critical evaluation of my thesis.

My paranympths, Aswin and Suzanne, I am looking forward to having you by my side on that important day for me.

Thank you to my friends, Julia, Victor, Paulien, and, AJ, your support during these four years in Holland was invaluable! Paulien, thank you for helping with the translation of the summary to Dutch.

My dearest husband, Matthias, thank you for your support during all this journey. My children, Kirill and Sofia, your smiles were inspiring me. Mama, я люблю тебя, спасибо!

## Curriculum vitae

Daria Kokova was born on January 25<sup>th</sup> 1986, in Abakan, USSR. After graduating from secondary school in 2003, she moved to Tomsk to study Chemistry at the Tomsk State University. During her study at the university, she was interested in physical chemistry, with her master thesis focusing on the development of heterogeneous catalysts for partial oxidation and analysis of products of catalytic reactions. During her university study, she started to work in the Laboratory of catalytic research of the Tomsk State University (2008-2011). However, after graduation, she realized that analytical chemistry interested her more. The board of the Chemistry Department of the Tomsk State University supported her concept for establishing a mass spectrometry-based analytical laboratory. Daria Kokova led and managed the laboratory until 2016. The focus of the laboratory was the development of analytical methods for complex organic/biological samples (GC-MS, HPLC-MS/MS, HTLC). The experience of working at the crossroads between biology and chemistry triggered her interest in metabolomics. She has received personal funding for two consecutive internships in the Center for Proteomics and Metabolomics (CPM) at Leiden University Medical Center. The area of research at the intersection between biology and chemistry triggered her interest and prompted her to see a PhD studentship in the field of metabolomics. She won a personal fellowship and joined the Department of Parasitology of LUMC, as a PhD student in 2016. Under the supervision of prof. dr. M. Yazdanbakhsh and dr. O.A. Mayboroda, the comprehensive host metabolic response to *Opisthorchis felineus* infection was explored during her PhD study.

Currently, Daria Kokova is leading the Laboratory of Clinical Metabolomics at the Tomsk State University. Her research interests are focused on applying metabolomics for the investigation of infectious diseases. She is interested in using UPLC-MS and NMR techniques for metabolomics profiling and in data processing and multivariate data analysis.

## List of publications

1. **D. Kokova**, A. Verhoeven, E.A. Perina, V.V. Ivanov, M. Heijink, M. Yazdanbakhsh, O.A. Mayboroda. Metabolic homeostasis in chronic helminth infection is sustained by organ specific metabolic rewiring. *ACS Infect. Dis.* 7: 4 (2021) (thesis Chapter 6)
2. **D. Kokova**, A. Verhoeven, E.A. Perina, V.V. Ivanov, E.M. Knyazeva, I.V. Saltykova, O.A. Mayboroda. Plasma metabolomics of the time resolved response to *Opisthorchis felineus* infection in an animal model (golden hamster, *Mesocricetus auratus*). *PLoS Negl Trop Dis* 14(1): e0008015 (2020) (thesis Chapter 4)
3. **D. Kokova**, O.A. Mayboroda. Twenty years on: metabolomics in helminth research. *Trends in Parasitology*, V. 35, I. 4, pp 282-288 (2019) (thesis Chapter 2)
4. **D. Kokova**, S. Kostidis, J. Morello, N. Dementeva, E.A. Perina, V.V. Ivanov, L.M. Ogorodova, A.E. Sazonov, I.V. Saltykova, O.A. Mayboroda. Exploratory metabolomics study of the experimental opisthorchiasis in a laboratory animal model (golden hamster, *Mesocricetus auratus*). *PLoS Negl Trop Dis* 11(10): e0006044 (2017) (thesis Chapter 3)
5. S. Kostidis, **D. Kokova**, N. Dementeva, I.V. Saltykova, H.K. Kim, Y.H. Choi, O.A. Mayboroda.  $^1\text{H}$ -NMR analysis of feces: new possibilities in the helminthes infections research. *BMC Infectious Diseases*. 17:275 (2017) (thesis Chapter 5)
6. N. Dementeva, **D. Kokova**, O.A. Mayboroda. Current Methods of the Circulating Tumor Cells (CTC) Analysis: A Brief Overview. *Curr Pharm Des* 23:32 (2017)

# Portfolio

PhD student:	drs. D Kokova	F
Primary thesis advisor:	prof.dr. M Yazdanbakhsh	
Other thesis advisor(s):	dr. O Maiboroda	
Research programme:	50401 Host-parasite interaction	
Title of Thesis:	The non-invasive and minimally invasive approaches for metabolomics screening of the helminth infection.	

## PhD training

	Year	Hours
<b>Mandatory courses</b>		
- PhD Introductory Meeting (done)	2017	
- Basic Methods and Reasoning in Biostatistics (done)	2017	
- BROK Course (done)	2018	
<b>Generic/disciplinary courses</b>		
- General English Course 3B	2016	
- Hands-on NMR Spectroscopy for Metabolic Profiling	2017	
- General English Course	2017	
- EMBO Practical Course on Metabolomics Bioinformatics for Life Scientists	2018	
- Scientific Conduct for PhDs	2018	
- Metabolomics Data Processing and Data Analysis	2017	
<b>Attended lectures, LUMC presentations, participation in meetings</b>		
- Metabomeeting 2017	2017	
- TOPIC	2017	
<b>Other activities (such as journal club)</b>		
- MOVISS: Metabolomics Bio&Data	2018	
<b>Congress attendance and poster or oral presentations</b>		
- ICOPA 2018	2018	
- EMBO/EMBL symposium	2019	
<b>TOTAL number of hours</b>		

## Publications

	Year
<b>Publications in peer reviewed journals (article, review, editorial, letter to editor)</b>	
- Current Methods of the Circulating Tumor Cells (CTC) Analysis: A Brief Overview; Dementeva Natalia, Kokova Daria, Mayboroda Oleg A.; 2017; Journal article	2017
- Exploratory metabolomics study of the experimental opisthorchiasis in a laboratory animal model (golden hamster <i>Mesocricetus auratus</i> ); Kokova Daria A., Kostidis Sarantos, Morello Judit, et al.; 2017; Journal article	2017
- H-1-NMR analysis of feces: new possibilities in the helminthes infections research; Kostidis Sarantos, Kokova Daria, Dementeva Natalia, et al.; 2017; Journal article	2017
- Plasma metabolomics of the time resolved response to <i>Opisthorchis felineus</i> infection in an animal model (golden hamster, <i>Mesocricetus auratus</i> ); Kokova D, Verhoeven A, Perina EA, et al.; 2020; Journal article	2020
- Metabolic Homeostasis in Chronic Helminth Infection Is Sustained by Organ-Specific Metabolic Rewiring.; Daria Kokova, Aswin Verhoeven, Ekaterina A Perina, et al.; 2021; Journal article	2021
- Twenty Years on: Metabolomics in Helminth Research; Kokova Daria, Mayboroda Oleg A.; 2019; Review	2019